

SKI Report 00:48

The Use of Risk Based Methods for Establishing ISI-Priorities for Piping Components at Oskarshamn 1 Nuclear Power Station

Björn Brickstad

**Det Norske Veritas
Box 30234
SE-104 25 Stockholm**

November 2000

Project team

**Björn Brickstad, DNV AB (Project Manager)
Roger Axelsson, OKG Aktiebolag
Tomas Jelinek, OKG Aktiebolag
Jan Lundwall, Ringhals AB
Pål Efsing, Barsebäck Kraft AB
Kostas Xanthopoulos, SKI
Anders Hallman, SKI
Tomas Elmeklo, ÅF-PPA
Dan Wilson, NUSAB Aktiebolag
Torbjörn Andersson, Safetech Engineering AB**

This report concerns a study which has been conducted for the Swedish Nuclear Power Inspectorate (SKI). The conclusions and viewpoints presented in the report are those of the author and do not necessarily coincide with those of the SKI.

SKI Project Number 98162

1 INTRODUCTION	5
1.1 Program Objectives	6
1.2 Program Organisation.....	6
1.3 Description of Program Tasks	6
2 OSKARSHAMN NUCLEAR POWER STATION UNIT 1	7
2.1 Current Selection Procedure of ISI, Control Group Division	7
2.2 Considered Pipe Systems	8
3 DAMAGE MECHANISMS	10
4 ESTIMATION OF COMPONENT LEAK- AND RUPTURE PROBABILITIES.....	12
5 ESTIMATION OF CONSEQUENCES.....	14
6 EVALUATION OF RISK FOR CORE DAMAGE	17
6.1 Basis for Crediting Leak Detection in the Evaluation of Risk.....	17
6.2 Core Damage Frequency with no Credit for Inspection.....	18
6.2.1 System 315, Auxiliary Condensor	20
6.2.2 System 313, Main Circulation System.....	23
6.2.3 System 326, Top Head Cooling System.....	25
6.2.4 System 321, Shutdown Cooling System	25
6.2.5 System 331, Cleaning System.....	27
6.2.6 System 354, Hydraulic Control Rod System	27
6.2.7 Core Damage Frequency per system, no inspections.....	29
6.2.8 Core Damage Frequency, all systems, no vibrations	30
6.3 Core Damage Frequency with Credit for Inspection.....	31
6.3.1 Inspection Assumptions	31
6.3.2 Core Damage Frequency for the Current ISI Selection	34
7 RISK RANKING	37
7.1 Suggestion for a New Risk Based Inspection Program.....	38
7.2 Optimization of Inspection Intervals	45
7.3 Unknown Damage Mechanisms	48
8 RISK BASED INSPECTION PROCEDURE BY EPRI	49
9 VALIDATION.....	50
9.1 Comparison with Actual Leak Frequencies	51
9.2 Benchmarking with the Code WinPRAISE.....	52

9.3 Sensitivity Analyses	54
10 CONCLUSIONS AND RECOMMENDATIONS	54
11 ACKNOWLEDGEMENTS	55
12 REFERENCES	57
APPENDIX A: PROBABILISTIC COMPUTER CODE PIFRAP FOR ESTIMATING FAILURE PROBABILITIES	59
A1 Theory and Model Assumptions.....	59
A2 Some Remarks on the Numerical Procedure	62
A3 Assumptions about Input Data	64
APPENDIX B: SENSITIVITY ANALYSES.....	71
B1 Sensitivity of crack growth rate	72
B2 Sensitivity of leak rate detection limit	73
B3 Sensitivity of dead weight load.....	74
B4 Sensitivity of thermal expansion load.....	75
B5 Sensitivity of safety relief valve load	75
B6 Sensitivity of weld residual stress level.....	76
B7 Sensitivity of vibration stress.....	78
B8 Sensitivity of fracture toughness.....	78
B9 Sensitivity of yield stress	79
B10 Sensitivity of initial crack length distribution	80
B11 Sensitivity of initial crack depth	81
APPENDIX C: COLLATION OF IGSCC-CASES IN STRAIGHT PIPE AUSTENITIC STAINLESS STEEL GIRTH WELDS IN SWEDISH BWR-PIPING UP TO 1998.....	83

1 INTRODUCTION

The most important objective of a non-destructive examination (NDE) of a primary component of a Nuclear Power Plant, is to be able to detect possible degradation at an early stage in order to prevent the damage to cause leakage and further on to a possible rupture. The inspection programs that are based upon ASME XI are primarily devoted to areas within the plant where one, at the design stage, has indicated that the likelihood of fatigue, high stresses or large plastic deformations is the greatest. However, experiences from detected degradations in nuclear power plants, have shown that other causes that in general were not anticipated during design, are responsible for most of the damages. Examples are IGSCC in austenitic stainless steel piping, erosion-corrosion in ferritic piping and thermal fatigue in mixing tees. Obviously, there is a need for an In-Service Inspection (ISI)-program that has the capability of more accurately finding the components where the probability of degradation is the greatest.

During the latest ten years, a number of procedures have been suggested where the focus is set on the risk (as measured by Core Damage Frequency CDF or Large Early Release Frequency LERF). ASME CRTD (Center for Research and Technology Development) in co-operation with Westinghouse Owners Group WOG, have defined a procedure [1]-[4], where the failure probability at different locations is combined with the failure consequence to produce the risk for core damage. Electric Power Research Institute EPRI, has defined another procedure [5]-[7], where the likelihood of failure is determined from failure statistics for US Nuclear Power Plants. The basic idea with these procedures is to focus inspection locations to areas where the risk is the highest.

The US Nuclear Regulatory Commission NRC has been very active in defining these procedures. In August 1995, the NRC adopted a policy statement [26] regarding the use of PRA (Probabilistic Risk Assessment) as a tool for decisionmaking. This policy statement states in part that:

1. The use of risk-based analyses should be increased in all regulatory matters as a complement to deterministic methods and to support the NRC's philosophy of defence in depth.
2. PRA technology should be used in regulatory matters to reduce unnecessary conservatism associated with current regulatory requirements.

Also in Europe the activity to formulate and apply RBI-procedures for Nuclear installations is high. A network called EURIS (EUropean network of Risk-Informed in-Service inspection) has been created [8]. EURIS is sponsored by the European Commission as a "Concerted Action". The main objective of EURIS is to develop a European methodology for risk based assessment relevant for the needs of plant operators. The recommended procedure document is planned to be published at the beginning of the year 2000.

In Sweden, a qualitative risk-informed system for selecting pressurized components in Nuclear Power Plants for inspections has been in operation since 1987. This system, described in SKIFS 1994:1 [9], defines a qualitative measure of risk for core damage which is used to guide the ISI selection.

Since 1987, there has been a strong development in the plant specific PSA studies in Sweden. It is now common to directly include pipe breaks into the PSA and not only malfunctioning pumps and valves etc. Also, there has been a worldwide development in estimating failure probabilities, both from historical data and by using probabilistic fracture mechanics. In Sweden, where the dominating damage mechanism in the BWR primary piping is IGSCC, efficient tools to estimate leak- and rupture probabilities for IGSCC have

been developed. Therefore, it has been a natural step to take advantage of these developments to make quantitative estimates of the risk for core damage and use this information to check and develop the existing risk based inservice inspection program in Sweden.

1.1 Program Objectives

The objective of the program is to estimate the risk for core damage in a BWR-plant in Sweden (Oskarshamn, unit 1) due to pipe leaks and breaks and use this information to select components for ISI. Also, probabilistic methods to estimate the length of inspection intervals shall be investigated. The new ISI selection shall be compared against the existing system and possible improvements shall be suggested.

1.2 Program Organisation

SAQ Kontroll AB has been managing the program and has also worked as the principal investigator. Members of the project team include Swedish Nuclear Power Inspectorate SKI, OKG Aktiebolag, Barsebäck Kraft AB, Ringhals AB, ÅF-PPA, Safetech Engineering AB and NUSAB Aktiebolag. The program has been financed jointly by SKI and all the Swedish Nuclear Power Plant Owners. In the project team is included people with experiences from PSA, probabilistic fracture mechanics, material data, inspection methods and Nuclear Power Plant systems and functionality.

1.3 Description of Program Tasks

The following list defines the basic steps of the program.

1. Identify the relevant damage mechanisms in the primary piping systems. These are mostly IGSSC (more than 95% of all cases) and in some few cases fatigue and erosion-corrosion.
2. Collect the statistical properties of IGSCC in Swedish BWR regarding number of accumulated detected cases, number of leaks and the distribution of crack lengths. The information is gathered in part directly from the Nuclear Power Plants in Sweden and in part from the damage data base STRYK [11], operated by SKI.
3. Gather information of the geometry, loading conditions, material properties and inspection data for each component that is to be included in the pilot study. All primary piping components with a potential for IGSCC are included in the study.
4. Collect information of the plant specific PSA to obtain the consequences of leaks and ruptures. All systems inside the containment with a diameter exceeding 50 mm are included in the PSA which means about 3500 components. Pipe ruptures and disabled leaks are directly modeled in the PSA. Small leaks have to be treated separately as well as breaks outside the containment.
5. Use the structural reliability code PIFRAP [32] to calculate leak- and rupture probabilities. Account can be taken to inspection (interval and effectiveness) as well as leak detection.
6. Validation of PIFRAP by comparing against Swedish failure statistics (leaks) and benchmarking against WinPRAISE [23].
7. Compile the leak- and rupture probabilities (P) and the conditional core damage frequencies (C) into P-C risk diagrams. No influence of inspections are taken at this stage. The basic equation to evaluate the risk for each component is given by

$$CDF = P(\text{small leak}) \cdot C(\text{small leak}) + P(\text{large leak}) \cdot C(\text{large leak}) + P(\text{rupture}) \cdot C(\text{rupture})$$

8. Calculate risk reduction worth RRW and risk achievement worth RAW.
9. Perform sensitivity analyses.
10. Perform a new selection of components for ISI based on high relative risks or high RRW-values.
11. Compare the new risk based selection with the current Swedish regulation system SKIFS 1994:1 and the procedures developed by EPRI.
12. Calculate the change in total core damage frequency $\Delta CDF = CDF(\text{new selection}) - CDF(\text{old selection})$. Account both for inspection interval and effectiveness in the risk evaluations of the components selected for inspection.
13. Investigate the possibilities to optimise the risk by determining the inspection interval by probabilistic methods.

2 OSKARSHAMN NUCLEAR POWER STATION UNIT 1

The plant selected for the pilot study is Oskarshamn-1 (O1) which is the oldest BWR in Sweden. O1 started its commercial operation in 1972 and has a thermal output of 1375 MW and an electric output of 462 MW. O1 is designed by ABB-Atom and has 4 external main recirculating loops and 2 trains of auxiliary feedwater and low pressure core spray. There are some differences of O1 compared to the other BWRs in Sweden. One special feature is that O1 has an auxiliary condensor. In cases when the turbines are unavailable, the auxiliary condensor can cool the residual heat of the reactor without the necessity to provide auxiliary feedwater.

2.1 Current Selection Procedure of ISI, Control Group Division

The current system for ISI-selection is based on a division into so called control groups from A to C. It is described in SKIFS 1994:1 [9], where a damage index and a consequence index from 1 to 3 are defined, Fig. 1.

		Consequence Index		
		1	2	3
Damage Index	1	A	A	B
	2	A	B	C
	3	B	C	C

Fig. 1. Matrix used in Sweden to select components for ISI [9].

The damage index is an engineering estimate of the likelihood of failure. Basically a damage index equal to 1 corresponds to a damage mechanism present whereas a damage index 3 represents a situation where essentially no damage mechanism at all is present. The consequence index is based on the margin in system capacities to mitigate the component failure and the margin in fuel temperature to reach a critical level. In practice, this means

that the consequence index is determined basically by the component diameter and if the system is connecting above or below the water level in the reactor pressure vessel. A consequence index of 1 corresponds to the most severe consequence. By combining these indexes, a qualitative measure of risk for core damage is obtained and used to guide the ISI selection.

The matrix in Fig. 1 defines a Control Group (CG) from A to C for each component. In control group A, 100% of the components shall be selected for inspection. Within control group B the selection is random and shall correspond to at least 10% of the components. In group C the rules for inspection of conventional pressurized equipments are endorsed which normally means an extent of ISI-selection that is much lower than for control group B. This means that the main interest for inspection is focused on the components where a damage mechanism is potentially expected which is a very good basis for a risk based inspection selection. However, as is seen by Fig. 1, there are also inspection sites in control group B where no damage mechanism is expected (damage index 3 and consequence index 1). These locations should in general represent a very low risk for core damage.

In the O1 plant, the control group division is applied on all class 1-3 piping components with a diameter exceeding 50 mm from the reactor to the high pressure turbines.

2.2 Considered Pipe Systems

Initially, the intention was to cover only a few pipe systems in this pilot study. However, a major disadvantage is then that the evaluated core damage for the selected systems will not represent the total risk coming from pipe failures. When investigating alternative ISI-programs for inspections, it is important to be able to calculate the change in risk for a new ISI-selection relative to the current ISI-selection. In this respect it is essential that the total risk of core damage from pipe failures can be evaluated. This is only possible if all the essential pipe systems that have degradation mechanisms are included in the risk evaluation. Also, if a risk ranking procedure is used for an ISI-selection for locations representing only a few pipe systems, low risk locations in these pipe systems may not stay low risk any longer in a relative sense, if all relevant pipe systems are considered. It was therefore decided to extend the pilot study to all relevant pipe systems that have a potentially known damage mechanism. Pipe systems that do not have a damage mechanism will have a very small contribution to the risk of core damage. The following pipe systems are included in the pilot study with the number of considered welds given

1. System 313, main circulation system, 257 welds.
2. System 315, auxiliary condensor, 39 welds.
3. System 326, top head cooling, 23 welds.
4. System 321, shutdown cooling, 80 welds.
5. System 331, cleaning system, 43 welds.
6. System 354, hydraulic control rod system, 750 welds.

This gives a total of 1192 welds. This includes all components in these pipe systems that are located in control group A or B according to the current ISI-selection procedure, see Table 1. The reactor pressure vessel itself, internal parts, valves and pumps are not included in the pilot study (apart from welds connecting to the latter components). Certain elbows made of stainless steel and manufactured by cold bending, have earlier experienced IGSCC-problems in the elbow itself (intrados and extrados). However, these are all replaced in O1 which means that with respect to elbows, there are only welds connected to the elbows that still may have a potential mechanism for IGSCC.

System	No of comp with damage mechanisms	No of comp with CG = A	No of comp with CG = B	Current ISI-selection CG = A	Current ISI-selection CG = B
313 circumf	78	78	149 ⁽¹⁾	78	24 ⁽¹⁾
313 axial	30	30	0	30	0
315	20	20	19 ⁽¹⁾	20	7 ⁽¹⁾
326	12	12	11 ⁽¹⁾	12	2 ⁽¹⁾
321	63	10	70 ⁽²⁾	10	50 ⁽³⁾
331	43	0	43	0	6
354	750	0	750	0	118
	Sum 996	Sum 150	Sum 1042	Sum 150	Sum 207

(1) No known damage mechanism present.

(2) No known damage mechanism present in 17 components.

(3) No known damage mechanism present in 5 components.

Table 1. Considered pipe systems with information of number of components within each Control Group (CG) division and current extent of ISI-selection.

In Table 1 the different pipe systems that are included in the RBI-study are listed and a subdivision are made with respect to the control groups. The potential damage mechanisms are in most cases IGSCC and in some cases IGSCC and vibration fatigue. In most cases IGSCC in form of circumferential cracks may occur in the heat affected zones (HAZ) of pipe butt welds in stainless steel pipes. In some cases, where the weld material itself is susceptible to IGSCC, cracks may also initiate and grow in the axial direction of the pipe but essentially confined to the butt weld. This is the case for the main circulation system 313 which contains 30 butt welds of the Nickel base weld material Alloy 182. This is the reason for the division of circumferential and axial orientation of defects in system 313. For the rest of the systems the potential damage mechanism is IGSCC and the components are butt welds in stainless steel pipes and the orientation of the cracks is circumferential. Very few carbon steel components have a potential damage mechanism. Further discussions on damage mechanisms are given in the next section.

From Table 1 it is seen that a total of 1192 components (welds) are included in the control group division. Of these, 996 welds have a potential damage mechanism whereas 196 welds are considered not to have any known damage mechanism. In the current ISI-selection, all the 150 components in control group A and 207 components in control group B are selected for inspection. This gives a total of 357 components to inspect. In 38 cases, the current ISI-procedure is selecting components for inspection that has no known damage mechanism.

It should be noted that there are currently no known damage mechanism in the feedwater system (312), the auxiliary feedwater system (327) and the emergency core cooling system ECCS (323). High carbon content stainless steel pipe segments, located at warm parts of the pipe systems, have been replaced in these systems. Remaining high carbon content stainless steel pipe segments are all located in colder parts, far from the reactor pressure vessel.

3 DAMAGE MECHANISMS

Fig. 2 shows how the control group division for the pipe systems in O1 have resulted in a number of locations which are connected to different potential damage mechanisms.

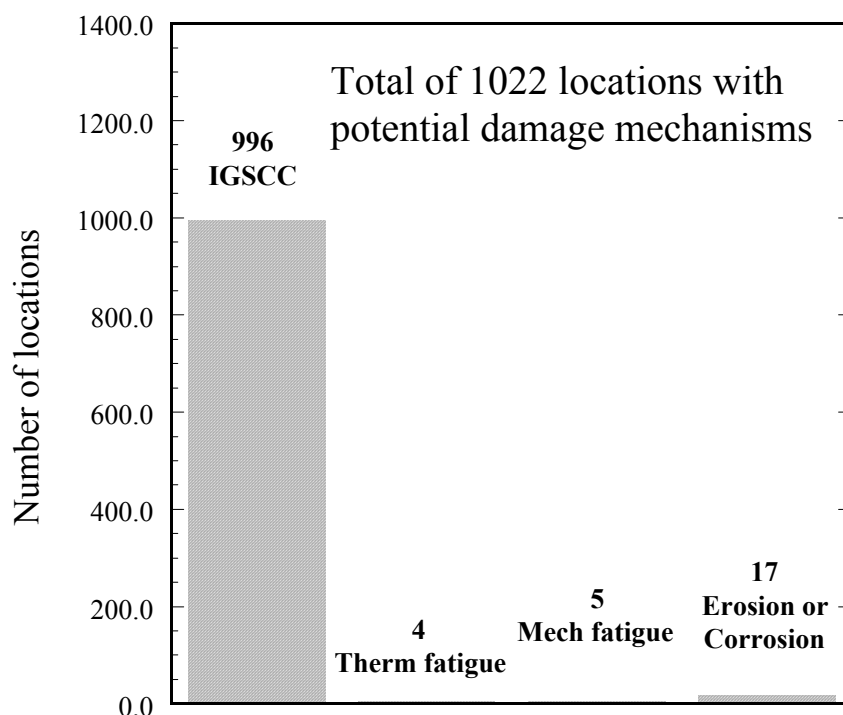


Fig. 2. Locations with potential damage mechanisms for the primary piping systems in O1.

IGSCC is assessed to be the dominant potential damage mechanism for O1. The following criteria is used in the assessment of IGSCC:

- Weld material of Alloy 182, Alloy 600 or carbon content $> 0.03-0.04\%$ in the stainless steel base material.
- Water temperature above $100-150\text{ }^{\circ}\text{C}$.
- Sensitized material due to welding.

In the pilot study, the mechanisms IGSCC and mechanical fatigue are accounted for. Thermal fatigue in mixing tees and erosion-corrosion in the steam lines have not been considered in this study. Components where there are a potential for these latter damage mechanisms, have to be treated separately. A special inspection program for erosion-corrosion is developed for O1. This program is based on operating experiences and reports from other Nuclear Power Plants of similar design. Since potential damage mechanisms other than IGSCC and mechanical fatigue are very scarce in O1, it is believed that this pilot study can give a good estimate of the total risk for core damage coming from leaks or breaks in the primary piping systems.

Apart from the damage mechanisms in Fig. 2, there are also high cycle vibrations present in some components in the pipe systems 313 and 315. As is going to be demonstrated later, vibration fatigue is only a concern in connection with IGSCC. This combination is valid for

approximately 15 welds but can give a considerable contribution to the overall core damage frequency.

A relevant question is now if the assessment that IGSCC is the dominant potential damage mechanism for O1 is also reflected in actual failure statistics. Several failure data bases have been developed during the recent years. A useful Swedish failure data base is the one called STRYK [11] and the data in Figs. 3 and 4 are taken from this data base with an entry date of March 31, 1999.

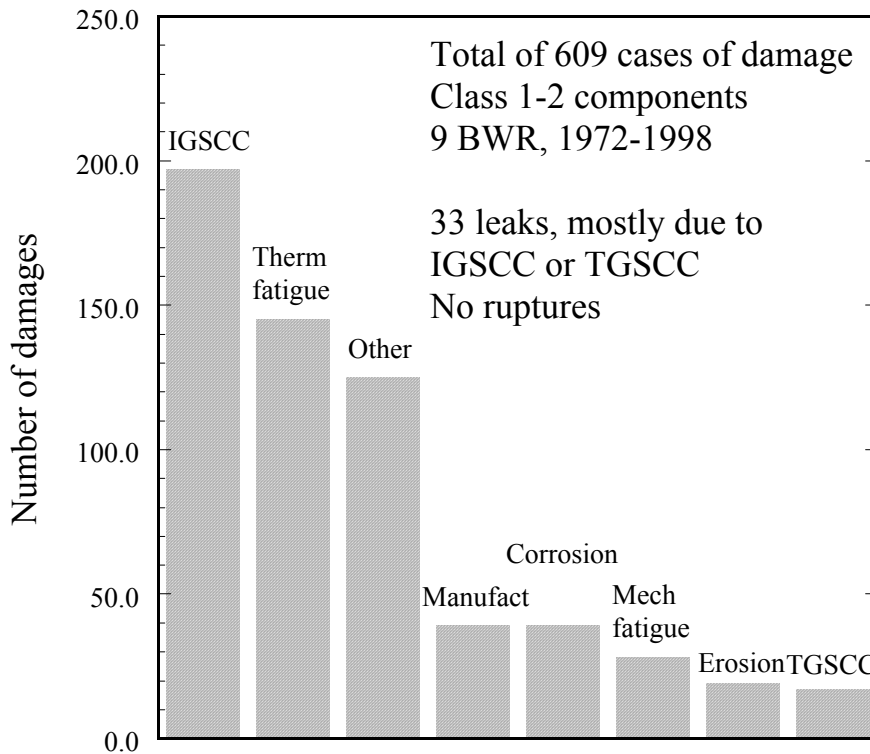


Fig. 3. Number of damages occurred in Swedish BWR-components 1972 to 1998.

In Fig. 3 all class 1 and 2 components are included from the 9 BWR-plants in Sweden. This involves the reactor pressure vessel, internal parts, piping components (pipes, elbows, tees, pumps, valves) and other components like thermal sleeves, snubbers, flanges and fastening screws. Most damages are non-penetrating and discovered by inspections and testing. In 33 cases, leaking failures have been discovered, mostly due to IGSCC or TGSCC. No case of a pipe rupture has been experienced. IGSCC is the dominating cause of the occurred damages. Thermal fatigue is the second most common cause. However, in many cases thermal fatigue has occurred in the reactor pressure vessel nozzles, internal parts and fastening screws. In the primary piping system, thermal fatigue has also occurred in mixing tees. In many of these tees, where cold and warm water are mixed, special thermal mixers have been installed in O1. The term "other" in Fig. 3 represents cases when the cause of the damage could not be established. Fig. 4 represents a subdivision of Fig. 3, where only damages in straight pipes are shown.

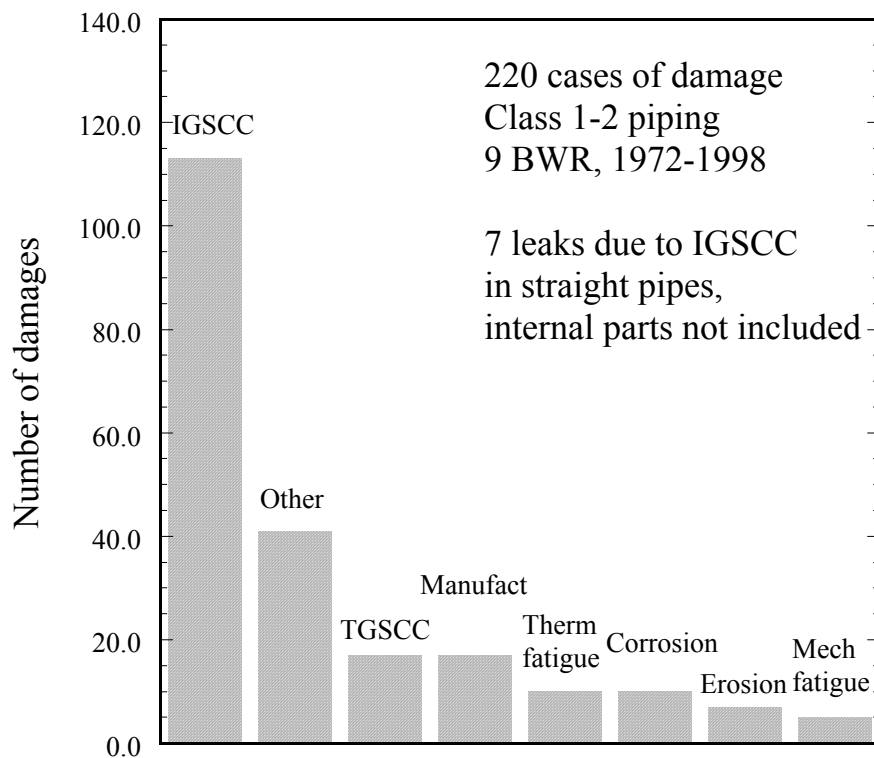


Fig. 4. Number of damages occurred in Swedish BWR-components, straight pipes.

When the occurred damages are restricted to straight pipes in the primary piping system, the dominance of IGSCC is even more remarkable. In 7 cases, leaks due to IGSCC in the HAZ of welds in stainless steel piping have been detected. This information can be used later to calibrate the predicted leak frequencies.

The information in Fig. 4 confirms the assessment of the potential damage mechanisms for O1, given in Table 1 and Fig. 2. The control group division is thus used as a screening procedure, to identify which locations that has a degradation mechanism and where, in a qualitative sense, the risk for core damage may be the largest.

4 ESTIMATION OF COMPONENT LEAK- AND RUPTURE PROBABILITIES

For many types of components observed failure frequencies are available and of such quality that they can be used in the assessment. For other types of equipment this is not the case. This is for instance not the case for rupture frequencies in nuclear piping. In the past, crude estimates about the probability of a pipe break in nuclear plants have been employed in PSA studies. Mostly the data from WASH-1400 [13] or variations of this basic study have been used. In recent years development of so called Probabilistic Fracture Mechanics (PFM) has shown that alternatives to the data of WASH-1400 may be obtained.

The practical experience indicates that IGSCC is the most important process for pipe failures in Boiler Water Reactors in Sweden. Very few actual failures have actually occurred, however, and this state of affairs precludes any estimation of the failure probability based on observed data, other than perhaps small leak probabilities. To estimate the failure probability, analytical methods have to be used instead. The perhaps best known

analytical tool for estimation of IGSCC failure probabilities is the PRAISE code described by Harris *et al* [6]. This code is however rather complicated and yet has several simplifications that makes it less suitable for the kind of stress corrosion problems that is experienced in Sweden, see section 9.2. A perhaps more robust procedure was developed by Bergman *et al* [12]. In Ref. [12] a procedure for evaluating the rupture probability due to IGSCC was formulated. This is extended also to leak probabilities in this study.

One goal of the present study has been to develop a procedure with accompanying computer software that can be used to estimate the failure probability for a specific pipe section with prescribed local loading. The failure probability is strongly dependent on the actual loading conditions which makes it necessary to treat pipe systems on joint by joint basis. It is the intention of formulating the procedure and the software in such a way that operators of nuclear facilities can use it as an instrument in their continuing safety assessments. It therefore important to make the procedure simple and robust as well as easily adaptable to changes of input assumptions such as probability distributions. In Appendix A, a detailed description of the theory, model assumptions and input data is given. Only a short discussion in relation to Fig. 5 is given here.

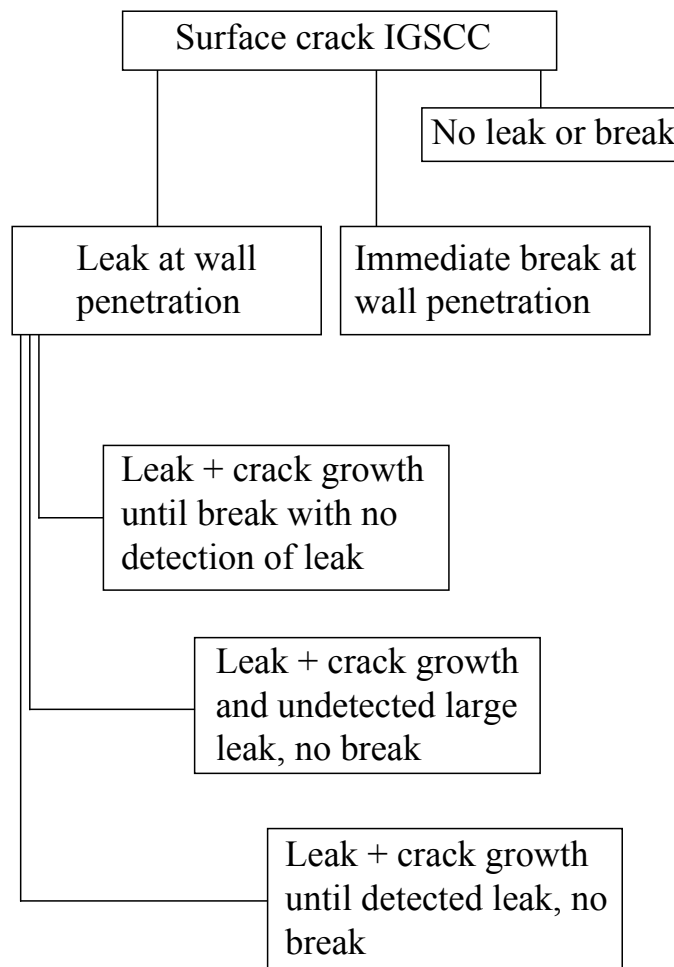


Fig. 5. Flow chart of different events for a stress corrosion crack in a pipe.

The starting point is the existence of a stress corrosion crack in the circumferential direction of a butt-welded pipe. Note in this study that we are not using a special model for how the crack is initiated by stress corrosion. Instead the probability of the existence of a stress corrosion crack is given by the crack initiation rate f_{i0} , which is taken from actual statistics of observed stress corrosion cracks in Swedish BWRs, see Appendix A. An initiated crack is in general assumed to have a depth of 1 mm but can also be varied in the analyses. The crack length is assumed to be random with an exponential distribution. Assuming that this crack starts to grow both in the depth- and length direction, the following mutually excluding events may occur within the total operating time of the station:

1. No leak or break.
2. Leak at wall penetration.
3. Immediate break at wall penetration.

Of interest here is the leak- and break probability. The non-Leak Before Break (non-LBB) situation in the third event is only one part of the contribution to the rupture probability. There is also the possibility of a leaking crack that remains undetected (both by inspection and leak detection) and that after growth in the circumferential direction of the pipe, eventually a break occurs, see Fig. 5. Both these contributions are considered by the developed software PIFRAP, Bergman [32] to give the rupture probability $p_f(\text{rupture})$. The leaking crack may also develop a large undetected leak within the total operating time. This is denoted the leak probability $p_l(\text{large leak})$ at the leak rate level m_1 . Of interest in the risk evaluation is a level of leak rate m_1 , above which a loss in a system function occurs (disabling leak). The probability that the crack is penetrating the wall to a leak (second event above) is denoted $p_l(\text{small leak})$. The leak rate at the instant of wall penetration is often too small to be detected, if one considers the complex crack shapes that gives a much smaller crack opening along the outer part of the pipe compared to the inside, see Brickstad and Sattari-Far [33]. The PIFRAP code gives all these probabilities $p_l(\text{small leak})$, $p_l(\text{large leak})$ and $p_f(\text{rupture})$, measured per weld, per year, in a single computer run. From Fig. 5 it is noted that $p_l(\text{small leak})$ also contains contributions to $p_l(\text{large leak})$ and $p_f(\text{rupture})$. However, this is not a problem since both $p_l(\text{large leak})$ and $p_f(\text{rupture})$ are generally much smaller than the small leak probability. Note also that detected cracks, either by inspections or by leak rate detection, do not contribute to the failure probability. If a crack is detected, it is assumed that either an effective repair is made or that the crack is kept under close surveillance in order to avoid a leak until the next inspection. This is standard procedure if stress corrosion cracks are detected during operation in a Swedish Nuclear Power Plant.

5 ESTIMATION OF CONSEQUENCES

In nuclear applications a methodology to systematically analyse and quantify sequences that may lead to severe consequences are used. These are called PRA (Probabilistic Risk Assessment) or PSA (Probabilistic Safety Assessment). PSA can be made at different levels according to the type of damage produced. Level 1 is dealing with the risk for core damage. Level 2 is going a step further by estimating the frequency of radioactive release above a certain level to the environment. The frequency of consequences (such as human life casualties) due to radioactive releases is studied in PSA level 3. For the O1 plant, the PSA level 1 is used in this study. PSA analyses are also classified due to the type of initiators. The initiators can be internal events like transients, pipe breaks or Common Cause Initiators CCI. CCI are failures that cause a transient and at the same time are degrading a safety

system. Also external events like internal fires, flooding and seismic events are analysed in the PSA studies.

PSA in its standard form is dealing with structures consisting of discrete components or functions and the sequences how a combination of events, involving e.g. malfunctioning components, may lead to a core damage. The PSA model is built by using event and fault trees. The component and function failure probabilities are mostly based on direct observations, for example the frequency of a valve not closing. When all the initiators considered are analysed, the PSA analysis will give you lists (minimal cut sets) of component or function failures that will lead to a core damage (level 1), and also the probability of core damage for every initiating event.

Here we are especially concerned with pipe breaks as an initiating event. Pipe breaks of different sizes are postulated directly in the PSA analyses for O1. These are classified according to the size and location of the break and the different feed water systems capacities to make up for the loss of coolant. The following approximate limits of leak rates apply for these pipe breaks:

1. Large LOCA, leak rates > 2000 kg/s. Core cooling by ECCS.
2. Medium LOCA, 30 kg/s $<$ leak rate < 2000 kg/s. Core cooling by ECCS and forced blowdown of relief valves.
3. Small LOCA, Leak rate < 30 kg/s. Core cooling can be achieved by the normal feedwater systems.

The postulated breaks in O1 involve over 3500 components with a diameter exceeding 50 mm inside the containment. For system 354, pipe diameters exceeding 32 mm are included. Depending on where the breaks are postulated, different probabilities of core damage can be obtained. For the O1 plant, 6 large LOCAs above the core water level, 10 large LOCAs below the core water level, 4 medium LOCAs and 8 small LOCAs have been analysed in the PSA. They are classified with respect to similar consequences for core damage. For the initiating events, i.e. the LOCA frequencies, the WASH-1400 study [13] has been used in the PSA for O1. The WASH-1400 study is not very detailed for specific degradation mechanisms and it can not give reliable predictions of the different pipe breaks that are analysed in this study. Therefore, only the consequence part of the PSA study for O1 is used here. These are called System Barriers SB or Conditional Core Damage Probability CCDP and are defined as the probability of core damage given that a pipe break of a certain size has occurred. The pipe break probabilities are estimated by probabilistic fracture mechanics as described in section 4 and Appendix A.

The core damage for O1 may occur basically due to three reasons, inability to shutdown the reactor (CD1), inability to cool the reactor core (CD2) and inability to remove the residual heat (CD3). It turns out that the most severe consequences are dominated by CD2 for pipe breaks. The system barriers due to CD2, Wretås [25], have been determined for the O1 plant due to postulated pipe breaks and are given in Table 2. The following comments are given with respect to Table 2:

1. In the pipe systems 313, 315 and 326, there are only components inside the containment (PS). In system 321, there are components (with degradation mechanisms) both inside and outside PS. In systems 331 and 354 most components are located outside PS. Since the PSA study for O1 are mainly concerned with pipe breaks inside PS, special considerations have been given to breaks outside PS. Particularly for system 321 a rupture can have a more severe consequence ($SB = 1.0E-5$) compared to other pipe systems located outside the containment (system 331 and 354). The reason for this is

that system 321 is connected to the reactor pressure vessel below water level. Besides the fact that the containment barrier is absent for a rupture outside the containment, the loss of cooling water at a rupture event will not be transferred back to the wetwell. Also, the leak rate detection limit is higher outside the containment. This makes the rupture probability higher since it is more difficult to detect leakages. For system 331, all components with a degradation mechanism are located far from the reactor pressure vessel with many valves in between. Therefore, the system barrier for a rupture in system 331 is set equal to $4.67E-7$. This is the barrier for a normal plant shutdown with initially all operating systems available. The same barrier is assumed for a rupture in system 354. Here the internal control rods will limit the leak area that can drain the reactor pressure vessel to a hole with a diameter of 20 mm.

Pipe System	Large LOCA (rupture)		Medium LOCA (large disabling leak)		Small LOCA (small leak)	
	With operator action	No operator action	With operator action	No operator action	With operator action	No operator action
313	3.34E-3	4.30E-2	3.67E-3	7.65E-3	4.67E-7	7.40E-7
315	3.34E-3	4.30E-2	3.67E-3	7.65E-3	4.67E-7	7.40E-7
326, bottom	3.34E-3	4.30E-2	3.67E-3	7.65E-3	4.67E-7	7.40E-7
326, top	2.14E-5	3.45E-5	2.14E-5	3.45E-5	4.67E-7	7.40E-7
321, inside PS	2.70E-3	6.65E-3	3.39E-3	7.36E-3	4.67E-7	7.40E-7
321, outside PS	1.0E-5	-	1.0E-5	-	4.67E-7	7.40E-7
331	4.67E-7	7.40E-7	4.67E-7	7.40E-7	4.67E-7	7.40E-7
354	4.67E-7	7.40E-7	4.67E-7	7.40E-7	4.67E-7	7.40E-7

Table 2. System barriers for pipe breaks for inability to cool the reactor core (CD2) in the considered pipe systems in O1.

2. In system 326, a more severe system barrier is set for a break below water level compared to a break above water level covering the core. For the pipe systems 313 and 315, the piping components with degradation mechanisms are located below water level only.
3. The system barrier $4.67E-7$ for a small LOCA in Table 2, actually corresponds to a much smaller leak rate than the limit 30 kg/s. This is used to quantify the consequence when the growing surface crack is just penetrating the pipe wall thickness. Initially the leak rate at wall penetration will be very small, usually below 1 kg/s. The plant response to a small leak rate of this size is a plant shutdown, $SB = 4.67E-7$. This value is assumed for all small leaks of this size in all the considered pipe systems in the O1 plant and is used as a lower limit for the system barrier.
4. The effects of manual operating actions are shown in Table 2. For CD2 the effect is rather small due to a quite high failure frequency for operating actions in this category. For CD3, insufficient residual heat removal, the effect is larger due to the longer time

periods involved. This makes an operating action failure less probable. For the risk evaluation in this study, the system barriers in Table 2 with credit for manual operating actions have been used.

5. There are no damage mechanisms in standby systems such as the ECCS or the auxiliary feedwater system. Thus no special considerations have been made in standby systems in O1.
6. Indirect effects such as pipe whips have been accounted for inside the containment. A guillotine break of a pipe system is then assumed to cause a break also on a nearby system which has a pipe diameter less than or equal to the first pipe system.

6 EVALUATION OF RISK FOR CORE DAMAGE

In this study, the following equation is used for evaluating the Risk for Core Damage, i.e. the Core Damage Frequency CDF:

$$\text{CDF} = P(\text{small leak}) \cdot C(\text{small leak}) + P(\text{large leak}) \cdot C(\text{large leak}) + P(\text{rupture}) \cdot C(\text{rupture}) \quad (1)$$

where P is the failure probability (per year) and C is the consequence resulting from the corresponding piping failure. Note that C is actually the probability for core damage given that a pipe failure has occurred. The core damage occurs mainly due to insufficient core cooling. Eqn. (1) is used by WOG [4] in their application of RBI. A question now arises which terms in Eqn. (1) that should be included in the risk evaluation, considering that not all terms are mutually exclusive. This would not cause problems if one term is dominating over the others. It was found for O1 that the consequence of a large disabled leak was of a similar magnitude as the consequence of a rupture, see Table 2. Moreover, the limiting leak rate for a disabled leak at the plant is set to 30 kg/s, above which a decrease of pressure is needed to inject water through the ECCS. With a conservative estimate of the leak rate just before rupture (see Appendix A), the probability for a large disabled leak is approximately the same as the rupture probability. In order not to double count risk contributions for rupture and a large disabled leak, only the first and third term in Eqn. (1) were used for the risk evaluations in this study. This can be slightly unconservative since the consequence of a large disabled leak is in some cases larger than consequence of a rupture as shown in Table 2. However, the difference in these consequences is very small and for the O1 plant the error of using this procedure is insignificant. Note that small leaks (at wall penetration) and rupture can occur as mutually excluding events. Normally the probability of a small leak is much larger than the rupture probability.

6.1 Basis for Crediting Leak Detection in the Evaluation of Risk

In NUREG-1661 [14], it is recommended that neither inspections nor leak detection should be credited when evaluating risks for ISI-selection. That no credit for inspections should be taken is quite natural since it is the purpose of the risk categorization to select locations for ISI. Thus it would be wrong to credit inspections before the selection process is done. The question of accounting for leak detection is more difficult. In NUREG-1661, the main argument for not crediting leak detection is the assumption that this would mask important piping segments that warrant inspection, to identify the degradation before failure. Thus leak detection systems are only recognized as an additional mechanism that ensure defense-in-depth. The observation that most probabilistic fracture mechanics codes (besides PIFRAP) assumes immediate leak detection at a defined leak rate and subsequent shutdown and

repair, is probably also a reason for this conservative standpoint in NUREG-1661. However, there are a number of reasons for crediting leak detection in risk evaluations, at least in the light of the findings in this pilot study. The following reasons can be formulated:

1. The major contribution to the risk for core damage for the high risk locations is the rupture term and not the term for small leak. For rupture, the leak detection capabilities play an important role.
2. If leak detection is neglected, operators have to ignore large leak rates over very long periods of time before rupture occurs. This is not realistic. Leak detection systems are active in the plant regardless of whether the component are selected for inspection or not.
3. If leak detection is ignored, and if no inspections are assumed, the probability of a rupture will approach the leak probability for these kind of stress corrosion problems. If, from a starting initial surface crack, rupture is predicted to occur within the expected operating time of the plant, then there is nothing that will stop the crack from leading to a leak or a rupture. Remember that the major contribution to rupture in this study is the stress corrosion crack that leads to wall penetration followed by further subcritical crack growth until rupture occurs without detecting the leak. The non-LBB situation (immediate break at wall penetration) is a possible but rare event, which is supported by failure statistics. Thus if leak detection is ignored, there will be less possibility to perform a realistic risk categorization and the selection procedure will be driven more by consequences than the actual risk for core damage, see also section 6.2.1.
4. The developed software PIFRAP does not assume an immediate detection of the leak but is accounting for uncertainties in the leak rate evaluations. Even if the mean value of the calculated leak rate is exceeding the leak detection level, PIFRAP assumes that there is a certain probability that the actual leak rate is smaller than the leak detection level and thus that the crack remains undetected. Furthermore, PIFRAP is accounting for complex crack shapes that in general gives a much smaller crack opening along the outer part of the pipe compared to the inside, see Appendix A. Finally, a conservative procedure is used to estimate the leak rate before rupture. This is explained in more detail in Appendix A.

The above arguments are the basis for crediting leak detection in the evaluation of risk for core damage in this study. This is also supported by recent studies by Simonen *et al* [15].

6.2 Core Damage Frequency with no Credit for Inspection

By evaluating the risk in terms of Eqn. (1) for every component, risk diagrams can be developed. Fig. 6 shows the CDF (measured per year) for all the 1192 evaluated components (see Table 1) that are included in the pilot study.

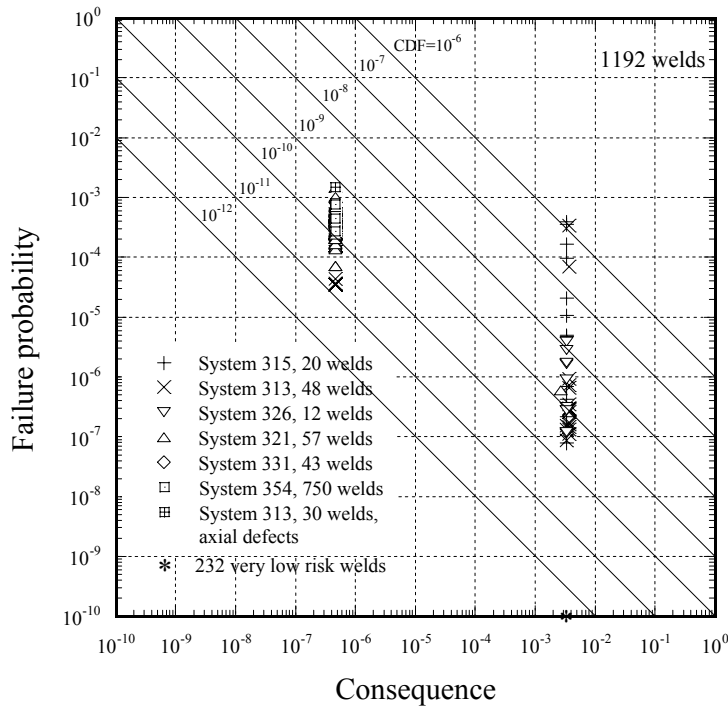


Fig. 6. Core damage frequency per weld, no inspections.

The following general comments should be noted, valid for all the individual risk diagrams in this report:

- The failure probability represents either the probability of a small leak or the probability for a rupture, measured per reactor-year as a mean value for the remaining operating time of the plant.
- With the term "Consequence" is meant the conditional core damage frequency, i.e. the probability of core damage, given that a leak or rupture has occurred. This quantity is dimensionless.
- The diagonals in the risk diagram connect points with a constant risk for core damage.
- Every point in the risk diagram represents the risk for one particular weld. In the general case, two terms (small leak and rupture) are contributing to the risk. For the sake of clarity, only one point (C_{plot} , P_{plot}) per weld is marked in the risk diagram. The consequence C_{plot} is the consequence C_i in Eqn. (1) whose term $P_i C_i$ is dominating the contribution to the CDF. The corresponding failure probability P_{plot} is then obtained by dividing the actual CDF for the weld by C_{plot} . In this way the actual risk for core damage is always correctly given in the risk diagram, but in cases when the risk terms for small leak and rupture are of the same order, the plotted failure probability P_{plot} is adjusted upwards by at most a factor of 2. The advantage is that each point represents only one weld and it is immediately seen if the risk is dominated by leak or rupture.
- The points in the diagram are clustered basically at two consequences, either at small leak or at the rupture consequence. The consequence of a rupture (large LOCA) is almost the same (of the order $3.3E-3$) for a wide range of pipes inside the containment. The exception is system 331 (cleaning system) and system 354 (hydraulic control rod system), where most of the welds are located outside the containment, far from the reactor pressure vessel. Here, the rupture consequence is much lower and is set equal

to the consequence for a small leak, corresponding to a plant shutdown (of the order $4.7E-7$).

The difference in consequences will cause all the high risk locations to be dominated by the risk due to a pipe rupture (or possibly a large disabled leak).

- f) Leak rate detection are in general accounted for in the risk evaluations with a probabilistic model for leak rates as described in Appendix A. The leak rate detection limit is set to 0.3 kg/s inside the containment and 2 kg/s outside the containment. Leak rate detection will not influence the probability of a small leak but can have a large influence on the rupture probability.
- g) In 232 out of 1192 welds, the resulting CDF was very small. This is in most cases due to that no damage mechanism is present, but they are still included in Control Group B. These very low risk welds are indicated by a star in Fig. 6 and special comments for these locations are given in the following sections for each pipe system.

In the following, comments are given for the CDF for each pipe system in Fig. 6.

6.2.1 System 315, Auxiliary Condensor

The dimensions of system 315 are a pipe diameter between 170 and 250 mm and a pipe thickness from 14.2 to 19.5 mm. The pipes are all made of stainless steel with stainless steel welds using Gas Tungsten Arc Weld GTAW, Shielded Metal Arc Weld SMAW or Submerged Arc Weld SAW. This pipe system has only 20 welds that have a potential damage mechanism IGSCC, all located inside the containment. However, it is the one that contributes most to the total CDF from all pipe systems. The reason for this is that for 12 welds the mechanisms IGSCC and high cycle vibrations occur at the same time. The vibration levels have been determined by measurements and subsequent stress analyses for the pipe system. What happens is that IGSCC is the crack driving mechanism for surface cracks. The high cycle vibration amplitudes are sufficiently small (of the order 1-2 MPa) that the range of stress intensity factors ΔK will not exceed the vibration threshold (assumed here to be $4 \text{ MPa}\sqrt{\text{m}}$) as long as the crack is a surface crack. When wall penetration occurs, the crack geometry changes and will in general be of a complex nature with the outer crack length much smaller than the crack length along the inside of the pipe. This causes initially a small leak rate that can be difficult to detect. The undetected through wall crack then continues to grow by IGSCC in the circumferential direction. Relatively soon after wall penetration the vibration threshold will be exceeded along some part of the crack front. PIFRAP then assumes an immediate rupture. (This is somewhat conservative in the sense that the rupture will not take place instantly. The time to rupture will be of the order hours to several days. However, account has been taken to the fact that it is only a small part of the vibration spectrum that is vibrating with a high frequency (10-20 Hz)). If the vibration amplitude is sufficiently high, the crack opening area and thus the leak rate, when the vibration threshold is exceeded, is quite small. This makes the benefit of leak rate detection small. Along with the reduced time to rupture this causes a relatively high probability for a rupture which combined with the rupture consequence will give high risk contributions. Fig. 7 shows a risk diagram for the welds in system 315 with damage mechanism IGSCC. All the high risk locations with a CDF above $1E-8$, are due to the influence of IGSCC and vibration fatigue.

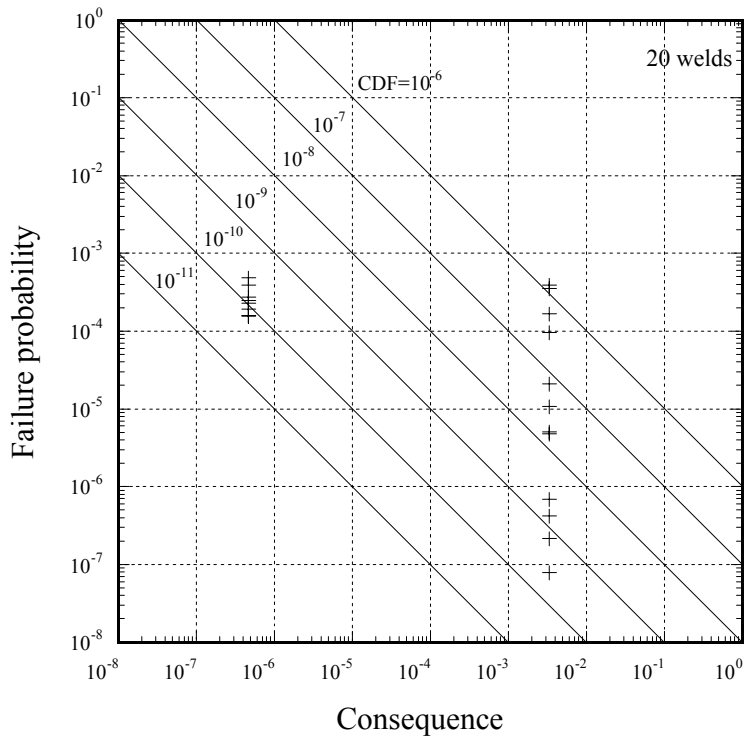


Fig. 7. Core damage frequency per weld for system 315, no inspections.

Note that at the current levels of vibration amplitudes (of the order 1-2 MPa), all surface cracks (even long and deep) are harmless with respect to vibration fatigue. For this reason, the existence of vibrations in system 315 has not attracted any special interest in the control group division. It is not until the cracks have penetrated the pipe wall, that a more severe situation occurs. For these particular pipe locations, the vibration amplitudes have to be below about 0.7 MPa in order for the welds not to be more risk significant than those with no vibrations. It should be observed that the suppression of the leak rate at the vibration limiting critical crack size, is promoted by large local bending weld residual stresses (such as those occurring for thin-walled pipes) and small operating loads (dead weight and thermal expansion), see the sensitivity analysis in appendix B. All these factors tend to limit the COD and the leak rate at the critical crack size, which tend to increase the rupture probability due to the larger probability of non-detection of leak rates before rupture.

Note also that it is the combination of IGSCC and high cycle vibrations that can cause a high risk situation. High cycle vibrations alone have in general too small amplitudes to initiate cracks. Thus one would never have noticed that these particular locations would represent a high risk if only deterministic analyses had been performed. Deterministic analyses are in general only performed for surface crack geometries.

A final important note on this aspect is that it is because leak detection is actually credited in the analyses, that these particular locations are having a high risk for core damage. This can be demonstrated in Fig. 8, where the CDF for system 315 is replotted, but with all leak rate detection suppressed.

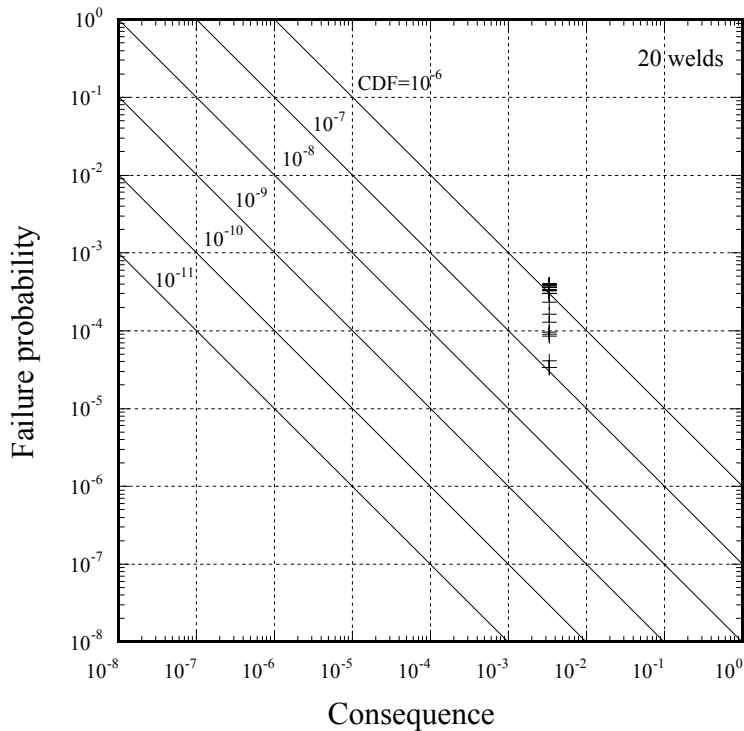


Fig. 8. Core damage frequency per weld for system 315, no inspections, no leak rate detection.

In this case the CDF is dominated by rupture for all welds. Due to that no leak detection are credited, the rupture probabilities for welds with and without vibrations will not differ by more than a factor of 10. This makes it more difficult to perform a discriminating risk ranking. If leak detection is accounted for, the locations with low or no vibrations will represent lower risks due to that the probability of not detecting the leak rate before rupture occurs is small for these locations. Normally, the critical through wall crack length, at which rupture is predicted, is exceeding one third of the pipe circumference if no vibrations are present. Thus in this case, one can conclude that by not taking account for leak rate detection, important piping segments that warrant inspection would be masked.

In system 315, there are also 19 welds in control group B that have no known damage mechanism, see Table 1. For these welds the software PIFRAP gives zero leak- and rupture probability. This is a result of that PIFRAP only considers growing cracks with deterministic inputs for starting crack depth and material data. However, there may still exist non-growing pre-service defects from the welding process that will have a non-zero failure probability, albeit very small. For this purpose the software PROPSE [16] is used that is applying a FORM method to obtain the failure probability for non-growing cracks with probabilistic inputs for yield stress, ultimate tensile stress, fracture toughness and defect size. In general normal distributions are assumed for the material data with a standard deviation of 10% of the mean values. The defect size is assumed to be lognormally distributed with a mean value of 25% of the wall thickness and a standard deviation of 20% of the mean value, i.e. 5% of the wall thickness. For the stress conditions (assumed to be deterministic in PROPSE) for these 19 welds in system 315, the resulting failure

probabilities were found to be very small. A cut-off of the failure probability is here set to 1E-11 per year. This will cause the core damage frequency per weld to be less than 1E-12 and this is indicated by a star in the risk diagram in Fig. 6. This illustrates the general observation in this study that there is a distinct difference, in terms of risk for core damage, between those components which have a damage mechanism and those which have not.

6.2.2 System 313, Main Circulation System

The dimensions of system 313 are a pipe diameter between 112 and 670 mm and a pipe thickness from 8 to 35 mm. The pipes are made of stainless steel or carbon steel with a stainless steel cladding. The welds are made of stainless steel with GTAW, SMAW or SAW and in some cases using the Inconel electrode Alloy 182 (for 30 welds of a 670 x 35 mm cladded carbon steel piping). The pipe system has 78 welds that have a potential damage mechanism IGSCC, all located inside the containment. Fig. 9 shows the risk diagram for these welds.

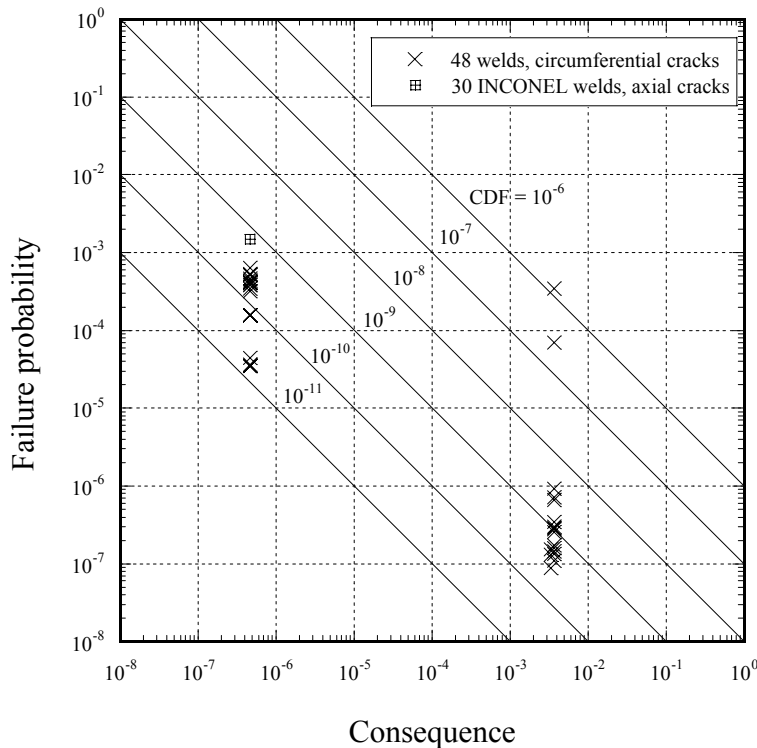


Fig. 9. Core damage frequency per weld for system 313, no inspections.

It is observed that two welds have a significantly higher CDF. They are located in a small diameter (114 mm) by-pass piping in system 313. Similar to system 315, these two welds have the mechanisms IGSCC and high cycle vibrations occurring at the same time. Apart from these two welds, high risk values are obtained for thin-walled pipes that have large operating stresses combined with in some cases a stainless steel weld SAW, which has less ductile material properties. As observed from Fig. 9, all the high risk locations are dominated by the risk due to pipe ruptures and not due to small leaks.

Not shown in Fig. 9 is 30 welds with a crack in the circumferential direction for which PIFRAP predicts zero leak- and rupture probability even though IGSCC is a potential

damage mechanism. These welds are welded with Alloy 182 in carbon steel piping clad with a stainless steel layer. The outer diameter is 670 mm and the pipe thickness is 35 mm. The reason why PIFRAP is predicting zero failure probabilities are mostly due to low operating stresses. This includes the weld residual stresses. Delfin *et al* [17] have made very detailed weld simulations of these welds which show that at about 20% of the wall thickness, a distinct region of compressive axial residual stresses occurs. This acts as an effective way of arresting a growing circumferential stress corrosion crack. Even setting the residual stresses to zero and using conservative crack growth data and using a starting crack depth of 5 mm, PIFRAP will never predict that leak (or rupture) will occur within the operating time (40 years) of the plant. Small operating stresses and the fact that the pipe wall thickness is quite large which a stress corrosion crack has to penetrate, are the explanation for this prediction. Also, there are no history of leaks in these large diameter piping. For these 30 welds with a crack in the circumferential direction, the software PROPSE [16] has been used to evaluate the failure probability for a pre-service defect or an arrested stress corrosion crack. The same kind of input assumption were made as for system 315. The resulting failure probabilities were found to be very small. A cut-off of the failure probability was again set to 1E-11 per year. This will cause the core damage frequency per weld to be less than 1E-12 and this is indicated by a star in the risk diagram in Fig. 6. This is also valid for the 149 welds in control group B (see Table 1) that have no known damage mechanism. Sample calculations using PROPSE for the welds in this group that have the highest operating stresses, verify that these welds represent a very low core damage frequency.

In Fig. 9 is also included risk estimations for axial cracks in the girth welds. Axially oriented stress corrosion cracks in seamless pipes are unusual since the stainless steel weld material itself is not susceptible to IGSCC. However, certain Nickel-based alloys are susceptible to stress corrosion cracking. This is the case for the weld electrode Alloy 182 as mentioned above. There has been a few historical cases of axial IGSCC in these kind of girth welds, e.g. in the Nuclear Power Station Chinsan 2 in USA. PIFRAP can not in general account for axial cracks. Instead the following procedure has been used to estimate the failure probability. First the crack existence frequency is determined by evaluating the number of detected axial stress corrosion defects in the weld material Alloy 182 in all the Swedish BWRs. During the past years 11 such defects have been detected up to the year 1998, ref. [11]. This leads to an average occurrence rate of $11/26 = 0.423$ cases per year. Estimating the total number of welds made of Alloy 182 in the primary piping for all the 9 BWRs to be 287, then implies that the mean crack existence frequency for an axial stress corrosion crack to occur in an Alloy 182 girth weld is $f_{i0} = 0.423/287 = 1.47E-3$ per year, per weld. Considering the quite large weld residual stresses in the hoop direction [17], the leak probability is conservatively set to this value f_{i0} . It is a conservative assumption since it corresponds to the situation that every axially oriented stress corrosion crack will eventually lead to a leak. The leak rate from such cracks will be small and thus represent a small consequence. The probability of a rupture from an axial crack in the weld is set to a cut-off value of 1E-11 per year. This is motivated by the argument that an axial stress corrosion crack will be confined to the weld region or possibly some small region outside the girth weld. The base materials in the piping systems in O1 are in general not susceptible to stress corrosion cracking. Evaluations have shown that axially oriented through wall cracks with a length limited to the weld region will have large margins to an axial rupture. The risk for core damage from such cracks are dominated by the leak term and is shown in Fig. 6 and 9. The same CDF is attributed to every one of these 30 welds with axially oriented cracks.

6.2.3 System 326, Top Head Cooling System

The dimensions of system 326 are a pipe diameter between 168 and 244 mm and a pipe thickness from 12.5 to 17.5 mm. The pipes are made of stainless steel. The welds are also made of stainless steel with GTAW, SMAW or SAW. The pipe system has 12 welds that have a potential damage mechanism IGSCC, all located inside the containment. Fig. 10 shows the risk diagram for these welds.

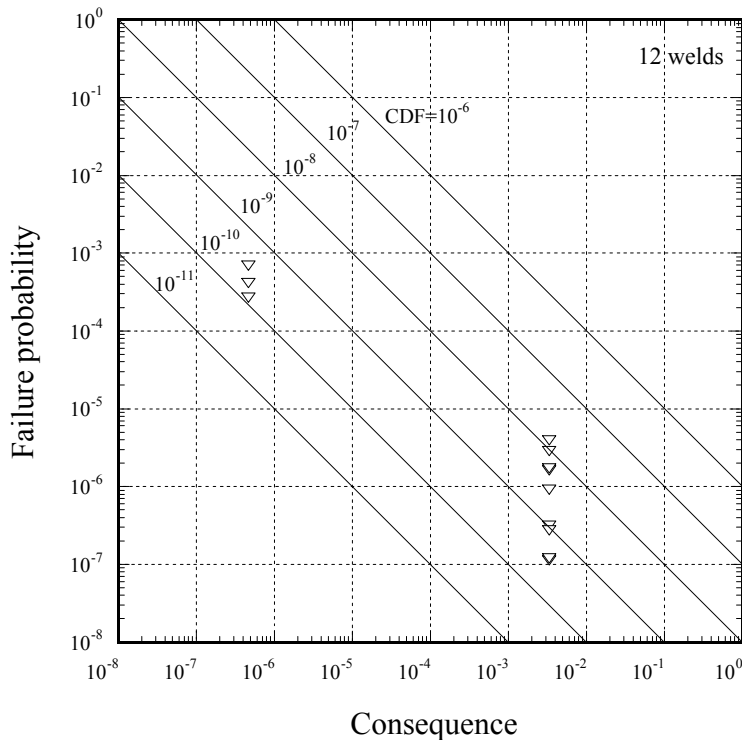


Fig. 10. Core damage frequency per weld for system 326, no inspections.

No significant vibrations are present in this system. Nevertheless, there are some high risk locations in Fig. 10 which can be explained by quite high operating loads, especially the thermal expansion stresses P_e and the Safety Relief Valve stresses P_{SRV} . For 9 out of 12 welds, the risk for core damage are dominated by a rupture event. Two out of the three welds in Fig. 10, for which the risk are dominated by a leak, are located above the core level where a rupture will have a less severe consequence.

In system 326, there are also 11 welds in control group B that have no known damage mechanism, see Table 1. Evaluations by aid of PROPSE for these welds for pre-service defects, verify that the failure probability can be estimated by a cut-off of $1E-11$ per year. The corresponding core damage frequency per weld is less than $1E-12$ which is indicated by a star in the risk diagram in Fig. 6.

6.2.4 System 321, Shutdown Cooling System

The dimensions of system 321 are a pipe diameter between 146 and 324 mm and a pipe thickness from 11 to 25 mm. The pipes are made of stainless steel. The welds are also made of stainless steel with GTAW, SMAW or SAW. The pipe system has 63 welds that have a

potential damage mechanism IGSCC. Of these, only 5 welds are located inside the containment and the rest outside the containment. Fig. 11 shows the risk diagram for these welds.

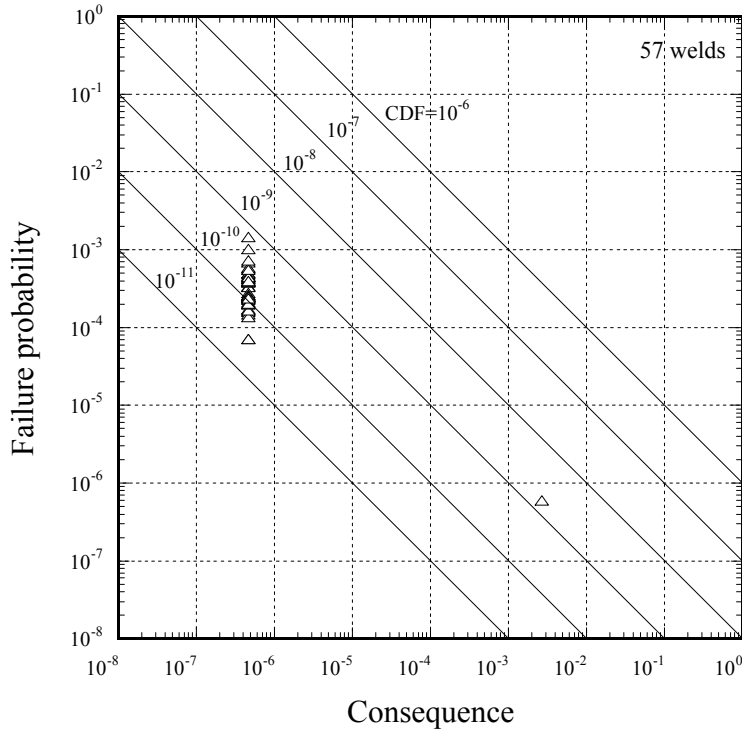


Fig. 11. Core damage frequency per weld for system 321, no inspections.

As shown in Fig. 11, for all welds but one, the risk for core damage is dominated by a leak event. This is explained by the fact that the majority of the welds are located outside the containment where a rupture will have a less severe consequence compared to ruptures inside the containment. The single weld for which the risk is dominated by a rupture event, is located inside the containment. Still, a rupture can have a larger consequence in system 321 compared to other pipe systems located outside the containment (system 331 and 354). The reason for this is that system 321 is connected to the reactor pressure vessel below water level. Besides the fact that the containment barrier is absent for a rupture outside the containment, the loss of cooling water at a rupture event will not be transferred back to the wetwell. Outside the containment, the leak rate detection limit is 2 kg/s. This makes the rupture probability higher since it is more difficult to detect leakages.

For 6 welds in system 321, PIFRAP predicts zero leak- and rupture probability even though IGSCC is a potential damage mechanism. These welds have a pipe wall thickness of about 25 mm and have very low operating loads. Some of these 6 welds are located in internal parts of valves, which are loaded essentially only by internal pressure. Calculations made by PROPSE for these 6 welds verify that the core damage frequency per weld is less than 1E-12 which is indicated by a star in the risk diagram in Fig. 6.

In system 321, there are also 17 welds in control group B that have no known damage mechanism, see Table 1. Evaluations by aid of PROPSE for these welds for pre-service defects, verify that the failure probability can be estimated by a cut-off of 1E-11 per year.

The corresponding core damage frequency per weld is less than $1\text{E-}12$ which also is indicated by a star in the risk diagram in Fig. 6.

6.2.5 System 331, Cleaning System

The dimensions of system 331 are a pipe diameter between 114 and 168 mm and a pipe thickness from 8.6 to 16.2 mm. The pipes are made of stainless steel. The welds are also made of stainless steel with GTAW, SMAW or SAW. The pipe system has 43 welds that have a potential damage mechanism IGSCC. All weld are located well outside the containment. Fig. 12 shows the risk diagram for these welds.

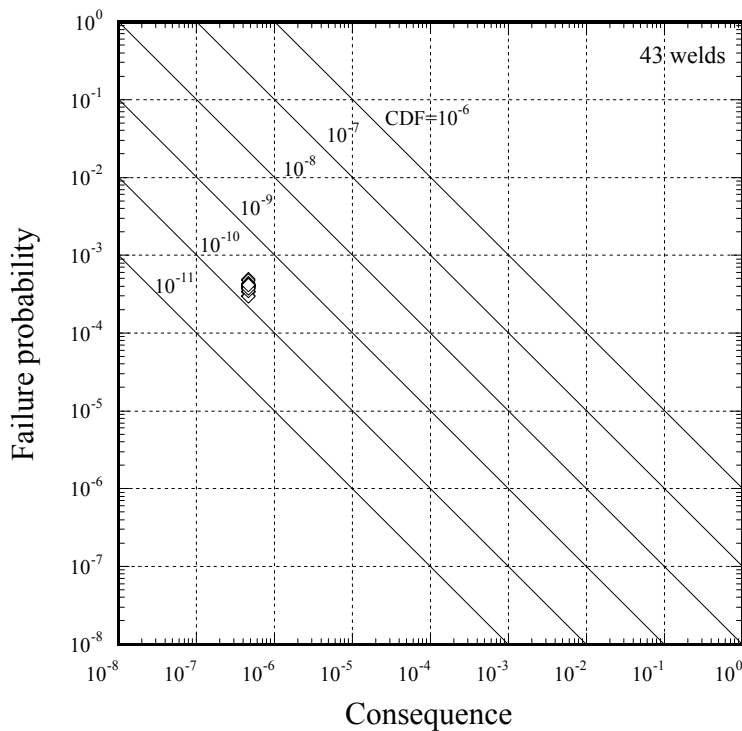


Fig. 12. Core damage frequency per weld for system 331, no inspections.

Many welds in system 331 have high thermal expansion stresses. Together with a high leak rate detection outside the containment (2 kg/s) will cause a relatively high rupture probability. Despite this, for all the welds in Fig. 12, the risk for core damage is dominated by a leak event. This is because all welds where a rupture will have a less severe consequence. Compared to system 321, the IGSCC-sensitive welds in system 331 are located further out from the reactor pressure vessel with more valves in between.

6.2.6 System 354, Hydraulic Control Rod System

System 354 differ from the other pipe systems in two aspects. Firstly, there are a large number of welds (750) that have a potential for IGSCC. Secondly, many welds are located in small diameter piping (diameters 60 or 76 mm). Some welds are also located at small pressure vessels with a diameter of 400 mm. The pipes are all made of stainless steel. The welds are also made of stainless steel with GTAW or SMAW. Most pipes are located

outside the containment (PS). The large amount of IGSCC-susceptible welds implies that it is necessary to evaluate the risk for core damage for this system even if the risk contribution from each individual weld is small. The following table defines the different types of welds which are studied for system 354:

Type	No of welds	Dimensions <i>D x h</i>	Welding technique	Carbon content	Inside or Outside PS
1	137	76.1 x 6.3 mm	SMAW	%C > 0.040	Outside
2	56	76.1 x 6.3 mm	SMAW	0.030 < %C < 0.040	Outside
3	56	76.1 x 6.3 mm	GTAW	%C > 0.040	Inside
4	56	76.1 x 6.3 mm	GTAW	%C > 0.040	Outside
5	109	60.3 x 5.5 mm	GTAW	%C > 0.040	Outside
6	103	60.3 x 5.5 mm	GTAW	%C = 0.039	Outside
7	37	76.1 x 6.3 mm	GTAW	0.030 < %C < 0.040	Outside
8	28	Welds to nozzle 60.3 x 5.5 mm	SMAW	%C > 0.040	Outside
9	28	Welds to nozzle 114.3 x 10 mm	SMAW	%C > 0.040	Outside
10	56	Pressure vessel 400 x 14 mm (a)	SMAW	%C = 0.040	Outside
11	28	Pressure vessel 400 x 14 mm (b)	SMAW	%C = 0.040	Outside
12	28	Fillet welds to nozzle 79.5 x 8 mm	SMAW	%C > 0.040	Outside
13	28	Fillet welds to nozzle 114.3 x 10 mm	SMAW	%C > 0.040	Outside

(a) Circumferential welds

(b) Longitudinal welds

Table 3. Specification of welds in System 354, hydraulic control rod system.

In system 354, there are 28 groups of pipe systems, each serving a group of control rods. The dimensions and configurations of these 28 groups are very similar. There exist stress evaluations for 20 welds in one of these groups. It is assumed here that the results for these 20 welds can be transferred to all 28 groups. Relatively large rupture probabilities (of the order 1E-4 per year) were obtained for the majority of the welds located outside the containment. The small pipe diameters will cause relatively small leak rates before rupture. This will cause little benefit of leak detection outside the containment where the leak rate detection limit is set to 2 kg/s. Also, the large weld residual stresses (local bending) for the thin walled pipes will cause relatively rapid crack growth once a stress corrosion crack has been initiated. Despite these factors that tend to increase the rupture probability, the risk for core damage is quite small and dominated by a leak event, as shown in Fig. 13.

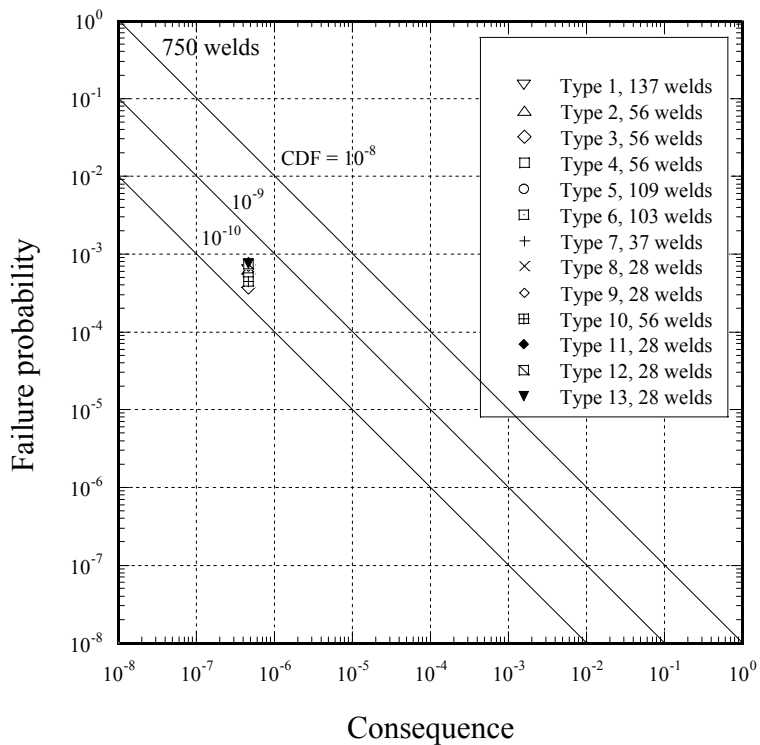


Fig. 13. Core damage frequency per weld for system 354, no inspections.

The reason for this is that the probability for core damage, given that a rupture has occurred, is small for system 354. The internal control rods will limit the leak area that can drain the reactor pressure vessel to a hole with a diameter of 20 mm. The rupture consequence is here set equal to the consequence for a small leak, corresponding to a plant shutdown (of the order $4.7E-7$). Thus the risk for core damage per weld will be small (of the order $3E-10$ per year) even if the risk integrated over the whole system is large.

6.2.7 Core Damage Frequency per system, no inspections

Integrating all risk contributions for the individual welds to each pipe system, the resulting risk diagram is shown in Fig. 14.

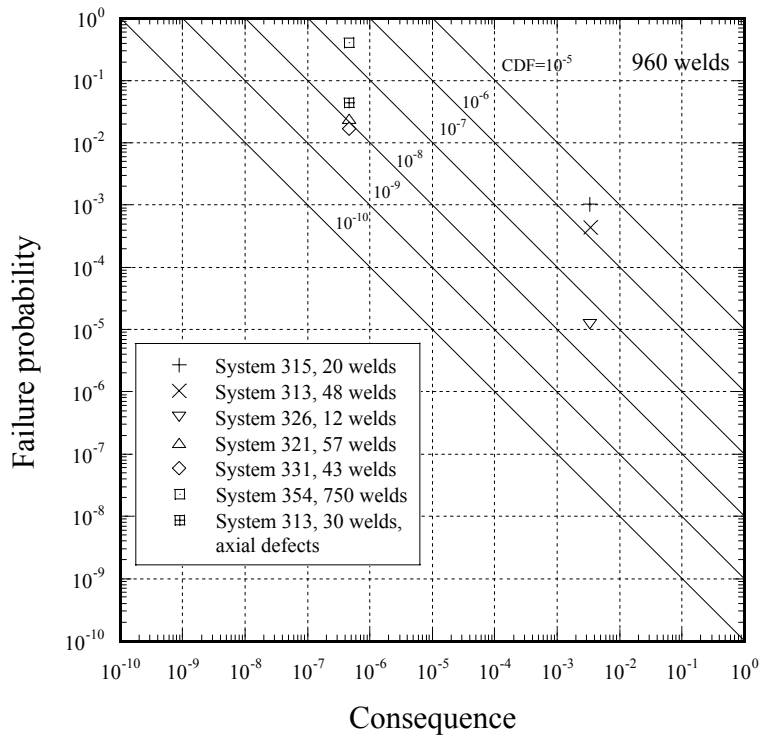


Fig. 14. Core damage frequency per system, no inspections.

From Fig. 14 it is observed that it is the pipe systems 315 and 313 that has the highest risks. This is due to the combined effect of IGSCC and high cycle vibration fatigue. The third most risk significant pipe system is 354, the hydraulic control rod system. The only reason for system 354 being risk significant is the large amount of IGSCC-susceptible welds in this pipe system. The core damage frequency per weld is quite small, as shown in Fig. 13.

6.2.8 Core Damage Frequency, all systems, no vibrations

If there would be no vibrations whatsoever, the resulting risk diagram for all individual welds in all systems is shown in Fig. 15.

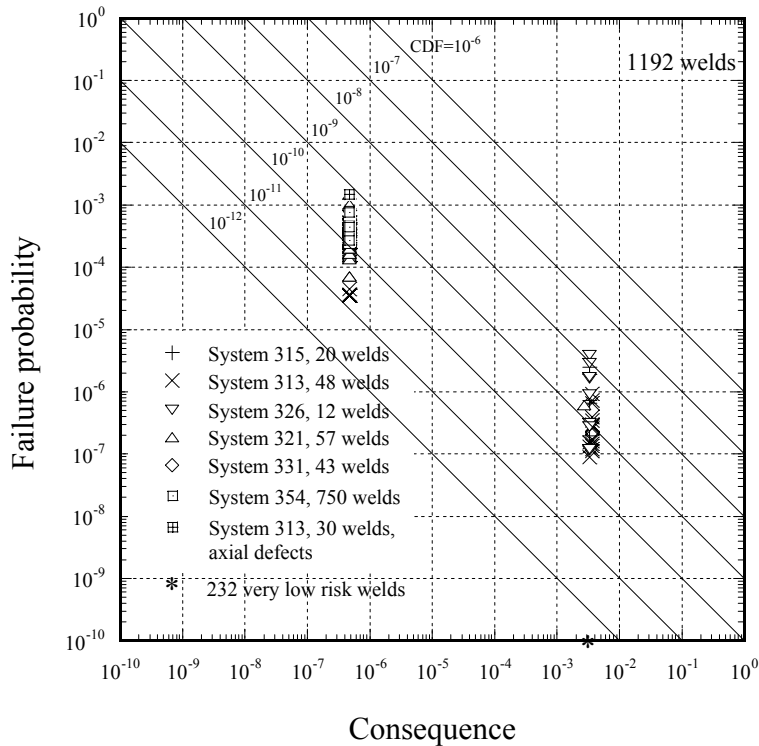


Fig. 15. Core damage frequency per weld, no inspections and no vibrations.

By comparing Fig. 15 with Fig. 6, it is clearly seen that the high risk locations are due to the combined effect of IGSCC and vibrations. Instead of a span of five decades, the risk span is decreased to three decades in Fig. 15.

6.3 Core Damage Frequency with Credit for Inspection

The risk ranking of components will be performed with no account for inspections. However, to compare different ISI selections in terms of risk, one has to quantify the effect of inspections.

6.3.1 Inspection Assumptions

To quantify the effect of inspection on the core damage frequency, a model for inspection has to be introduced. In this study, a model based on the probability of detection of stress corrosion cracks is used, Bergman et al [12]. This relation was given by Simonen and Woo [18] for the case of inspection of stainless steel pipes with access from the same side of the weld as where the potential crack is located. The details of this model is given in Appendix A. The terms "poor", "good" and "advanced" are referring to the inspection efficiency for probability of detection POD used in Ref. [18]. In Sweden one has recently introduced requirements of qualification for all inspections on the Nuclear Power Plants. This is an improvement compared to previous inspections performed with non-qualified systems. A qualified inspection is assumed to correspond to a POD for a "good" team. This inspection performance is similar to the best technique available used for the detection of stress corrosion cracks in stainless steel blocks in the PISC III project, cf Simula and Pulkkinen [19]. The following assumptions are made regarding inspections at Oskarshamn-1:

1. The first qualified inspection is performed at year 28 (equal to year 2000) and all risk evaluations with ISI are analyzed at this time.
2. Future qualified inspections are performed with intervals from year 28 as determined from deterministic damage tolerance analyses with intervals Δt varying from 3 to 10 years.
3. Previous non-qualified inspections are assumed to have been performed at an interval of 10 years since start of operation (1972).
4. Qualified inspections are assumed to correspond to a POD for a "good" team whereas non-qualified inspections are assumed to correspond to a POD for a "poor" team.
5. If an inspection is performed for a through-wall crack, $POD = 1.0$ is assumed.
6. To be conservative, all inspections are assumed to be completely dependent, i.e. credit is only taken for the last inspection.

The first assumption above (all inspected components are subjected to a qualified inspection at year 28) may seem to be a little too optimistic when the effects of the current inspection selection are investigated. However, this is used mainly to study the change of risk compared with a suggested new ISI-selection and for which the same kind of assumption is made.

If two inspections are independent, the effect of performing two successive inspections would be too much larger than if the inspection was made only once, (p_{nd}^2 vs p_{nd}). However, this can reflect an overestimation of the combined effect of the two inspections. If for some reason (e.g. due to a discontinuity in geometry), the crack was undetected during the first inspection, it is likely to be missed also during the next inspection. Therefore, as a conservative assumption, all inspections are assumed to be dependent for which in a sequence of inspections, only the effects of the last inspection is considered. On the other hand, it may be argued that if the crack is missed at the first inspection due to a tight crack or a discontinuity in geometry at the weld location, then subsequent inspections will not do you any good anyhow. The problem is that it is almost impossible to have precise information of this kind (local geometry effects) for every location in order to correctly treat the benefit of a series of inspections. At this time, it can be regarded just as a conservative assumption to assume all inspections to be completely dependent.

Fig. 16 shows the failure probability per year for a typical weld in system 315 (without vibrations) as function of current time and using the listed inspection assumptions. Note that it is the failure frequency that is shown and not the cumulative probability. "Poor team" inspections are assumed to be performed at the years 0, 10 and 20 and "good team" inspections are starting at year 28 after which different inspection intervals are assumed, 1 year, 3 years or 10 years. It is clearly seen with these assumptions, that the inspection interval will have a large effect on the failure probabilities. The effect is more pronounced for the rupture probability compared to the leak probability. This means that to a certain degree, the influence on the risk for core damage by a short inspection interval will depend on whether the risk is dominated by a leak or a rupture event.

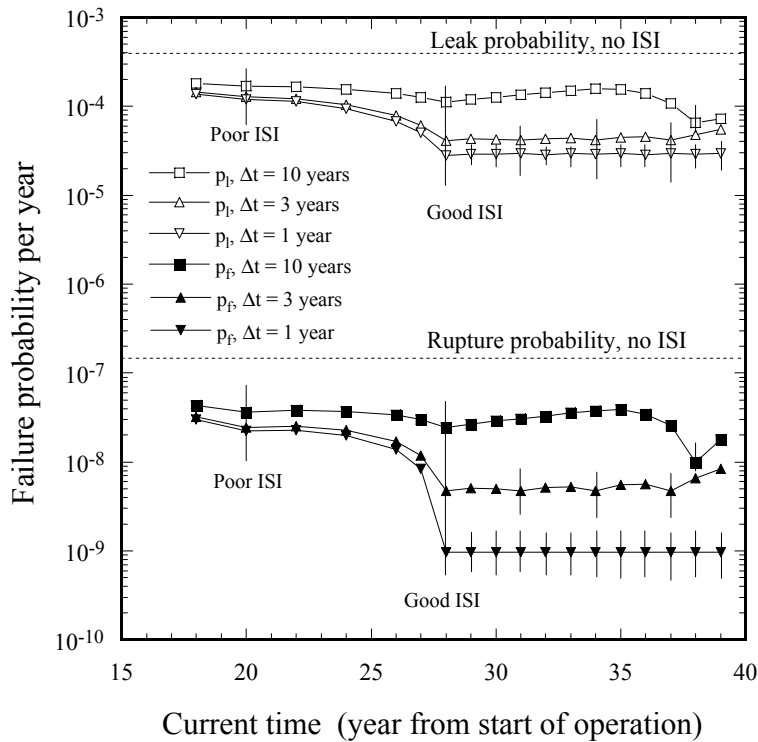


Fig. 16. Leak- and rupture probability per year as function of time. Effect of inspection interval. Stainless steel weld in system 315, pipe diameter 219 mm and wall thickness 14 mm.

Note also that the failure probability starts to decrease even before the actual inspection is performed. This may seem odd but it is a result of the model that is evaluating the failure probability per reactor-year as a mean value for the remaining operating time of the plant. It is possible that there exist stress corrosion cracks in the pipe today that earlier (non-qualified) inspections have not been able to detect. This means that if I know that I am going to perform an efficient inspection tomorrow, which will detect possible cracks with a high probability, the failure probability will also decrease today, compared to if I am not doing the efficient inspection until after two years from today. In this way the effect of future inspections can be better investigated. It is only a way to evaluate the result that, for the damage mechanism IGSCC, in this case is considered to be sensible. Note also that the failure probability per year, when no inspections at all are assumed, is almost independent of the current time. This is a result from the assumption of a constant distribution function for initiation time, i.e. the probability of a stress corrosion crack to initiate is constant in time. From Fig. 16, it may be concluded that if no qualified inspection has been done before, it is important to perform a qualified inspection as soon as possible in order to be able to detect earlier initiated stress corrosion cracks in the pipe.

The effect of different assumptions of the effectiveness of the inspections are seen in Fig. 17 for a constant inspection interval of 3 years starting from year 28. The same weld as in Fig. 16 is considered.

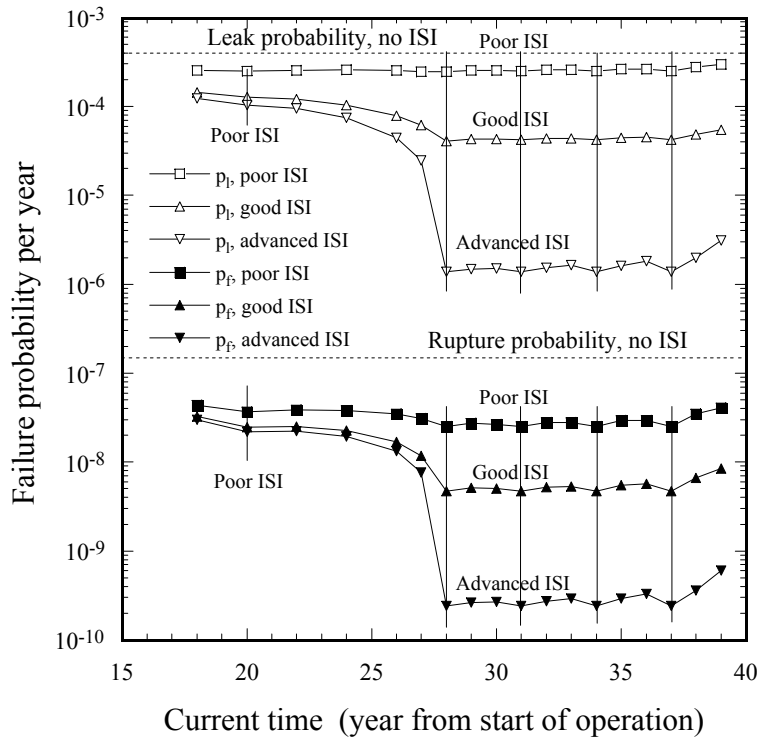


Fig. 17. Leak- and rupture probability per year as function of time. Effect of inspection effectiveness.

Fig. 17 illustrates the importance of performing effective inspections. However, an assumption of an advanced inspection would reflect a confidence in the probability of detection that is beyond the capabilities of the current techniques, see Appendix A. The upward trend for the failure probabilities after the year 37 are due to end effects. When the failure probability are evaluated as a mean value for the remaining operating time ($T-t$), T being 40 years and t representing the current time, the failure probability will be larger at $t = 39$ years compared to $t = 37$ years. Compare division with $(T-t) = 1$ year with $(T-t) = 3$ years.

6.3.2 Core Damage Frequency for the Current ISI Selection

In the current system for selecting components for ISI, 357 locations are selected in a proportion for the different pipe systems as shown Table 1. The inspections are required to be qualified and performed with an interval after year 28 as determined by deterministic damage tolerance analyses for each weld. In these analyses, a starting defect is postulated (with a size that should be able to be detected with a qualified inspection technique) and the interval is determined by the time it takes for this initial defect to grow by IGSCC to a limiting size that is still acceptable using ASME XI safety factors on flaw evaluation. The maximum interval shall not exceed 10 years. Also, the minimum interval may be set to 3 years according to the current regulations in Sweden, even if a conservative evaluation will result in a shorter interval. The motive for this is that a crack growth that penetrates the pipe

thickness in less than 3 years is in most cases not reflecting operating history. It is merely a result of conservative crack growth laws used in some of the evaluations.

Fig. 18 shows the risk diagram for all pipe systems evaluated at the year 28. 357 of the total 1192 welds are subjected to a first qualified inspection at year 28 whereas the rest of the welds are not inspected at all.

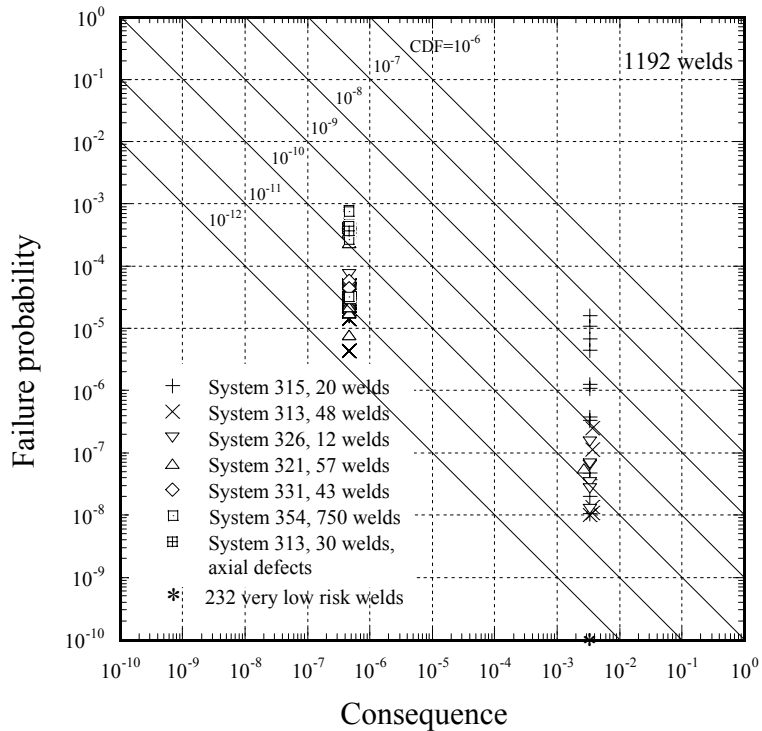


Fig. 18. Core damage frequency per weld, current ISI selection at 357 locations.

It is seen from Fig. 18 that some points (which have been subjected to inspections) have been reduced vertically, which means that the risk is reduced compared with Fig. 6. Note that inspections are only influencing the failure probability and not the consequence. Many of the high risk locations are reduced so that no weld has a higher CDF than $6E-8$ per year. The high risk locations in system 315 are still those welds which have with a potential for both IGSCC and high cycle vibration fatigue. However, the inspection interval for these welds are in many cases 10 years. At the other end, many already low risk locations without inspections are pushed down in risk even further. That is why some welds in Fig. 18 have a risk below $1E-11$ per year. Obviously, there are possibilities to optimize both the selection of locations for ISI and the inspection intervals. Note also that for system 354, for which 118 locations are selected for inspection, the majority of the inspections are performed with penetrating liquid (PT). This technique are not able to detect IGSCC from the inside of the components and the risk reduction has been set to zero in such cases. Only 6 locations are inspected by UT.

Fig. 19 shows the corresponding results for the CDF but with all the vibrations set to zero.

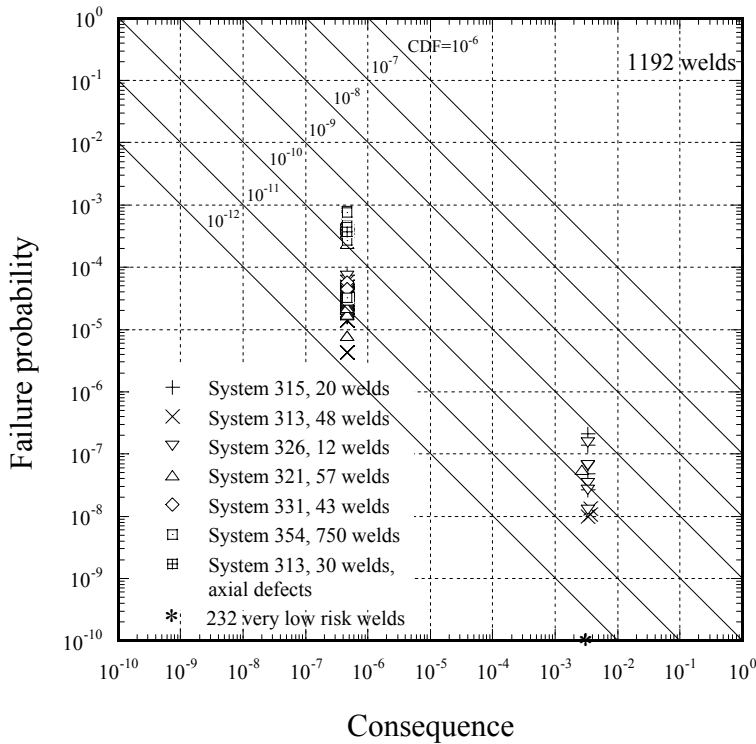


Fig. 19. Core damage frequency per weld, current ISI selection at 357 locations, no vibrations.

It is observed that if the vibrations are suppressed no weld has a higher CDF than 1E-9 per year.

Table 4 is showing the total core damage frequencies for the 4 studied cases, with and without inspections and with and without vibrations.

	CDF all systems no ISI	CDF all systems current ISI (357 locations)
With vibrations	5.31E-6	3.43E-7
No vibrations	3.15E-7	2.06E-7

Table 4. Total Core Damage Frequencies (per year) for O1 due to pipe failures.

From Table 4 the following observations can be made:

- i) Inspections are reducing the total CDF by a factor of 15.5 with vibrations considered.
- ii) If vibrations are not considered, the total CDF is only reduced by 35% by inspections. This is due to that the total CDF is then dominated by the risk from

system 354 (which has 750 welds potentially susceptible to IGSCC) for which only a small number of effective inspections are made.

7 RISK RANKING

When the risk for core damage for all the individual components have been determined, a procedure for risk ranking is needed. The objective of the risk ranking process is to form the basis for a new ISI-selection where the inspections in general are focused on the risk significant locations. The starting-point for the risk ranking is Fig. 6, where the individual risks are evaluated with no account for inspections. Using Fig. 6, Table 5 shows the total number of welds for all systems divided into risk intervals.

CDF-level per weld (no ISI)	Total number of welds	Number of welds, current ISI selection
Very high risk $CDF \geq 1 \cdot 10^{-7}$	6	6
High risk $1 \cdot 10^{-8} \leq CDF < 1 \cdot 10^{-7}$	5	5
Medium risk $1 \cdot 10^{-9} \leq CDF < 1 \cdot 10^{-8}$	15	15
Low risk $1 \cdot 10^{-10} \leq CDF < 1 \cdot 10^{-9}$	900	223
Very low risk $CDF < 1 \cdot 10^{-10}$	266	108

Table 5. Number of welds divided into different risk intervals.

Note that the expressions high and low risk in Table 5 are used only in a relative sense. A core damage frequency of 1E-11 is a very low risk compared to 1E-7. However, in another Nuclear Power Plant, a very low risk may have different CDF-values depending on the evaluated risks for that plant.

It is immediately seen from Table 5 that the current ISI selection is doing a very good job in the sense that the three highest risk levels (medium risk, high risk and very high risk) are covered by 100%. On the other hand, 108 locations representing very low risks are also selected for inspection. This indicates that there are possibilities for optimizations.

The welds given in each risk level can form the basis for a risk ranking. There exist also special risk ranking measures as defined by Eqns. (2) and (3).

$$RRW_i = \frac{R_0}{R_{i-}} \quad (2)$$

$$RAW_i = \frac{R_{i+}}{R_0} \quad (3)$$

where R_0 is the basic risk level for the total system as measured by the CDF related to piping pressure boundary failures, R_{i-} is the reduced risk for the total system assuming a zero failure probability for location i and R_{i+} is the increased risk for the total system assuming a failure probability of 1.0 for location i .

The Risk Reduction Worth RRW for location i is a measure of how much the total risk is reduced when a completely reliable component is assumed. It can also be seen as the effect on risk when a maximum effect of an inspection of that location is assumed (POD equals 1.0). A high RRW-value means that the particular component is a large relative contributor to the risk. The Risk Achievement Worth RAW for location i is a measure how much the risk is increased when the component is assumed always to fail. This means that there can be no effect of inspection (since the component always fails) and that RAW is only a measure of severity of consequence. These risk measures are used in the ASME/WOG procedure [4] to rank components for ISI. Normally the RRW index is used. For Surrey-1, a Westinghouse 3-loop PWR in the USA, pipe segments with RRW values greater than 1.005 were deemed high safety significant while segments with RRW values between 1.001 and 1.004 were deemed to be worthy of additional consideration by the plant expert panel. However, a pipe segment can contain many welds and is mainly defined as a portion of piping for which a failure at any point in the segment will result in the same consequence. Normally, the risk per weld is not quantified with the ASME/WOG procedure [4].

7.1 Suggestion for a New Risk Based Inspection Program

The inspection program can be defined by using the assessment of risk to answer the following questions:

- Which systems and locations shall be inspected?
- What kind of degradation mechanisms are appropriate for the different inspection sites?
- What kind of inspection technique shall be used and how shall the effectiveness requirements be defined?
- What is an appropriate inspection interval for the locations?

A good risk based inspection RBI-procedure shall be able to answer these questions. Also, the benefit of the new RBI-procedure should be able to be quantified in measurable terms. The following ambition, as expressed in Regulatory Guide 1.174 [10], can be defined for what can be regarded as a good inspection program:

Choose inspection sites, inspection intervals and inspection techniques that, by focusing on high risk locations, causes $\Delta CDF < 0$ ($\Delta LERF < 0$) or possibly only a small increase in CDF ($\Delta LERF$). In addition, remove very low risk locations from the ISI-program thereby reducing unnecessary radiation exposure to plant personnel.

The change in CDF (or LERF) is defined as

$$\Delta CDF = CDF(\text{new inspection program}) - CDF(\text{current inspection program}) \quad (4)$$

In this way, the benefit of the new RBI-procedure can be quantified in relation to the current inspection program. By focusing on high risk locations, this will often (but not always) lead

to a decreased total risk and at the same time defining less number of inspection sites compared to the old inspection program. NRC has defined acceptance guideline as to what can be regarded as acceptable changes in risk measures when using PRA in plant-specific changes to the licensing basis. Regulatory Guide 1.174 [10] states in part that (similar criteria are defined for the LERF):

- If $\Delta\text{CDF} < 0$, the change is considered to fulfil the NRC's requirement of a relevant risk-based regulation.
- If $\Delta\text{CDF} > 0$, the change should be small. How small is depending on the magnitude of the total CDF. If ΔCDF is less than 10^{-6} , the increase of CDF is regarded as sufficiently small, regardless of whether there is an evaluation of the total CDF.

One may argue in relation to the second statement above, that it is not suitable to have an acceptance criterion that is based on an absolute measure of risk. Depending on the chosen PRA-procedure, there will always be a certain degree of uncertainty of the CDF-levels. An alternative criterion would be to require that:

$$\Delta\text{CDF}/\text{CDF} \ll 1 \quad (5)$$

that is to require that the increase of CDF in a relative sense should be small. In practice, a combination of absolute and relative acceptance criteria is probably the best. A criterion based on an absolute measure of the CDF can still be desirable to achieve a general objective of a sufficiently small overall CDF for the plant.

The following criteria are suggested for a new ISI-selection for piping components in the O1 plant, with reference to Table 5:

1. Select 100% of all locations with $\text{CDF} \geq 1 \cdot 10^{-9}$ (very high, high and medium risk).
2. Select 10% of all locations with $1 \cdot 10^{-10} \leq \text{CDF} < 1 \cdot 10^{-9}$ (low risk).
3. Select 0% of very low risk locations, $\text{CDF} < 1 \cdot 10^{-10}$.

The values 100% and 10% are chosen by analogy with the current ISI selection procedure in Sweden [9]. Note that the specific values of the CDF-criteria are here suggested for this particular plant. For other Nuclear Power Plants, different CDF-values and criteria may be more appropriate depending on the features of the risk profile for the particular plant.

On a component level these limits correspond to quite low values of the Risk Reduction Worth. If vibrations are considered $\text{CDF} \geq 1 \cdot 10^{-9}$ corresponds to $\text{RRW} > 1.0002$ and $\text{CDF} < 1 \cdot 10^{-10}$ corresponds to $\text{RRW} < 1.00002$. These low values are a consequence of the large dominance in risk of the 10 locations that have both IGSCC and high cycle vibration as potential damage mechanisms. If all vibrations are set to zero, the corresponding RRW-values are changed to 1.0032 and 1.00032, respectively.

Using these selection criteria, Table 6 shows the results in form of number of selected locations and CDF per system in relation to the current ISI-selection.

System	CDF New ISI selection	CDF Current ISI selection	Δ CDF
313 circumf	7.32E-9 (13 welds)	1.95E-9 (102 welds)	5.37E-9
313 axial	1.91E-8 (3 welds)	5.19E-9 (30 welds)	1.39E-8
315	9.87E-8 (1) (11 welds)	1.37E-7 (27 welds)	-3.87E-8
326	2.64E-9 (7 welds)	1.31E-9 (14 welds)	1.33E-9
321	8.03E-9 (5 welds)	2.32E-9 (60 welds)	5.72E-9
331	7.29E-9 (4 welds)	6.94E-9 (6 welds)	3.57E-10
354	1.67E-7 (2) (75 welds)	1.88E-7 (118 welds)	-2.08E-8
All systems	Sum 3.10E-7 (118 welds)	Sum 3.43E-7 (357 welds)	-3.28E-8

(1) Involves a shorter inspection interval than in the current ISI program for some of the high risk locations in system 315.

(2) Involves UT-inspections for the new ISI program in system 354 instead of PT in the current ISI program.

Table 6. Number of selected locations and CDF per system, possible new ISI selection.

The suggested new ISI-selection leads to both a reduced number of welds for inspection and a reduction in overall risk. The reduced number of inspection sites in e.g. system 313 will of course lead to an increase in risk but since it is only the low risk locations that are excluded in the suggested new ISI program, the increase in risk is very small. This is the case for all systems except for system 315 and 354, where the CDF is decreased. Some of the high risk locations in system 315, which have inspection intervals of 10 years according to the current ISI Program, the inspection interval is decreased to 3 years in the new ISI Program. This has a significant effect on the risk reduction because these locations represent the highest risks of all locations. In system 354, where 112 welds in the current ISI Program are inspected with PT, the new ISI Program involves UT-inspections (at 75 welds) which are more suitable to detect IGSCC from the inside of piping components. This also leads to a risk reduction.

The CDF for the suggested new ISI Program leads to a reduction of risk with 9.5% relative to the CDF for the current ISI selection. The number of locations for inspection is 118 in the new ISI selection compared with 357 in the current ISI Program.

Fig. 20 shows the CDF diagram for the suggested new ISI Program.

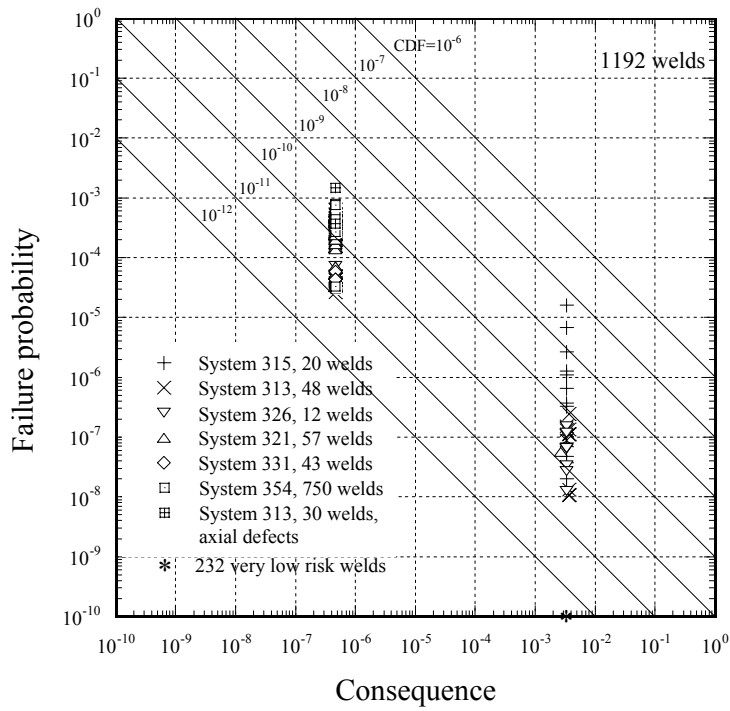


Fig. 20. Core damage frequency per weld, suggested new ISI selection at 118 locations.

It is observed that fewer welds are now located at the higher risk levels compared to the current ISI Program (Fig. 18). Furthermore, no location will obtain a risk level after inspection below $1E-11$. In this way a more flat risk profile after inspection is obtained.

The corresponding result for the number of selected locations and CDF per system, assuming all vibrations to be zero for both the current and new ISI Program, is shown in Table 7. Fig. 21 shows the corresponding risk diagram for this case.

System	CDF New ISI selection	CDF Current ISI selection	Δ CDF
313 circumf	6.54E-9 (12 welds)	6.86E-10 (102 welds)	5.85E-9
313 axial	1.91E-8 (3 welds)	5.19E-9 (30 welds)	1.39E-8
315	3.61E-9 (5 welds)	1.69E-9 (27 welds)	1.92E-9
326	2.64E-9 (7 welds)	1.31E-9 (14 welds)	1.33E-9
321	8.03E-9 (5 welds)	2.32E-9 (60 welds)	5.72E-9
331	7.29E-9 (4 welds)	6.94E-9 (6 welds)	3.57E-10
354	1.55E-7 (1) (120 welds)	1.88E-7 (118 welds)	-3.34E-8
All systems	Sum 2.02E-7 (156 welds)	Sum 2.062E-7 (357 welds)	-4.25E-9

(1) Involves UT-inspections for the new ISI program in system 354 instead of PT in the current ISI program.

Table 7. Number of selected locations and CDF per system, possible new ISI selection assuming no vibrations present.

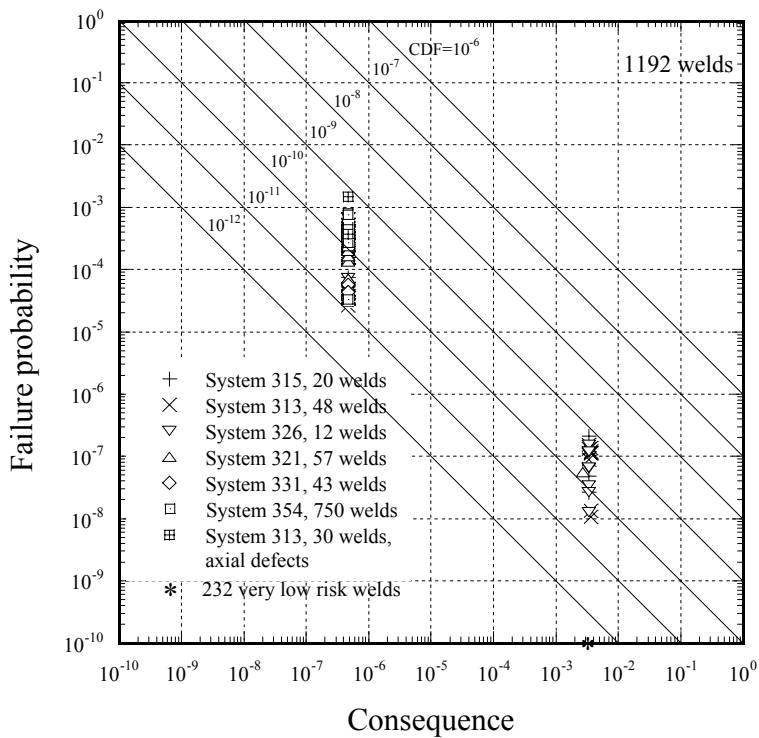


Fig. 21. Core damage frequency per weld, suggested new ISI selection at 156 locations

assuming no vibrations present.

The reduced overall risk is accomplished by an increased number of UT-inspections in system 354. If all vibrations are set to zero, the CDF for the suggested new ISI Program leads to a reduction of risk with 2.1% relative to the CDF for the current ISI selection. However, at the present time vibrations are existing at the plant. The most effective risk reduction is then achieved if both all vibrations are eliminated and the inspection method in system 354 is changed to UT instead of PT. In that case the suggested new ISI Program will have a total CDF of 2.02E-7 (156 locations) compared to a CDF of 3.43E-7 for the current ISI Program (357 locations). This corresponds to a reduced risk of 41%. The resulting CDF diagram in Fig. 21 shows a very flat risk profile with the individual risks after inspections located within only two decades.

It is also possible to evaluate the number of cumulated future inspections with the different suggested ISI-selections. Table 8 shows the result, assuming that the total operation time for the plant is 40 years and all inspection intervals in general follow the deterministic procedure (with intervals ranging from 3 to 10 years starting from year 28).

System	Number of future inspections Current ISI selection	Number of future inspections New ISI selection (with vibrations)	Number of future inspections New ISI selection (without vibrations)
313 circumf	271	45	40
313 axial	150	15	15
315	84	53	25
326	52	27	27
321	188	25	25
331	30	20	20
354	590	375	600
All systems	1365	560	752

Table 8. Number of future inspections to end of life in each pipe system with different ISI Programs.

It is observed from Table 8 that the suggested new ISI Programs will lead to a reduction in number of accumulated inspections mainly in system 313 and 321. This is because these systems contain many low risk locations where the current ISI Program is not particularly effective to reduce the risk for core damage.

There exist also other strategies to make risk priorities. Figs. 22-23 are showing risk ranking diagrams where all the individual risks have been normalized with the risk for the highest risk location. The risk values are then sorted in a way that site number 2 represents the second highest risk etc. Both the risk with and without inspection is shown in Fig. 22-23 where each risk value is sorted. This means that it is not necessarily so that the risk location with ISI corresponds to the same location as without ISI.

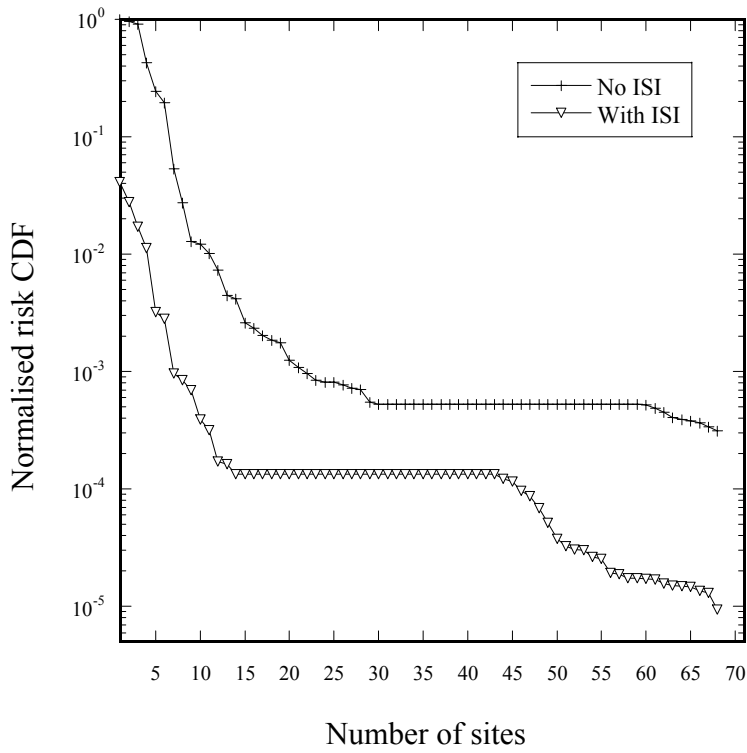


Fig. 22. Normalized risk ranking versus number of sites. Vibrations included.

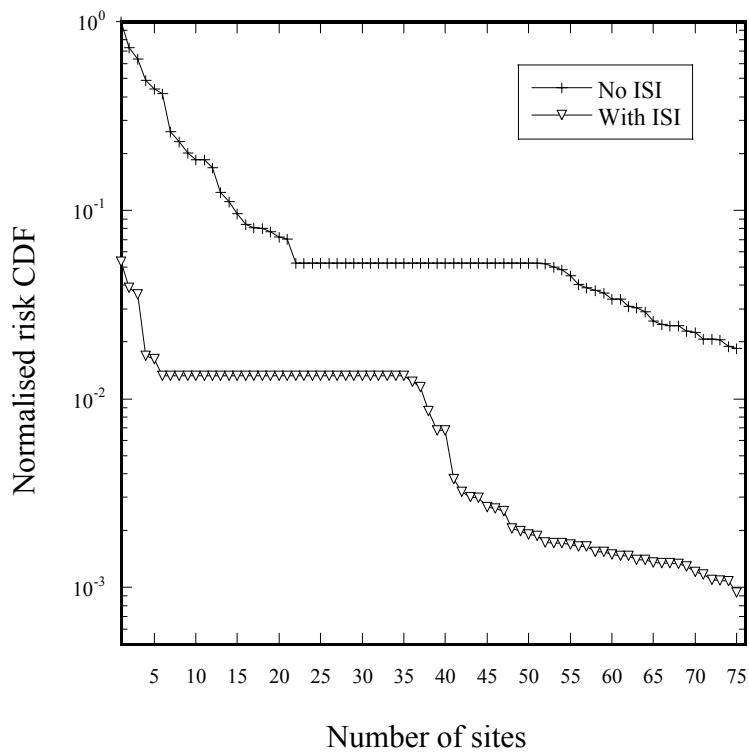


Fig. 23. Normalized risk ranking versus number of sites. Vibrations excluded.

The plateau in the central part of Fig. 22-23 represents the risk for core damage from system 313, axial defects. The CDF is here determined by small leaks and is the same for all welds of this type, see section 6.2.2. What is interesting to note in Fig. 22 is that if one is covering the individual risks by inspections, starting from the curve with no ISI and going from the highest risk to successively lower risks, at some point the next location in risk will not be the most risk significant location anymore. This is because the already inspected high risk locations will have a higher risk after inspection than the next location before inspection. One may then argue that it is not meaningful in trying to decrease the overall risk by performing inspections at successively lower risk locations, if the already inspected locations represent a higher risk. The optimum number of locations would then be only 10 locations in Fig. 22 even if the process is stopped when the normalized risk has decreased a factor of 50, allowing for some uncertainties in the risk evaluations. This is due to the large dominance of the total risk from the relatively few locations which have both IGSCC and vibrations. If the vibrations are removed (Fig. 23), the optimum number of locations would be about 75.

7.2 Optimization of Inspection Intervals

The inspection interval can have a large influence on the risk for core damage. Fig. 24 shows this dependence for 8 different welds in system 313 and 315.

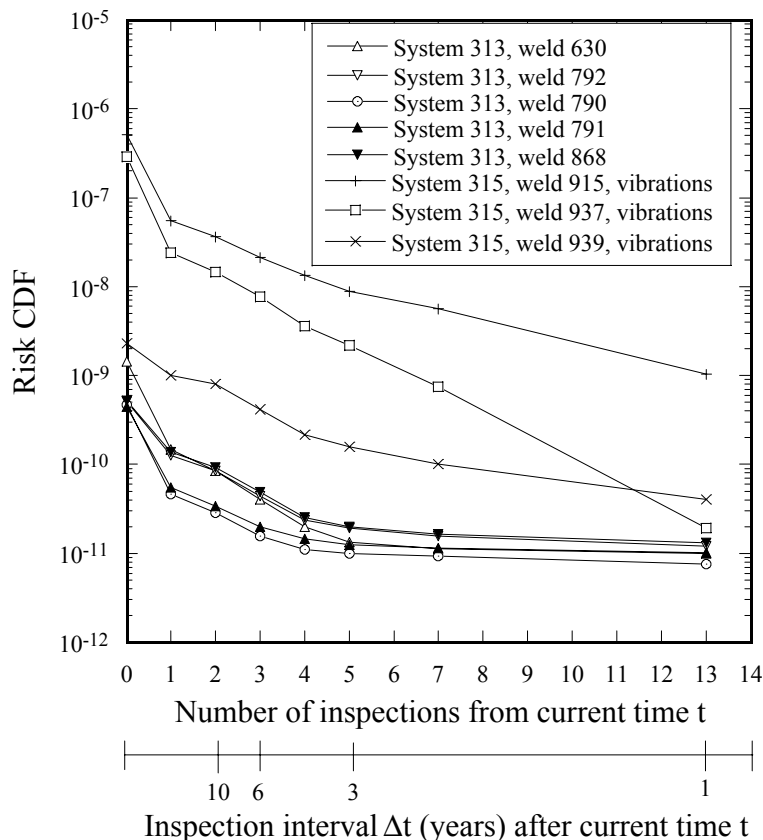


Fig. 24. Influence of inspection interval on the Core Damage Frequency.

The risk in Fig. 24 is plotted versus number of inspections (qualified, dependent inspections)

starting from the current time at year 28 until the assumed operating time 40 years. Thus an inspection interval of one year corresponds to 13 inspections whereas an interval of 10 years corresponds to 2 inspections. It is clearly seen from Fig. 24 that an increased number of inspections are reducing the risk. This is especially prominent for the welds with vibrations, where it is important to detect a possible crack before leakage occurs. On the other hand, for the welds without vibrations there seem to be an inspection interval of about 3 years below which only a further marginal decrease in risk is obtained. This indicates that is not meaningful to use too short inspection intervals. The results in Fig. 24 are replotted in Fig. 25 where all the CDF-values without inspection are normalized with the CDF-value with inspection.

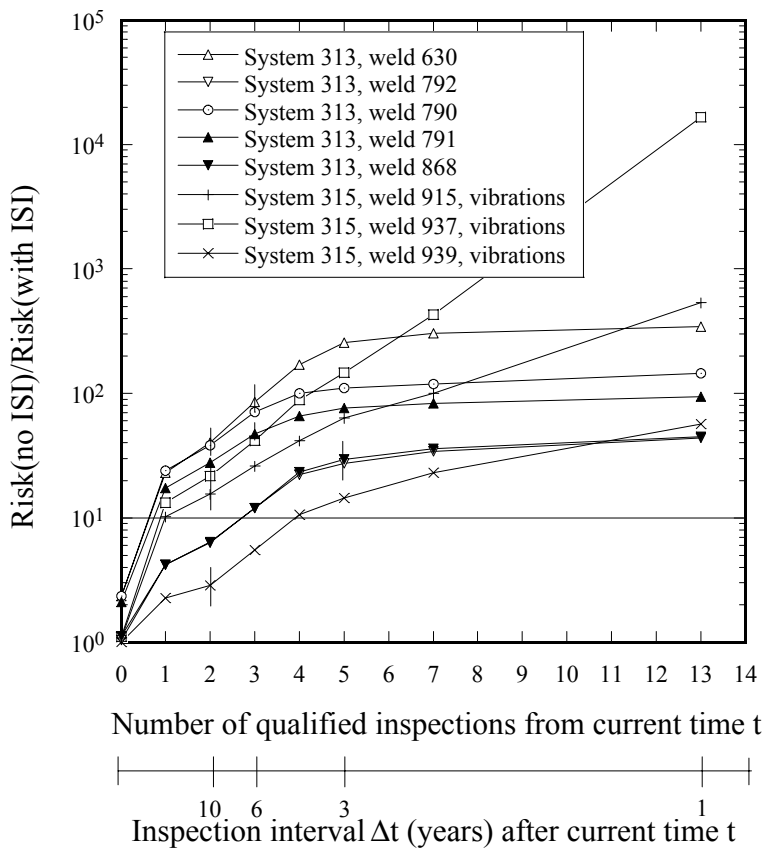


Fig. 25. Risk reduction factors on risk for different inspection intervals.

The results in Fig. 25 can be seen as a measure of how effective the inspection method with the corresponding inspection interval is to reduce the risk for core damage. Also indicated by short vertical lines are the inspection intervals (between 3 and 10 years) for each individual location that are determined by the current ISI Program. Now, it can be argued that a suitable goal for an ISI Program, is to reduce the risk by a factor of 10. If the inspections would reduce the risk by a lower factor than 10, the relevance of performing inspections at all can be questioned. On the other hand, a risk reduction goal by a factor of greater than about 10 can be difficult to justify because of limitations and uncertainties in the NDE flaw detection capabilities and the demands on the frequency of inspections. This is in line with the recommendations in NUREG-1661 [14].

To meet a risk reduction goal of 10, Fig. 25 indicates that the inspection interval should be

decreased for one weld, whereas some of the other welds could possibly increase the inspection intervals. The conclusions from this study is that there are possibilities to optimize the risk reduction by using different inspection intervals which can be determined by probabilistic methods in contrast to the deterministic procedure used in the current ISI Program in Sweden. However, a complete optimization of inspection intervals for all components is out of the scope of the present study.

For a typical weld in system 313, Fig. 26 is showing the effect on the leak- and rupture probability for different inspection intervals when using dependent versus independent inspections.

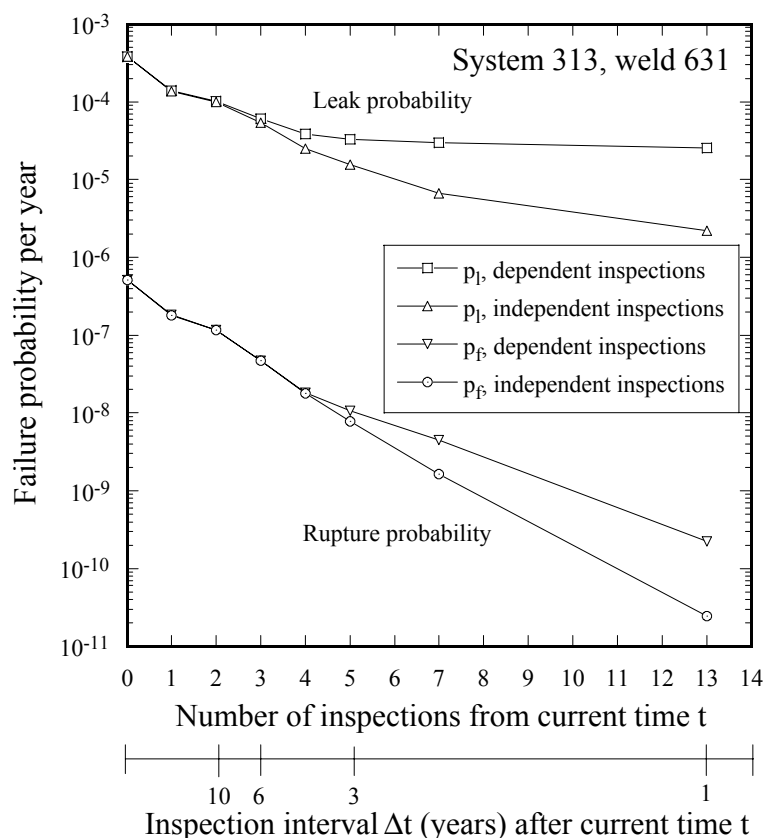


Fig. 26. Influence of inspection interval on the failure probability for dependent versus independent inspections.

The benefit of successive inspections is larger if the inspections are assumed to be completely uncorrelated, see section 6.3.1. However, Fig. 26 shows that the effect is not that important unless the inspection interval is short. All the risk evaluations in this study are performed with the assumption of dependent inspections in order not to overestimate the effect of inspection effectiveness.

The reason for that the rupture probability is decreasing more than the leak probability for very short inspection intervals in Fig. 26 is that inspections will also influence through wall cracks. The POD for inspection of a through wall crack is assumed to be 1.0. This means that if a leaking crack is not discovered by leak detection, it will always be detected by an inspection, if an inspection is performed between leak and rupture. If the inspection interval is short, then there is often sufficient time between leak and rupture for an inspection to take

place, at least for short initial crack lengths.

7.3 Unknown Damage Mechanisms

This section is based on the views put forward by EURIS [8]. Selection procedures based on risks are sometimes criticized for not accounting for unknown damage mechanisms. Since the basis for a risk based strategy is to be able to identify where degradation mechanisms occur and which they are, it is rather self evident that such procedures can not directly treat unknown mechanisms. The problem is actually a question of completeness, i.e. how can we be sure that there are not unknown mechanisms that may appear at some locations in the future and that may warrant inspections to keep the risk to an acceptable level at those locations. It is sometimes suggested that to account for unknown mechanisms a certain amount of random selection for inspection should be done. However, as shown in [8], a risk based selection of say 10% of all locations is just as effective to identify an unknown mechanism as if the selection of 10% would be performed at random. This is because the probability of detecting an unknown mechanism is dependent only on the size of the inspection sample and not whether or not it is risk based. Thus one may argue that by doing a risk based inspection one also has the ability to detect an unknown mechanism as long as inspections at all are performed. Also a risk based inspection is the best way to use the current knowledge. There is of course the problem of how the inspection method shall be qualified for a mechanism that is not known.

Another problem is the treatment of postulated mechanisms, i.e. although it may be felt that a particular degradation mechanism is not occurring, the mechanism can not be ruled out at a sufficient level of confidence. For example, if the carbon content for a stainless steel pipe is given as a low value in the material specifications but it is suspected in reality that the carbon content is sufficiently high in order to create a potential for IGSCC, one may postulate a stress corrosion crack at that location in order to provide confidence that the mechanism is in reality not there. Such locations can also be treated by a risk based procedure and it may turn out that they should be selected for inspection due to a high risk. It should be observed, however, that the primary objective of such an inspection is to find out if the postulate is true or false. For the above example one could also combine the risk evaluation with the probability of a false value of the carbon content given in the material specifications for the particular pipe. It may then happen that the location will not be a high risk site any more.

8 RISK BASED INSPECTION PROCEDURE BY EPRI

Electric Power Research Institute EPRI, has defined a procedure [5]-[7], where the risk for core damage is determined using a matrix shown in Table 9. The division into low, medium or high risk is determined by the Consequence- and Degradation category.

		Consequence Category			
		None	Low	Medium	High
Degradation Category	High	Low	Medium	High	High
	Medium (IGSCC)	Low	Low (3)	Medium (2)	High (1)
	Low	Low	Low	Low	Medium

Table 9. Risk categorization for O1 using the EPRI procedure.

The consequence category is used to rank the core melt potential given the occurrence of a pipe break in the pipe segment being considered. If a PSA evaluation is used, the probability of core damage given that a pipe break has occurred (or Conditional Core Damage Probability CCDP) is used to classify the severity of the consequence. The following limits define the boundaries between the consequence categories:

High Consequence Category:	$CCDP > 1E-4$
Medium Consequence Category:	$1E-6 < CCDP < 1E-4$
Low Consequence Category:	$CCDP < 1E-6$

The Degradation Category is determined by a qualitative procedure where the likelihood of a pipe break is estimated by examining the ratios of pipe ruptures to pipe leaks from different degradation mechanisms. This is done by using pipe failure statistics, reported by e.g. Bush et al [20]. For IGSCC, no pipe rupture has occurred which motivates that all components with a potential for IGSCC are placed in the Medium degradation category. This means that once the degradation mechanism is known, the degradation category is established. The EPRI procedure applied for O1 leads to the following number of welds in respective risk category with numbers (1), (2) and (3) as indicated in Table 9:

(1) High risk category:	78 welds in system 313, circumferential cracks 30 welds in system 313, axial cracks 20 welds in system 315 12 welds in system 326 5 welds in system 321
(2) Medium risk category:	58 welds in system 321
(3) Low risk category:	43 welds in system 331 750 welds in system 354

If these risk categories are compared with the quantitative risk evaluations performed in this

study, both similarities and differences are seen. For example the 78 welds in system 313, categorized as high risk (1), also include the 30 welds of Alloy 182 in the thick walled (670 x 35 mm) piping. These welds resulted in very low risk values in this study, see section 6.2.2. This merely illustrates the fact that only the presence of a damage mechanism like IGSCC does not necessarily mean that the component will have a high failure probability. On the other hand, all the low risk category (3) welds in system 331 and 354 were also evaluated as low risks in this study. These welds were mostly located outside the containment where the consequence of a pipe rupture is less severe in these pipe systems. For the definition of inspection programs there exist two ASME Code Cases, N560 and N578 that are based on the EPRI procedure. Basically, 10% of the high risk category welds shall be inspected in Code Case N560 whereas 25% of the high risk category welds and 10% of the medium risk category welds shall be inspected in Code Case N578. In the O1 plant, this would mean 15 locations to inspect using N560 and 43 locations to inspect using N578. Note that in the USA, the EPRI procedure is at the present time not approved by the NRC to be applied for components that are included in so-called "Augmented Programs". Augmented programs apply for certain degradation mechanisms like IGSCC and flow assisted corrosion. The inspection of components having these mechanisms is determined by special programs defined in Generic letters, issued by the NRC. The following conclusions can be drawn from using the EPRI procedure for evaluating risks at the O1 plant:

- i) The selection of locations for inspection is mostly controlled by high consequences.
- ii) The EPRI procedure is simple to apply since no quantitative failure probabilities are needed.
- iii) Relatively few locations for inspections were selected at O1 using the EPRI procedure, 15 welds with Code Case N560 and 43 welds with Code Case N578.
- iv) There is no guidance as to how the 10% or 25% should be selected within each risk category.
- v) There is in general not possible to investigate in quantitative terms, how the inspections using the EPRI procedure will influence the risk compared to the existing program for inspection.

It should be mentioned that there are attempts to quantify the change of risk using the EPRI procedure even if these evaluations are not done on a routine basis, cf [21].

9 VALIDATION

Perhaps the most difficult part of performing a quantitative RBI analysis is to estimate failure probabilities. Since for some locations a low risk significance is mainly a result of a low failure probability, it is essential that the Structural Risk and Reliability Analysis (SRRA) code can be validated. In this study, the developed software PIFRAP is used for which the following validation steps are performed:

- Comparison with actual leak frequencies.
- Benchmarking with the code WinPRAISE.
- Sensitivity analyses (see Appendix B).

9.1 Comparison with Actual Leak Frequencies

One of the best validation of SRRA codes is to compare predictions with actual failure frequencies. However, in many cases there are no or very few reported failures corresponding to the conditions addressed by the SRRA code. For example there has been no case of ruptures reported in Sweden from IGSCC in BWRs. This is consistent with the low predicted rupture probabilities using PIFRAP in this study. However, there have been several small leaks in BWR piping due to IGSCC as shown in Fig. 4. This offers a possibility to compare the PIFRAP predictions against the actual leak frequency.

The following equation is used to estimate the total leak probability per year for the O1 plant:

$$p_L = 1 - \prod_{i=1}^n \prod_{j=1}^N (1 - p_i) \cdot (1 - p_j) \quad (6)$$

where

p_L = probability per year of obtaining a leak due to IGSCC in the whole primary piping system of the plant.

p_i = leak probability per year of weld i , subjected to inspection (current ISI program).

p_j = leak probability per year of weld j , not subjected to inspection.

n = number welds subjected to inspection.

N = number welds not subjected to inspection.

Using PIFRAP for the individual p_i and p_j for small leak probabilities and performing the summation for all the 1192 welds which are included in the pilot study, p_L will be about 0.26 per year. The result is dominated by the contribution from system 354 (hydraulic control rod) due to the large amount of welds susceptible to IGSCC in this system. Note also that the current ISI program (using mostly PT for the inspections) is not capable to reduce the leak probability for this pipe system which means that the result for p_L is dominated by the not inspected welds of system 354.

From the failure statistics (Fig. 4) for all the nine BWRs in Sweden, there have been 7 small leaks due to IGSCC up to the year 1998. These leaks have occurred in the HAZ of girth welds in straight pipes. Several of the leaks have actually occurred in the hydraulic control rod pipe system of the BWRs and discovered in general by leak detection. The total number of cumulative reactor years for all the nine BWRs is 176 up to the year 1998. This gives an average leak frequency for one plant of $7/176 = 0.040$ per year. This means that PIFRAP is overestimating the actual leak frequency by a factor of 6.5 ($0.26/0.040$). It is believed that the major reason for this overestimation is the use of conservative stress corrosion crack growth data. In this study the following crack growth law is used

$$\frac{da}{dt} = 4.5 \cdot 10^{-12} K_I^{3.0} \quad (7)$$

where the growth rate is measured in mm/s and K_I is given in $\text{MPa}\sqrt{\text{m}}$. This is taken from a compilation of SCC growth data for different steels and water environments in Swedish BWRs, Jansson et al [22]. Eqn. (7) represents an upper estimate of stress corrosion crack growth in stainless steels (type 304) in normal water chemistry environment. If the crack growth rate would be reduced by a factor of 5 (the constant in Eqn. (7) equal to $9\text{E-}13$), which perhaps corresponds to more realistic crack growth data, PIFRAP will predict a total

leak probability p_L of about 0.11 per year. In this case, PIFRAP will overestimate the actual leak frequency by a factor of 2.8 (0.11/0.040). This represents a very good agreement. It should however be observed that PIFRAP is evaluating the leak probability measured per reactor-year as a mean value for the remaining operating time of the plant. It is not certain that the average leak frequency of 0.040 per year will be maintained also in the future.

9.2 Benchmarking with the Code WinPRAISE

In this section a discussion of the rupture probability will be given. The rupture probability will in general be small which means that often one is using information of frequency functions far out in the tails where the information is scarce. Also, validation against actual ruptures is difficult since no rupture due to IGSCC has ever occurred, at least not in Swedish BWRs. Therefore, it is important to benchmark different SRRA codes between each other. A well-known SRRA code is the PRAISE code (Piping Reliability Analysis Including Seismic Events). PRAISE was originally developed in 1980 in the USA for the assessment of seismic events and fatigue in PWRs. Later it was developed also for initiation and growth of stress corrosion cracks. The Windows version is called WinPRAISE, Harris and Dedhia [23]. WinPRAISE can treat fatigue from preexisting cracks or fatigue and stress corrosion from preexisting cracks or stress corrosion from purely initiated cracks using a Monte Carlo simulation technique. The random parameters are initial crack size, material properties (flow stress, time to initiation and crack growth rate) and stress state (thermal and residual stresses). WinPRAISE can give the failure probability for a small leak, a large disabled leak (at a given leak rate) and a rupture.

A quite extensive investigation has been performed within this pilot study to penetrate the PRAISE code and the underlying assumptions in order to make a meaningful comparison between PIFRAP and WinPRAISE. The benchmark evaluations have been performed to solve for the rupture probabilities for a sample of girth welds in all the six considered piping systems in the O1 plant. The following assumptions of input data have been made. References are given to both WinPRAISE and PIFRAP. If no reference is given, identical input data is used for both WinPRAISE and PIFRAP. Detailed information of the modeling assumptions in PIFRAP is given in Appendix A.

- Stress corrosion from preexisting circumferential cracks.
- Pipe diameters varying from 76 to 252 mm. The wall thickness varies from 6.3 to 20 mm.
- Starting crack depth equal to 1 mm (PIFRAP).
- Initial crack depth random with lognormal distribution (default) and a default mean value typically about 2.5 mm (WinPRAISE).
- Crack length random with exponential distribution and a mean value 10.66% of the pipe circumference (PIFRAP).
- Crack aspect ratio (length to depth) random with lognormal distribution (default) and a default mean value of 1.34 (WinPRAISE).
- Failure criteria controlled by a J -criterion or by net section collapse.
- Values of J_R , yield strength and flow stress for typical austenitic stainless steels, the same in WinPRAISE and PIFRAP.
- Values of oxygen content and conductivity of coolant in WinPRAISE to make the crack growth rate comparable with PIFRAP using Eqn. (7).
- Pipe stresses due to pressure, dead weight and thermal expansion, the same in WinPRAISE and PIFRAP for the respective pipes.

- Weld residual stress random with normal distribution and a default mean value of 34 MPa at the inside surface for pipes with diameters below 254 mm. Linear through thickness bending (WinPRAISE).
- Weld residual stress deterministic and linear through thickness bending. Magnitude at the inside surface of the pipes for a wall thickness h up to 25 mm according to $\sigma_{res} = 297 - 9.88 \cdot h$ MPa, Ref. [24] (PIFRAP).
- No in-service inspections performed.
- Crack existence frequency (measured as expected number of cracks per weld) set to 0.0106. This value are taken from damage statistics, STRYK [11], corresponding to 98 cases divided by 9240 welds susceptible to IGSCC (PIFRAP and WinPRAISE).
- Leak rate detection accounted for with leak rate detection limit 0.30 kg/s inside the containment and 2 kg/s outside the containment. Leak rate evaluation performed using the SQUIRT code. Crack morphology parameters, surface roughness = 0.08 mm, pathway loss coefficient PLC = 0.282 mm⁻¹. Deterministic leak rate evaluation in WinPRAISE. Leak rate assumed to be random in PIFRAP with normal distribution with a mean value given by the deterministic SQUIRT code and a coefficient of variation COV (standard deviation divided by mean) varying between 0.20 and 0.50.

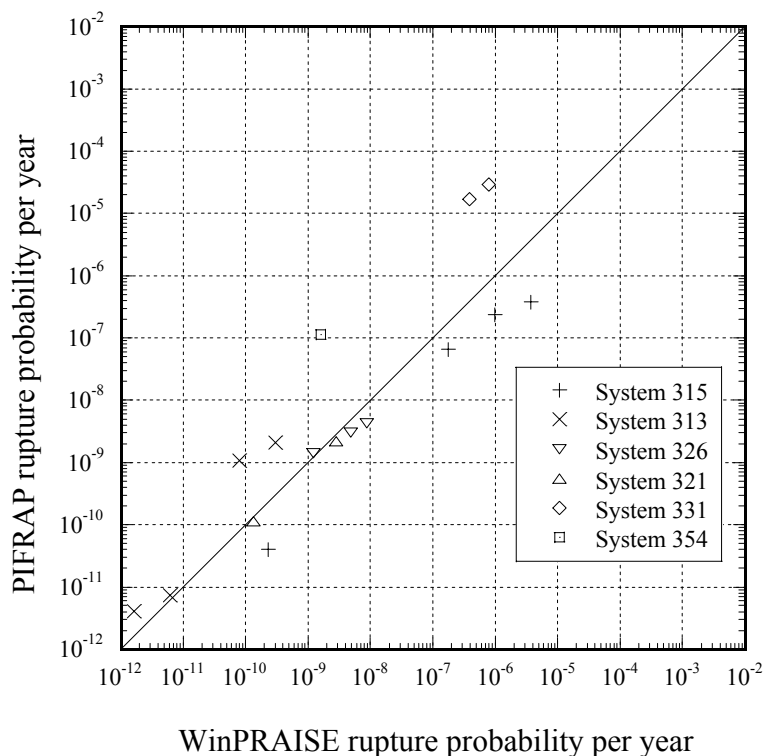


Fig. 27. Benchmarking study with PIFRAP and WinPRAISE.

Using the above assumptions the rupture probability per year was evaluated with both PIFRAP and WinPRAISE. In WinPRAISE, the mean rupture frequency per year was obtained by calculating the cumulative rupture probability after 40 years and then dividing the results by 40. The result is shown in Fig. 27.

The agreement of the results between the different codes is quite good for this particular class of problems. However, during the process of investigating the underlying assumptions

made in the WinPRAISE code for stress corrosion problems, a number of observations have been made, which in many cases can not be found in the code manual. The observations are listed in the following:

1. WinPRAISE does not seem to give the common Leak Before Break behavior, i.e. the normally expected result that $p(\text{rupture}) \ll p(\text{small leak})$, is not obtained. WinPRAISE will give about the same values for both the small leak- and the rupture probability for stress corrosion problems.
2. At wall penetration, WinPRAISE assumes that the crack opens up along its entire length at the inside and outside surface of the pipe (straight crack fronts).
3. WinPRAISE has a deterministic model for treating leak rates and their detection. A through-wall crack at wall penetration that has a larger leak rate than the detection limit, will not contribute to the rupture probability.
4. Residual stresses are not accounted for when considering through-wall cracks, not for the evaluation of J -integrals, critical crack sizes or for leak rate evaluations.
5. WinPRAISE can account for vibration fatigue by evaluating ΔK and comparing it against the vibration threshold. However, this is only done for surface cracks. No checks against the threshold value are made for through-wall cracks.
6. For materials for which failure is governed by a J -criterion, thermal expansion loads are treated as load controlled. This assumption is also made for the evaluation of leak rates.
7. The circumferential variation of bending loads (dead weight, thermal expansion), is not accounted for when evaluating J -integrals, critical crack lengths or leak rates.
8. There is no possibility in WinPRAISE to prescribe a user defined crack growth rate for stress corrosion problems.

Some of these observations are due to simplified assumptions made in the code that may influence the results to varying degrees, at least for stress corrosion problems. It is expected that the process of comparing the different SRRA codes will continue and that new information or better modeling assumptions will be incorporated into the codes so that the results from these codes reflect the best current knowledge in probabilistic fracture mechanics.

9.3 Sensitivity Analyses

It is important to perform sensitivity analyses covering all input parameters to demonstrate that changes to input values result in consistent changes in evaluated failure probabilities. Such analyses are reported in Appendix B. The results reported in Appendix B also give information about the uncertainties associated with the inputs to the probabilistic evaluations.

10 CONCLUSIONS AND RECOMMENDATIONS

1. Quantitative risk evaluations are an efficient way to guide inspection priorities for primary piping components.

2. The results of the pilot study have shown that:
 - it is important to include a model for leak rate evaluation and detection in order to obtain realistic estimations of risk.
 - the highest risk contributions are those components which have IGSCC and vibration fatigue as damage mechanisms at the same time.
 - if no qualified inspection has been done before, it is important for an effective risk reduction to perform a qualified inspection as soon as possible.
3. The current ISI-selection procedure for piping components (SKIFS 1994:1):
 - is efficient to select all high risk locations.
 - also selects many low risk locations.
 - is a very efficient starting point for making quantitative RBI-analyses. This is because it gives information of which damage mechanisms that are present and where in the plant they occur.
4. It is possible to apply both the ASME/WOG- and the EPRI-procedure for RBI for Swedish nuclear power plants. However, if quantitative risk levels are needed, only the ASME/WOG-procedure seems to be a realistic alternative.
5. With a quantitative RBI-analysis for O1, it is possible to combine a reduced number of inspection sites with a reduction of overall risk. This is possible due to:
 - a shorter inspection interval is suggested for some of the high risk locations in system 315 which have both vibrations and IGSCC.
 - a more effective inspection technique is suggested for system 354.
6. Many low risk locations are suggested not to be included in the new ISI-selection. This means that the radiation exposure to plant personnel can be reduced and resources can be redirected to other safety related issues.
7. The present pilot study with quantitative risk evaluations can be used to:
 - optimise the selection of inspection locations.
 - optimise the inspection interval.
 - give quantitative information of the changes in risk and costs due to plant modifications, for example when:
 - a qualified inspection technique is introduced.
 - an inspection interval is changed.
 - in case of an inaccessible location that makes it impossible to inspect.
 - the water chemistry is changed, for example from NWC to HWC.
8. It is possible to validate the software PIFRAP used in the pilot study against actual leak frequencies. Also for a certain class of problems, good agreement has been demonstrated for the rupture probability between using PIFRAP and the software WinPRAISE.

11 ACKNOWLEDGEMENTS

The author acknowledge with great appreciation the members of the project team who have assisted in providing valuable information and support for this study. The project team members have been:

Roger Axelsson, OKG Aktiebolag
Tomas Jelinek, OKG Aktiebolag
Jan Lundwall, Ringhals AB
Pål Efsing, Barsebäck Kraft AB
Kostas Xanthopoulos, SKI
Anders Hallman, SKI
Tomas Elmeklo, ÅF-PPA
Dan Wilson, NUSAB Aktiebolag
Torbjörn Andersson, Safetech Engineering AB

The financial support from SKI, OKG Aktiebolag, Barsebäck Kraft AB, Ringhals AB and Forsmarks Kraftgrupp AB is gratefully acknowledged.

The help from the following persons at OKG Aktiebolag is highly appreciated:
Ulrika Wretås, Lars Yvell and Percy Hermansson (Consultant).

The help from the following persons at SAQ Kontroll AB is very much appreciated:
Dag Danielsson, Ali Akhtar, Otto Jörpeland, Carl-Johan Börjesson, Peter Dillström and Mats Bergman.
Special thanks are also given to Weilin Zang (SAQ) for the additional programming of the PIFRAP code and for some of the FEM analyses and to Lena Nilsson (SAQ) for the work on the graphical user interface to PIFRAP.

The author is also indebted to the following persons for helpful discussions during the project:
Anders Enerholm, RELCON AB
Fred Nilsson, The Royal Institute of Technology
Fred Simonen, PNNL, USA
David Harris, Engineering Mechanics Technology, USA
Gery Wilkowski, Engineering Mechanics Corporation of Columbus, USA
Nu Ghadiali, Battelle, USA
Victor Chapman, Rolls Royce Power Engineering, UK

12 REFERENCES

- [1] ASME CRTD, *Risk-Based Inspection - Development of Guidelines*, Volume 1, General Document, ASME CRTD-Vol. 20-1, USA, 1991.
- [2] ASME CRTD, *Risk-Based Inspection - Development of Guidelines*, Volume 2 - Part 1, LWR NPP Components, ASME CRTD-Vol. 20-2, USA, 1993.
- [3] ASME CRTD, *Risk-Based Inspection - Development of Guidelines*, Volume 2 - Part 2, LWR NPP Components, ASME CRTD-Vol. 20-4, USA, 1998.
- [4] *Westinghouse Owners Group Application of Risk-Informed Methods to Piping Inservice Inspection*, Topical Report, WCAP-14572, Rev. 1, Westinghouse Energy Systems, 1997.
- [5] Gosselin, S. R. et al, *Risk-Informed Inservice Inspection Evaluation Procedure*, EPRI TR-106706, 1996.
- [6] Gosselin, S. R., *EPRI's new in-service pipe inspection program*, Nuclear News, Nov. 1997.
- [7] Gosselin, S. R. and Fleming, K. N., *Evaluation of Pipe Failure Potential via Degradation Mechanism Assessment*, Proc. 5th Int. Conf. on Nuclear Engineering, May 1997, Nice, France.
- [8] European Network of Risk Informed In-service Inspection (EURIS). *Framework for Risk Informed Inspection of Nuclear Power Plants in Europe*, European Commission, Contract No F14S-CT98-0059, December 1999.
- [9] SKIFS 1994:1, *Regulations by Swedish Nuclear Power Inspectorate for Mechanical Components in Nuclear Power Plants*, SKI, Stockholm, Sweden, October 1994.
- [10] Regulatory Guide 1.174, *An Approach for Using Probabilistic Assessment in Risk-Informed Decisions on Plant-Specific Changes to the Licensing Basis*, USNRC, July 1998.
- [11] Damage Data Base STRYK, SKI, Stockholm, Sweden, 1999.
- [12] Bergman, M., Brickstad, B. and Nilsson, F., A Procedure for Estimation of Pipe Break Probabilities due to IGSCC, *Int. J. Pres. Ves. & Piping*, Vol. 74, pp. 239-248, 1997.
- [13] WASH-1400. *Reactor Safety Study: An Assessment of Accident Risks in US Commercial Nuclear Power Plants*, NUREG/CR-75/014, USNRC, 1975.
- [14] *Technical Elements of Risk-Informed Inservice Inspection Programs for Piping*, NUREG-1661, USNRC, January 1999.
- [15] Simonen, F. A., Harris, D. O. and Dedhia, D. D., *Effect of Leak Detection on Piping Failure Probabilities*, ASME Pressure Vessels and Piping Conference, San Diego, USA, 1998, PVP-Vol. 373, pp. 105-113.
- [16] Dillström, P., *Probabilistic Safety Evaluation - Development of Procedures with Applications on Components Used in Nuclear Power Plants*, SAQ FoU-Report 99/07, SAQ Kontroll AB, Stockholm, Sweden, 2000.
- [17] Delfin, P., Brickstad, B., Gunnars, J. and Josefson, B. L., *Residual Stresses in Multi-pass Butt Welded Bimetallic Piping, Part II*, SAQ FoU-Report 99/06, SAQ Kontroll AB, Stockholm, Sweden, November 1999.
- [18] Simonen, F. A. and Woo, H. H., *Analyses of the Impact of Inservice Inspections Using a Pipe Reliability Model*, NUREG/CR-3869, USNRC, 1984.
- [19] Simula, K. and Pulkkinen, U., *Statistical Models for Reliability and Management of Ultrasonic Inspection Data*, Report No KUNTO(96)10, VTT Automation, Finland, December 1996.
- [20] Bush, S. H., Do, M. J., Slavich, A. L. and Chockie, A. D., *Piping Failures in United States Nuclear Power Plants: 1961-1995*, SKI Report 96:20, Stockholm, Sweden, 1996.

- [21] EPRI Risk-Informed Inservice Inspection Workshop, Scottsdale, USA, February 15-17, 1999.
- [22] Jansson, C. and Morin, U., *Stress Corrosion Crack Growth in Nuclear Materials*, (in Swedish), MD-01, rev. 2.1, Vattenfall Energisystem, Sweden, April 1997.
- [23] Harris, D. O. and Dedhia, D. D., *WinPRAISE 98, PRAISE Code in Windows*, Engineering Mechanics Technology, Inc, USA, April 1998.
- [24] Brickstad, B. and Josefson, B. L., A Parametric Study of Residual Stresses in Multi-pass Butt Welded Stainless Steel Pipes, *Int. J. Pres. Ves. & Piping*, Vol. 75, pp. 11-25, 1998.
- [25] Wretås, U., *Oskarshamn 1 - Evaluation of PSA-O1, Rev.6*, (in Swedish), Report No 99-02660, OKG Aktiebolag, Sweden, March 1999.
- [26] USNRC, *Use of Probabilistic Risk Assessment Methods in Nuclear Activities: Final Policy Statement*, Federal register, Vol. 60, p. 42622, August 1995.
- [27] Bergman, M. and Brickstad, B., A Procedure for Analysis of Leak Before Break in Pipes Subjected to Fatigue or IGSCC Accounting for Complex Crack Shapes, *Fatigue Fract. Engng Mater. Struct.*, Vol. 18, No 10, pp. 1173-1188, 1995.
- [28] Doctor, S. R., Bates, D. J., Heasler, P. G. and Spanner, J. C., *NDE Reliability for Inservice Inspection of Light Water Reactors*, NUREG/CR-4469, Vol. 1-6, USNRC, 1984.
- [29] Ghadiali, N., Paul, D., Jakob, F. and Wilkowski, G., *SQUIRT User's Manual, Version 2.4*, Battelle, Columbus Ohio, 1996.
- [30] Ghadiali, N. and Wilkowski, G., *Effect on Crack Morphology on Leak Rates (Coefficient of Variation)*, Report to SAQ Kontroll AB, Battelle, Columbus, USA, 1996.
- [31] Zang, W. and Linder, J., *Fracture Toughness and Tensile Properties for Austenitic Stainless Steels and Welds*, SAQ/FoU-Report 98/01, SAQ Kontroll AB, Stockholm, Sweden, 1998.
- [32] Bergman, M., *PIFRAP User's Manual, Version 1.0*, SAQ FoU-Report 97/07, SAQ Kontroll AB, Stockholm, Sweden, 1997.
- [33] Brickstad, B. and Sattari-Far, I., *Crack Shape Developments for LBB-Applications*, SINTAP/SAQ/06, Report from the EU-project SINTAP, Contract No BR-PR-CT95-0024, SAQ Kontroll AB, Stockholm, Sweden, July 1998.
- [34] Rahman, S., Ghadiali, N., Wilkowski, G., Moberg, F. and Brickstad, B., Crack Opening Area Analyses for Circumferential Through-wall Cracks in Pipes - Part III: Off-center Cracks, Restraint of Bending, Thickness Transition and Weld Residual Stresses, *Int. J. Pres. Ves. & Piping*, Vol. 75, pp. 397-415, 1998.
- [35] Andersson, P., Bergman, M., Brickstad, B., Dahlberg, L., Nilsson, F. and Sattari-Far, I., *A Procedure for Safety Assessment of Components with Cracks*, SAQ/FoU-Report 96/08, SAQ Kontroll AB, Stockholm, Sweden, 1996.
- [36] Ikonen, K., Raiko, H. and Keskinen, R., *Leak Before Break Evaluation Procedures for Piping Components*, Finnish Centre for Radiation and Nuclear Safety, STUK-YTO-TR 83, Helsinki, December 1995.
- [37] Abramowitz, M. And Stegun, I. A., *Handbook of Mathematical Functions*, Applied Mathematics Series, Vol. 55, National Bureau of Standards, Washington DC, USA, 1964.

APPENDIX A: PROBABILISTIC COMPUTER CODE PIFRAP FOR ESTIMATING FAILURE PROBABILITIES

A1 Theory and Model Assumptions

D	Outer diameter of pipe
R_i	Inner radius of pipe
h	Wall thickness
d	Detection limit for leak rate
Δt	Inspection interval
T	Service life
t	Elapsed time since start up
$f_{al}(l_0)$	Probability density function for initial crack length
$p_{nd}(a)$	Probability for non-detection at in-service inspection
p_{ld}	Probability of non-detection of leakage rate of size d
$f_i(t_i)$	Probability density function for initiation time
a	Crack depth
a_0	Initial crack depth
l	Crack length
l_0	Initial crack length
t_L	Time to leakage
t_F	Time to rupture
m	Leakage flow
$m(t_F)$	Leakage flow just before rupture
μ_l	Mean value of leak rate
σ_l	Standard deviation of leak rate
$p_{f0}(t, T, l_0)$	Conditional rupture probability for given initial crack length
p_f	Rupture probability for pipe section

The present model is intended for evaluation of the leak- and rupture probability of a specific pipe cross section with a certain stress state and possibly containing a circumferential crack growing due to stress corrosion cracking. The following assumptions are made for the probabilistic analysis.

- The stresses are assumed to be deterministic.
- The crack growth law and its parameters are assumed to be deterministic
- The initial crack depth is assumed to be fixed to 1 mm.

- d) The probability that a crack with the assumed depth is initiated during the time interval $(t_i, t_i + dt)$ is given by $f_i(t_i)dt$.
- e) The initial length of the crack is random with the probability density function $f_{al}(l_0)$.
- f) The probability of not detecting a crack at an in-service inspection is $p_{nd}(a)$.
- g) The probability of not detecting a leak rate of a size corresponding to the detection limit d is p_{ld} .

Due to the assumptions made, the growth of the crack will be deterministic and will only depend on the initial crack length for a given geometry and given stresses. A procedure for calculating growth of such cracks has been developed by Bergman and Brickstad [27] resulting in a computer code named LBBPIPE. In Ref. [27] both surface cracks and through wall cracks were considered. The surface cracks in their work are characterised by the length along inner periphery l and the maximum depth a . The through-wall cracks are characterised by the length along the inner and outer periphery, respectively. In both cases the shape of the cracks is given by parametric expressions so that reasonable shapes are obtained. By the computer program LBBPIPE the crack growth $(a(t), l(t))$ can be calculated to the time for penetration of the outer surface t_L (leak) and further to the time of rupture t_F . In addition the leak rate just before rupture $m(t_F)$ can be calculated. With rupture is here meant that either

$J > J_c$ or that the pipe suffers plastic collapse due to that the limit load is exceeded. J is here calculated by the R6-procedure and J_c is the corresponding fracture toughness. The evaluation of the J -integral is described in more detail in Ref. [27].

A certain surface crack of initial length l_0 and of initial depth a_0 in a pipe of inner radius R_i and wall thickness h is considered. The initial depth is taken as common for all cracks and set to a small value (1.0 mm). The development of this crack can be calculated by the procedure in Ref. [27]. In particular the time of rupture $t_F(l_0)$ and the leak rate just before rupture $m(t_F)$ can be obtained. Note that these two quantities are only functions of the initial crack length and that $m(t_F) = 0$ for cracks that lead to rupture without penetrating the pipe wall (non-LBB situation).

Such a crack initiated at the time t_i is now considered. The following mutually excluding possibilities exist:

- 1) $t_i + t_F > T$, where T is the service life. Obviously this event gives no contribution to the rupture probability.
- 2) $t_i + t_F < T$ and $m(t_F) > d$. This event also gives no contribution to the rupture probability.
- 3) $t_i + t_F < T$ and $m(t_F) < d$ and the crack is detected by in-service inspections. This event gives no contribution to the rupture probability. Detected cracks, either by inspections or by leak rate detection are assumed not to contribute to the failure probability. If a crack is detected, it is assumed that either an effective repair is made or that the crack is kept under close surveillance in order to avoid a leak until the next inspection. The probability that the leak rate is not detected is handled through assuming a random behaviour of the leak rate so that

$$\text{Prob}(m(t_F) < d) = p_{ld}(l_0) \tag{A1}$$

- 4) $t_i + t_F < T$ and $m(t_F) < d$ and the crack is not detected by in-service inspections. This event gives contribution to the fracture probability.

The probability for the alternative 4) to happen can be expressed as

$$p_{f0}(t, T, l_0) = p_{ld}(l_0) \cdot \int_{t_i=\max(0, t-t_F)}^{T-t_F} f_i(t_i) \prod_{j=j_1}^{j_2} p_{nd} [a(t_j - t_i)] dt_i \quad (A2)$$

where t_j denotes the inspection times and the number of possible inspections are determined by (A3) and (A4)

$$(j_1 - 1) < \frac{t_i}{\Delta t} < j_1 \quad (A3)$$

$$j_2 < \frac{t_i + t_F}{\Delta t} < j_2 + 1 \quad (A4)$$

The relation (A3) ensures that no inspection before the initiation time may be accounted for and likewise relation (A4) ensures that no inspections after rupture may enter. Δt denotes the inspection interval which needs not to be constant. The product of non-detection of successive inspections in (A2) implies that the inspections are completely independent. However, the inspections need not to be independent. If completely dependent inspections are assumed, only the last inspection before rupture is credited for in (A2).

The lower integration limit of the time integration in (A2) accounts for the fact that a crack that has not led to rupture before the time instant t must have had an initiation time that is larger than $t - t_F$. Likewise the maximum initiation time is $T - t_F$ if rupture is to occur before end of service life T . Here t is the time elapsed (current time) since start up, for the period which the calculation is intended. In the calculation it is also assumed that $p_{nd}(a = h) = 0$, i.e. leaking cracks will always be detected if an in-service inspection is performed between leak and rupture.

The expression (A2) gives the conditional probability of rupture given the initial crack length l_0 . To obtain the rupture probability of the pipe section, the random properties of the initial crack length have to be taken into account. This is done by integration of (A2) with respect to crack length with the probability density functions for this variable as weight.

$$p_f(t, T) = \int_{l_c}^{2\pi R_i} p_{f0}(t, T, l_0) f_{al}(l_0) dl_0 \quad (A5)$$

The lower length limit l_c is the solution of the equation $t_F(l_c) = T$. Finally p_f is divided by the time $(T - t)$, i.e. p_f represents the probability for a rupture, measured per reactor-year as a mean value for the remaining operating time of the plant.

The equations (A1) to (A5) are given for the evaluation of the rupture probability. Likewise, the probability of a leak, p_L at a certain leak rate level $m(t_L)$ at the time t_L , can be obtained by replacing all variables t_F by the time to leak t_L . Instead of rupture, the end event is a leaking crack which is leaking at a specified leak rate level. In the evaluations, if the specified leak rate level is set to a large value, it may happen that for a certain initial crack length the leak rate just before rupture $m(t_F)$ is less than the specified leak rate level. In that case t_L is set to t_F . If this happens for all initial crack lengths, the probability of a (large) leak will be equal to the probability for a rupture. However, for more moderate specified leak rates, the rupture probability will always be considerably less than the leak probability. The

probability of an initial leak at the instant of wall penetration, is obtained by specifying the leak rate, at which the leak probability is evaluated, to zero.

A2 Some Remarks on the Numerical Procedure

In order to perform the probabilistic evaluations according to the procedure described, a computer code named PIFRAP (Pipe FRActure Probabilities) has been developed, Bergman [32]. PIFRAP contains the earlier described programs LBBPIPE and SQUIRT for the evaluation of crack growth and leak rates. PIFRAP calls upon these programs for different values of initial crack length and required quantities for the integration are obtained to give the leak- and rupture probability. Fig A1 shows an example of an evaluation of successive crack shapes for IGSCC in a stainless steel pipe using LBBPIPE and PIFRAP.

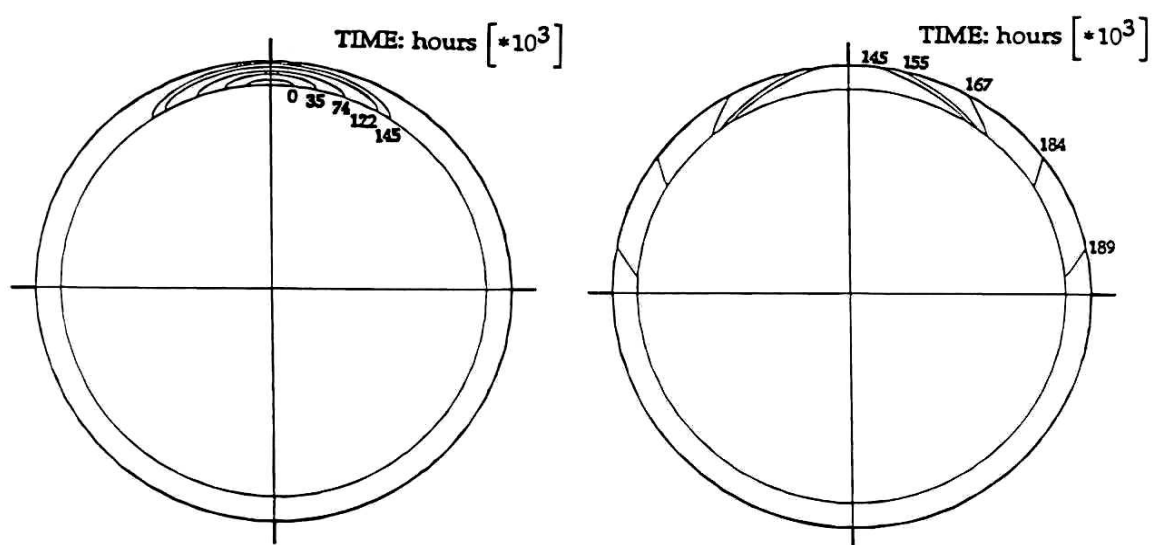


Fig. A1. Successive crack shapes for a growing stress corrosion crack starting from an initial surface crack. Wall penetration at $t_L = 18.1$ years and rupture at $t_F = 23.6$ years, Ref. [27].

One of the notable features of PIFRAP and LBBPIPE is the ability to treat complex crack shapes. At the instant of wall penetration the outer crack length will in general be considerably smaller than the crack length along the inside of the pipe. This has been confirmed by comparison with experiments performed both in Japan and in UK, Brickstad and Sattari-Far [33]. A criterion for the crack geometry at wall penetration has been suggested in [27] and is shown to agree quite well with experiments [33].

The version of LBBPIPE and PIFRAP used here is somewhat modified in comparison between the previously released version, Ref. [32]. A database containing influence functions for the stress intensity factor, limit load solutions and crack opening areas for circumferential surface cracks and complex through-wall cracks in a pipe has been extended to cover longer cracks than before. Up to complete circumferential surface cracks and through-wall cracks with a lengths up to 80% of the inner periphery can now be analysed.

Another new feature is that the effects of plastic deformation on the Crack Opening

Displacements COD and Crack Opening Areas COA for through-wall crack geometries, are now accounted for. Ref. [32] assumed linear elastic behaviour for the determination of COD. Elastic-plastic FEM-calculations using ABAQUS have been performed in this study for a large number of circumferential through-wall crack geometries for a pipe with a ratio of inner radius to pipe wall thickness $R_i/h = 8.6$. The yield properties in Table A3 together with isotropic hardening for typical stainless steel pipes have been used. Through-wall crack angles from $2\theta = 45^\circ$ to $2\theta = 180^\circ$ (half circumference) are covered for a wide range of membrane and global bending stresses. Fig. A2 shows the result in form of the ratio of elastic-plastic to elastic COD (centre) and COA, at the outside of the pipe for a crack angle of $2\theta = 90^\circ$. L_r is the plastic collapse parameter given for combined tension and bending in the handbook by Andersson et al [35].

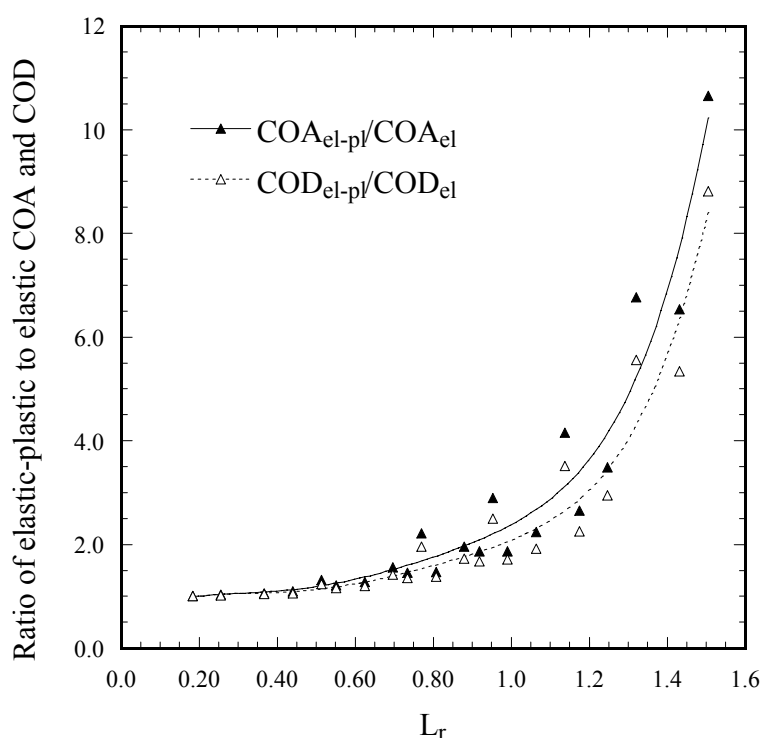


Fig. A2. The ratio of elastic-plastic to elastic COD and COA versus L_r for a crack angle of $2\theta = 90^\circ$.

The scatter in Fig. A2 is due to that different combinations of tension and bending can result in the same L_r -value. In the PIFRAP code linear interpolation is performed between the actual data points in Fig. A2 (determined by the specific stress conditions for the pipe) and used as correction functions to the elastic COD and COA for primary stresses in PIFRAP. The same procedure is used for all the studied crack geometries. As shown in Fig. A2, plastic deformation can have a large effect on the COD and COA, especially for large values of L_r . This will also have a large influence on the leak rate evaluations. For $L_r < 0.5$ the effect is small, even for large crack angles. These results have been compared against similar evaluations by Ikonen et al [36] and the results agree quite well.

The integrations to provide the failure probabilities are performed using an extended trapezoidal rule. In case of evaluation of the normal Gaussian distribution function, special care is taken for integration at the tails where a series expansion according to Abramowitz

and Stegun [37] is used.

A3 Assumptions about Input Data

The probability density function for initial crack length $f_{al}(l_0)$ was estimated from a total of 98 IGSCC-cases in Swedish stainless steel girth welds in straight pipes. The individual data are given in Appendix C, collected from 9 BWRs. In most cases the IGSCC was confirmed by metallographic evaluations. The frequencies of initial crack length relative to the inner circumference of each pipe are shown in Fig. A3.

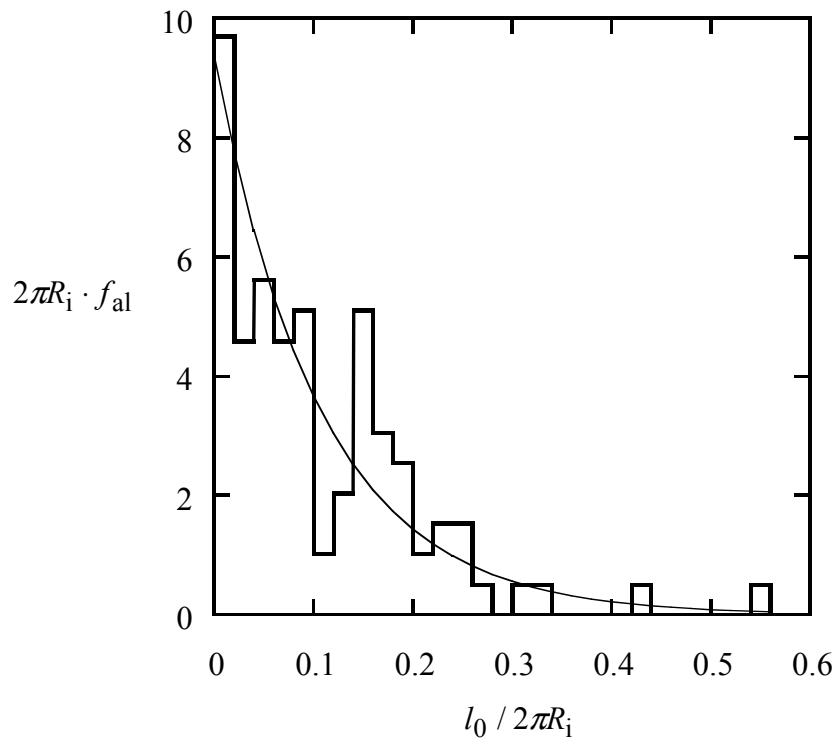


Fig. A3. Observed lengths for IGSCC cracks that have been measured in Swedish BWRs together with assumed probability density function for initial crack length.

A correction was made for the observed crack lengths in order to obtain the initial crack lengths by subtracting an amount of crack growth at each crack-tip equal to the observed crack depth. This procedure was motivated by the observation that once the crack has been initiated the absolute crack growth in the depth and length direction is of the same order. A truncated exponential distribution, Eqn (A6), was fitted to this sample and is also shown in Fig. A3.

$$f_{al} = \frac{\lambda}{2\pi R_i} \exp\left(-\frac{\lambda l_0}{2\pi R_i}\right) (1 - e^{-\lambda})^{-1} H(2\pi R_i - l_0) \quad (\text{A6})$$

Here H is the Heaviside step function. The last two factors in Eqn (A6) are due to the truncation. The choice of an exponential distribution is not obvious but is motivated by its mathematical simplicity and that it is monotonously decreasing. The parameter λ was

chosen with λ_0 equal to 9.380 so that the mean values of the observed and fitted distributions coincided. This corresponds to a mean value $1/\lambda_0$ of 10.66% of the inner pipe circumference.

Fig. A4 shows the cumulative number of IGSCC-cases in Sweden as function of number of service years.

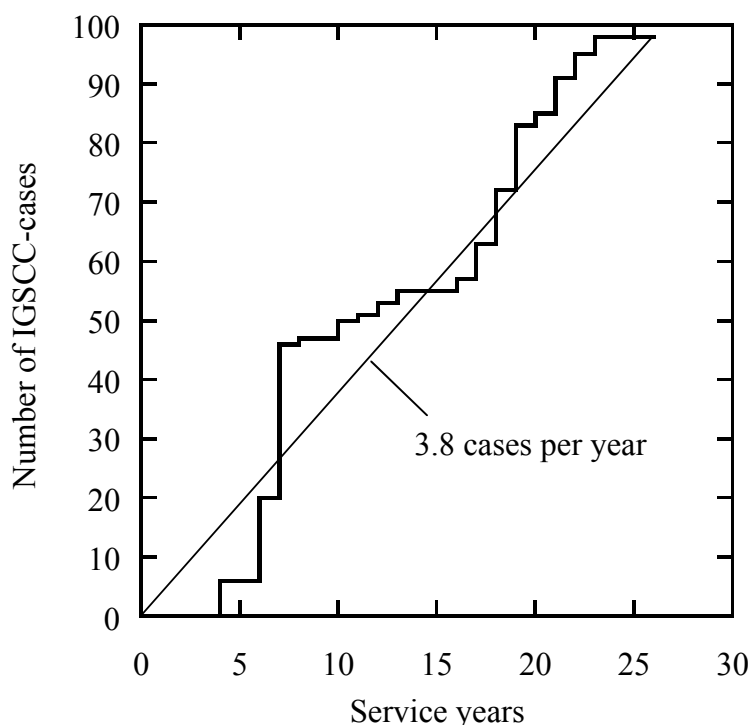


Fig. A4. Cumulated number of IGSCC cases in Swedish BWR piping.

The sample represents 98 cases in nine Swedish BWR piping up to the year 1998. No elbow cracking is included in this sample, only girth welds. The straight line fit in Fig. A4 corresponds to an average occurrence rate of 3.8 cases per year. Estimating the total number of austenitic stainless steel and Alloy 182 girth welds in Swedish BWR-plants to be 9230 then implies that f_i is constant and equal to $f_{i0} = 4.08 \cdot 10^{-4}$ per year per weld. This represents a total average such that if one would take an arbitrary weld from any one of the 9230 welds, f_{i0} would represent the probability of that weld to contain a stress corrosion crack. Subdivisions are possible on individual pipe systems with respect to different dimensions, material and environmental conditions. This may cause f_{i0} to be both smaller and larger than the total average value. However, since the number of IGSCC-cases will be smaller for each subdivision the uncertainty in f_{i0} can be large for individual pipe systems. The relation for the non-detection probability at in-service inspections has been taken from a study by Simonen and Woo [18] for the case of inspection of stainless steel pipes with access from the same side of the weld as where the potential crack is located.

$$p_{\text{nd}}(a) = 1 - \phi[c_1 + c_2 \ln(a/h)] \quad (\text{A7})$$

Here ϕ denotes the normalised Gaussian distribution function. c_1 and c_2 are constants taken from Ref. [18] and are shown in Table A1.

Type of inspection team	c_1	c_2
poor	0.240	1.485
good	1.526	0.533
advanced	3.630	1.106
From Ref. [19]	1.64	0.75

Table A1. Coefficients of non-detection function.

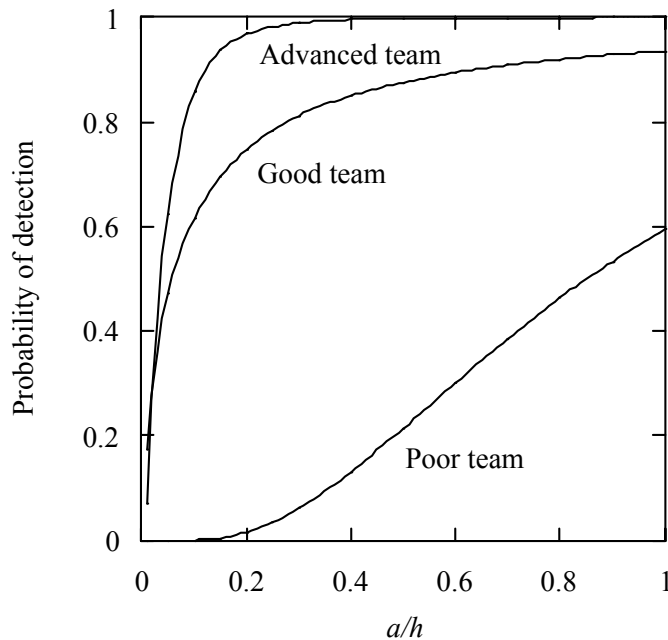


Fig. A5. The probability of detection.

The detection probability ($1-p_{nd}$) is shown in Fig. A5. The term "poor" represents a lower bound performance among the teams that participated in programs to assess inspection efficiency (*cf.* Doctor *et al.* [28]). "Good" represents a team with over average performance in round robin trials that have been conducted and "advanced" represents a performance that may be achieved with further improved procedures. For qualified inspection procedures used in Sweden, the coefficients corresponding to "good" are assumed. No dependence on the crack length appears in Eqn (A7) and no such information has been uncovered in this study. In an investigation by Simola and Pulkkinen [19] no significant length dependence of the detection probability was found.

The author of this report have not been able to find any results for the non-detection probability that are significantly different from those used here. Ref. [19] have analysed the outcome from the PISC-III programme for IGSCC in stainless steel components and the

results are very similar to those of Eqn. (A7). Simola and Pulkkinen assumed a functional form of the non-detection probability of the same type as in Ref. [19] and the coefficients obtained in their analysis are given for comparison in Table A1.

The leak rate in LBBPIPE is calculated using the computer code SQUIRT, Ghadali *et al* [29]. The random properties of the leak rate are taken into account calculated by aid of the results from Ghadali and Wilkowski [30]. Their simulations indicate that the leak rate is normally distributed with a mean value μ_l given by the deterministic SQUIRT code and a standard deviation σ_l given by

$$\sigma_l = 0.4671199 \mu_0 \left(\frac{\mu_l}{\mu_0} \right)^{\left(0.8675548 - 0.0062139 \ln \left(\frac{\mu_l}{\mu_0} \right) \right)} \quad (\text{A8})$$

$$\mu_0 = 0.063093 \text{ kg/s}$$

This result was obtained by numerical simulations using the SQUIRT code with lognormally distributed morphology parameters. This gives a COV = σ_l / μ_l between approximately 0.20 and 0.50. In the present simulations the normal distribution was truncated at zero leak rate in order not to obtain unphysical results for small leak rates.

The basic input data for PIFRAP consists of the data given above together with the specifications according to Tables A2-A6.

Wall thickness h	σ_0 [MPa]	a_0	a_1	a_2	a_3	a_4	a_5
$0 < h \leq 7$ mm	228	1.0	-2.0	0	0	0	0
$7 < h \leq 25$ mm	$297 - 9.88 \cdot h$	1.0	-2.0	0	0	0	0
$h > 25$ mm	79.4	1.0	3.8116	-99.82	339.97	-404.59	158.16

Table A2. Parameters for the definition of axial residual stress distribution in the HAZ of austenitic stainless steel girth welds at a temperature of 288 °C, Ref. [24].

Type of weld	Yield stress σ_y [MPa]	Tensile strength σ_U [MPa]	Fracture toughness J_c [kJ/m]	Vibration threshold ΔK_{th} [MPa \sqrt{m}]
GTAW	150	450	721	4.0
SMAW	150	450	357	4.0
SAW	150	450	320	4.0

Table A3. Material properties at a temperature of 288 °C.

K_I [MPa \sqrt{m}]	Growth rate [mm/s]
$K_I \leq 50 \text{ MPa}\sqrt{m}$	$\frac{da}{dt} = 4.5 \cdot 10^{-12} K_I^{3.0}$

$K_I > 50\text{MPa}\sqrt{\text{m}}$	$\frac{da}{dt} = 5.6 \cdot 10^{-7} \text{ mm/s}$
-------------------------------------	--

Table A4. Crack growth rate for IGSCC in austenitic stainless steels in Swedish BWRs, normal water chemistry at a temperature of 288 °C, Ref. [22].

Surface roughness	Pathway loss coefficient PLC	Discharge coefficient	External pressure	Leak rate detection limit d
0.08 mm	0.282 mm ⁻¹	0.95	0.1 MPa	0.3 kg/s inside containment 2.0 kg/s outside containment

Table A5. Parameters for leak rate evaluation through stress corrosion cracks.

Type of inspection	c_1	c_2	T [years]	t [years]	Number of hours per year of operation
Non-qualified	0.240	1.485	40	28	8000
Qualified	1.526	0.533	40	28	8000

Table A6. Inspection parameters.

The information in the tables A2-A6 needs some explanatory remarks. The specifications for the weld residual stresses are taken from a numerical investigation by Brickstad and Josefson [24]. The axial weld residual stress distribution through the thickness in the heat affected zone HAZ is described in the following form

$$\frac{\sigma}{\sigma_0} = \sum_{k=0}^5 a_k \left(\frac{u}{h}\right)^k \quad (\text{A9})$$

Here u is a coordinate with origin at the inside of the pipe, σ_0 and a_k are constants given in Table A2. For the thin walled (small diameter) piping this corresponds to a pure local through thickness bending whereas for the thick walled (large diameter) piping a more complicated distribution is obtained. Furthermore, all weld residual stresses are assumed to be axisymmetric.

The operating loads in terms of membrane stress due to internal pressure, bending stress due to dead weight and thermal expansion are used in PIFRAP for each individual weld section according to the stress reports for each pipe system. Besides the service loads (which contribute to the crack growth due to IGSCC), an additional load denoted complementary failure load, can be analysed. This can be a load that may occur regularly, such as a thermal stress during a turbine trip, or a load with lower probability, such as water hammer or seismic loads. PIFRAP checks at every time instant if these additional loads will limit the time to leakage or rupture. For every complementary failure load, an occurrence probability is also assigned which is included as a multiplicative factor in the failure probability. It is then not always the complementary failure load that is the most limiting loads that controls

the failure probability. In the majority of the evaluations for the O1 plant, a safety relief valve load occurs as a primary global bending load. This load is generally larger than the dead weight load. The safety relief valves are tested once a month which creates a complementary failure load with an occurrence probability of 1.0. This has an effect on the rupture probability as is demonstrated in the sensitivity analysis in Appendix B.

The material data used are shown in Table A3 and correspond to a stainless steel weld in a type 304 base material. The yield properties refer to the base material whereas the fracture properties are valid for the welds and are taken from a study by Zang and Linder [31]. The J_c -values in Table A3 are actually evaluated at 2 mm stable crack growth to allow for the increased ductility after initiation. The welds are GTAW (Gas Tungsten Arc Welds), SMAW (Shielded Metal Arc Welds) and SAW (Submerged Arc Welds).

The IGSCC growth data are given by a compilation by Jansson and Morin [22]. The growth rates in Table A4 are an upper estimate of IGSCC for type 304 stainless steels in a Normal Water Chemistry (NWC) environment. NWC is characterised as having an oxygen content of less than 0.6 ppm, a conductivity less than 0.2 $\mu\text{S}/\text{cm}$ and a maximum electrochemical potential of -70 mV.

The leak rates are evaluated using the program SQUIRT [29]. Only the thermo-hydraulic part of SQUIRT is used in PIFRAP. The crack opening areas are calculated by separate evaluations using the updated LBBPIPE software. The input data given in Table A5 are taken from recommendations in [29] for stress corrosion cracks. However, the value of the coefficient PLC in Table A5 is smaller than the default value in [29]. PLC characterises the number of turns or changes in direction the fluid must make when flowing through the crack. For a tight crack, PLC can be quite high reflecting the surface roughness of the crack. In the PIFRAP evaluations, the interest is focused on the leak rate just before rupture and for which the crack opening displacements COD are expected to be relatively large. For such cases the PLC can be much smaller. For very large COD it can even be zero. That is why a smaller PLC is used in this study. Note also that only the two-phase flow solution in SQUIRT is used in PIFRAP. This is because the current single-phase model in SQUIRT is very crude and is actually not recommended to be used with the current SQUIRT version [29]. Using only the two-phase flow solution in SQUIRT will result in conservative (smaller) leak rate estimations. Note also that the effect on the leak rate from weld residual stresses are accounted for by PIFRAP. This is done by using the standard crack face pressure method. Weld residual stresses can have a large influence on COD as demonstrated by Rahman et al [34].

The starting crack in PIFRAP is always assumed to be located at the part of the pipe section where the global bending stresses (dead weight and thermal expansion) are tensile. Note that this is not necessarily a conservative assumption. If the starting crack would be located at the compressive side of the global bending stresses, this would slow down the crack growth rate which tends to decrease the rupture probability. On the other hand, the compressive bending stresses would also suppress the leak rate before rupture which tends to increase the rupture probability. In many cases these two factors are cancelling out.

APPENDIX B: SENSITIVITY ANALYSES

In order to check the procedure and also to obtain information about the importance of different quantities, a number of computer runs have been performed. For these runs a specific set of data referred to as the basic case was defined. By varying the parameters sensitivity analyses have then been performed. These analyses give information about the uncertainties associated with the inputs to the probabilistic evaluations.

Using the code PIFRAP it is very convenient to perform sensitivity analyses. One quantity at a time is varied while the others are fixed to their respective reference values. Two stress corrosion sensitive pipe welds in the main circulation system 313 have been analysed, one with vibrations (weld no 865) and the other with no vibrations (weld no 792). The following specifications define the reference values for the input data. These are normally the actual values (or best estimates) for stress state and material data. Notations follow Appendix A.

Geometry

Pipe weld number 865, $D = 112.5$ mm, $h = 8$ mm.

Pipe weld number 792, $D = 114.3$ mm, $h = 8$ mm.

Mean value of initial crack length $1/\lambda_0 = 10.66\%$ of inner circumference of pipe.

Stress conditions

Internal pressure 7.0 MPa at 288 °C, $P_m = 23$ MPa due to internal pressure.

Dead weight bending stress $P_b = 3.3$ MPa for weld 865, $P_b = 13.1$ MPa for weld 792.

Thermal expansion bending stress $P_e = 6.4$ MPa for weld 865, $P_e = 4.9$ MPa for weld 792.

Weld residual stress: local through-wall thickness bending stress $\sigma_b = 218$ MPa.

Vibration stress amplitude = 1.0 MPa for weld 865, vibration stress = 0 for weld 792.

Complementary failure load: Safety relief valve bending stress $P_{SRV} = 15.9$ MPa for weld 865, $P_{SRV} = 25$ MPa for weld 792. Occurrence frequency once per month.

Material data (at 288 °C)

Stainless steel weld, type GTAW. Base material type 304 stainless steel.

Yield stress $\sigma_Y = 150$ MPa, ultimate tensile stress $\sigma_U = 450$ MPa (base material).

Fracture toughness $J_c = 721$ kN/m (weld material).

Vibration fatigue threshold $\Delta K_{th} = 4$ MPa \sqrt{m} .

IGSCC growth rate:

Normal Water Chemistry (NWC) $\frac{da}{dt} = 4.5 \cdot 10^{-12} K_I^{3.0}$, $K_I \leq 50 \text{MPa}\sqrt{m}$.

$\frac{da}{dt} = 5.6 \cdot 10^{-7} \text{mm/s}$, $K_I > 50 \text{MPa}\sqrt{m}$.

Occurrence rate of IGCC, $f_{i0} = 4.08 \cdot 10^{-4}$ per year, per weld.

Leakage

Surface roughness 0.08 mm.

Pathway loss coefficient 0.282 mm⁻¹.

Discharge coefficient 0.95.

External pressure 0.1 MPa.

Detection limit for leak rate $d = 0.3$ kg/s, inside the containment.

Inspection

No inspections assumed.

Total service life $T = 40$ years.
 Elapsed time since start of operation $t = 28$ years (current time).
 1 year of operation = 8000 hours.

The assumption of no inspection in most of the sensitivity analyses is due to the selection of components for inspections that should be based on risk evaluations with no inspections accounted for. The following figures show the leak and rupture probability per year as well as the resulting core damage frequency CDF for variations in different input parameters. The reference values are indicated with vertical lines in the figures. For the evaluation of the risk for core damage, Eqn. (1) has been used (Section 6), where only the small leak and the rupture terms are included. The small leak corresponds to initial leak at wall penetration. For the evaluation of consequence terms in Eqn. (1), the values of system barriers in Table 2 (Section 5) have been used with credit for operator actions.

B1 Sensitivity of crack growth rate

In Fig. B1 the leak and rupture probability per year per weld and the CDF are shown as function of different growth rates for stress corrosion. The reference case corresponds to a crack growth rate factor of 1.0. A crack growth rate factor of e.g. 0.5 then represents a factor of 2 lower growth rate etc. For weld no 865 with vibrations, the CDF will be quite high in the reference case due to the large rupture probability. The vibrations will here make it less probable to detect the leak rate before rupture is predicted. When no vibrations are present, the non-detection probability of the leak rate before rupture will be small which will cause the rupture probability to be smaller.

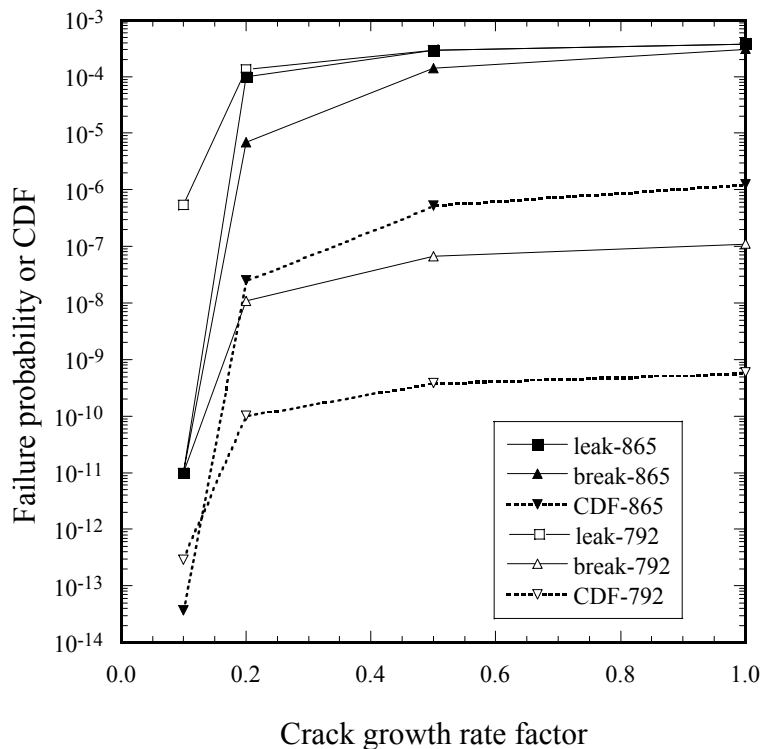


Fig. B1. Failure probabilities and CDF as function of crack growth rate.

Fig. B1 shows only a moderate influence upon the results from the crack growth rate, unless

the growth rate is below a certain limiting value. For a crack growth rate factor of 0.1, rupture is not predicted to occur within the total service life of the plant. For this case a cut-off value of 1E-11 has been used for the rupture probability.

B2 Sensitivity of leak rate detection limit

Fig. B2 shows the sensitivity of the results from different leak rate detection limits.

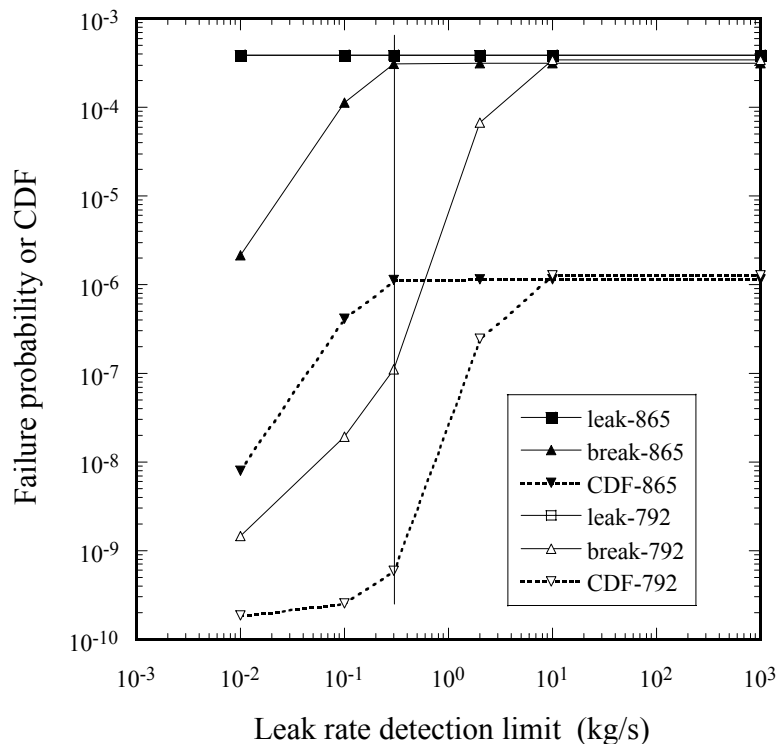


Fig. B2. Failure probabilities and CDF as function of leak rate detection limit.

The reference value $d = 0.3$ kg/s (4.8 gpm) is motivated by the technical specifications for the BWR-plants in Sweden which stipulates that the plant must be brought to a cold shutdown within one hour if an unidentified leak rate above 0.3 kg/s is discovered inside the containment. Fig. B2 clearly demonstrates that leak detection is a very important factor for the failure probability and CDF. A detection limit above 10 kg/s implies that virtually no leak rate is detected before break for this small diameter pipes. Typically the leak rate $m(t_F)$ just before rupture is predicted to about 3 kg/s for weld no 792. For this weld there will be a decrease of the rupture probability with more than 3 orders of magnitude between the case of no leak detection and a detection limit of 0.3 kg/s. If d is decreased to very small values, all leak rates will be detected, no matter how small they are. This implies that the rupture probability will tend to very small values unless break occurs before leak.

For weld no 865, the vibrations will cause very little benefit of leak detection unless the leak rate detection limit is very small.

Note that there will be different degree of sensitivity of the leak rate detection limit depending on the pipe diameter. The leak rate before rupture will be larger for a large diameter pipe.

B3 Sensitivity of dead weight load

Fig. B3 shows the sensitivity of the results for different values of the dead weight load, acting as a primary global bending stress. The reference values of the load are indicated with vertical lines for the respective weld.

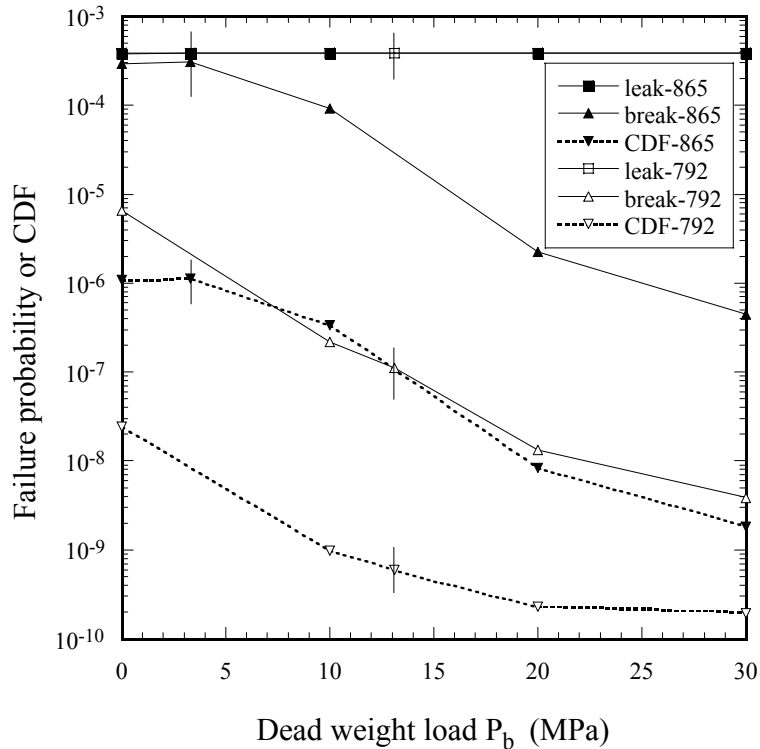


Fig. B3. Failure probabilities and CDF as function of dead weight load.

What may seem surprising in Fig. B3 is that the rupture probability decreases with increasing dead weight load. This is because there are two competing factors involved. The critical crack length at rupture and the time to rupture is decreased but the leak rate just before rupture is increased (due to an increased COD) when the dead weight load increases. The latter effect is dominating and through the smaller non-detection probability of the leak rate before rupture, the rupture probability will then decrease. A dead weight load of 30 MPa will cause the leak rate just before rupture to increase to typically about 8 kg/s instead of 3 kg/s for the reference value of dead weight load for weld no 792. Note also that a primary load will have a large effect on the COD and the COA due to plastic deformations effects, compare Fig. A2.

A large dead weight load is also beneficial for weld no 865 with vibrations. Here the critical crack size is limited by the vibrations (through exceeding of the vibration threshold) and is not affected by a dead weight load. Thus a large dead weight load will only increase the COD and leak rate just before rupture which will decrease the rupture probability and the CDF-values for this weld. For sufficiently small rupture probabilities, the CDF will be dominated by the small leak term. The small leak probability is not affected by leak rate detection. This is why the CDF flattens out for larger values of the dead weight load.

B4 Sensitivity of thermal expansion load

Fig. B4 shows the sensitivity of the results for different values of the thermal expansion load, acting as a secondary global bending stress. The reference values of the load are indicated with vertical lines for the respective weld.

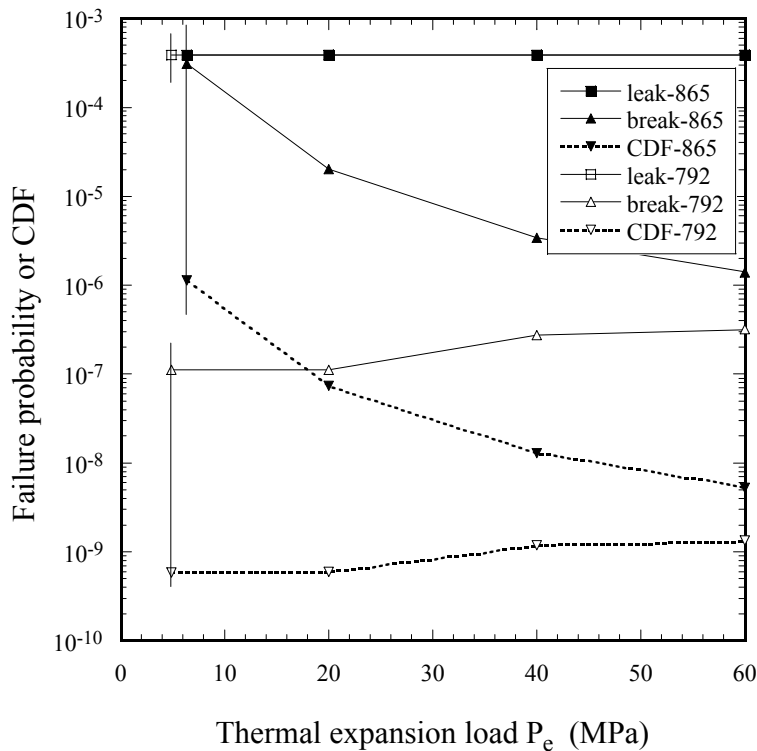


Fig. B4. Failure probabilities and CDF as function of thermal expansion load.

In Fig. B4, the rupture probability and CDF are shown to increase slightly with increasing thermal expansion load for weld no 792. In this case the first of the two competing factors dominates, i.e. the smaller critical crack length will increase the rupture probability. Thermal expansion stresses are considered as secondary stresses, not contributing to plastic deformation and collapse. Therefore, the effect on COD and leak rate for increasing thermal expansion load will be small. For weld no 865 with vibrations, the critical crack size is again limited by the vibrations and is not affected by the thermal expansion load. Thus a large thermal expansion load will only increase the COD and leak rate just before rupture which will decrease the rupture probability and the CDF-values. However, the effect is smaller compared to the influence of a (primary) dead weight load.

B5 Sensitivity of safety relief valve load

Fig. B5 shows the sensitivity of the results for different values of the safety relief valve load, acting as a primary global bending stress with an occurrence frequency of once a month. The reference values of the load are indicated with vertical lines for the respective weld.

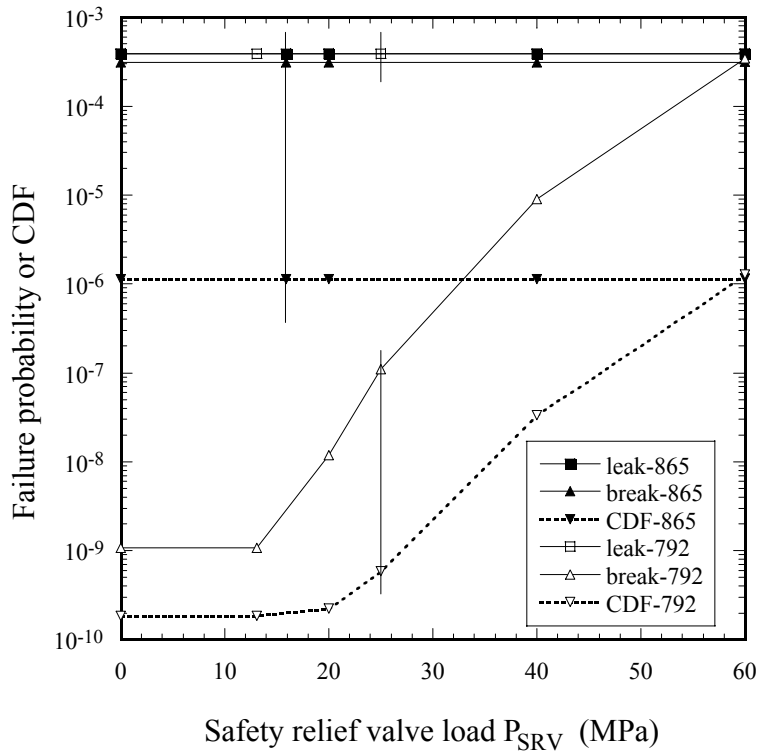


Fig. B5. Failure probabilities and CDF as function of safety relief valve load.

The safety relief valve load does not contribute to the growth of the crack or the load for which the leak rates are evaluated. The occurrence frequency is however sufficiently high in order to limit the critical crack length at rupture. This is why, for weld no 792, the rupture probability and CDF is shown to increase when the safety relief valve load is increased to larger values than the applied dead weight load. Weld no 865 is shown to be completely independent of the safety relief valve load in Fig. B5. For this case, the critical crack length at rupture is determined by the vibrations and therefore the complementary failure load will have no influence on the risk for core damage.

B6 Sensitivity of weld residual stress level

Fig. B6 shows the sensitivity of the results for different values of the weld residual stress level, acting as a secondary local bending stress through the thickness of the pipe. The reference value of the residual stress (weld residual stress factor 1.0) is indicated with a vertical line for the welds. The reference value is quite high, 228 MPa, which is typical for thin-walled pipes of this size, cf Ref. [24]. The hoop shrinkage during welding causes a local inward deformation in the vicinity of the weld. This will create a more or less linear axial bending stress with tension over the inner wall balanced by compression over the outer wall. The axial shrinkage of later weld passes is not resisted by earlier welding passes, since the whole thickness undergoes more or less the same thermal cycle for a thin-walled pipe. The reference case corresponds to a weld residual stress factor of 1.0. A weld residual stress factor of e.g. 0.5 then represents a residual stress of 114 MPa etc.

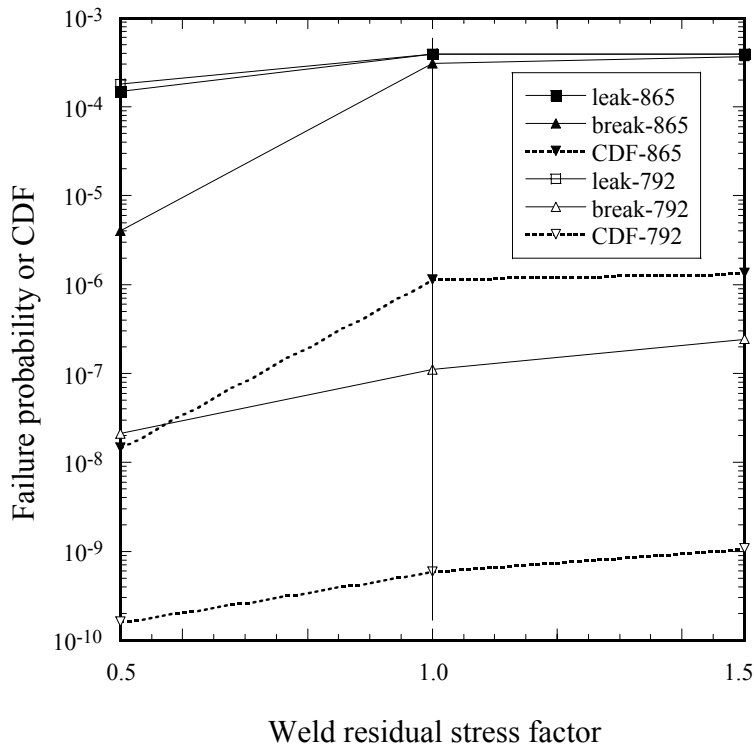


Fig. B6. Failure probabilities and CDF as function of weld residual stress level.

It is seen from Fig. B6 that the leak and rupture probability and CDF are shown to increase with increasing weld residual stress level. It is observed that at least for weld no 792 the influence from the weld residual stress level is rather small. The explanation for this behaviour can be found in the way the residual stresses are distributed through the pipe thickness as a linear local bending stress. The axial weld residual stress is more important for the surface crack growth than for the growth of the leaking crack. For a through-wall crack, a membrane stress or a global bending stress is more important contributors to the crack driving force and thus for the rupture probability. For weld no 865 with vibrations, the effect is larger for the smaller weld residual stress level. One explanation for a small leak rate just before rupture for a short critical crack size which is limited by vibration stresses, is that the weld residual stresses will act as a limiting factor on the leak rates. Initially, at wall penetration, the leak rate will be very small or even zero, due to the compressive stresses along the outside of the pipe. However, the crack will continue to grow at the inside of the pipe and eventually the crack will start to grow also along the outside of the pipe. When the critical crack size is small, limited by the vibration stress, the residual stresses will suppress the leak rate at the critical crack size and thus the larger non-detection probability of the leak rate before rupture will cause a higher rupture probability. If now the weld residual stress level is decreased, the limiting effect on the leak rate before rupture from the compressive residual stresses will be diminished. The leak rate just before rupture will then increase for weld no 865, which causes the rupture probability and CDF to be lower.

B7 Sensitivity of vibration stress

Fig. B7 shows the sensitivity of the results for different values of the vibration stress amplitude. Only weld no 865 is analysed. The reference value of the load, 1.0 MPa, is indicated with a vertical line for the weld.

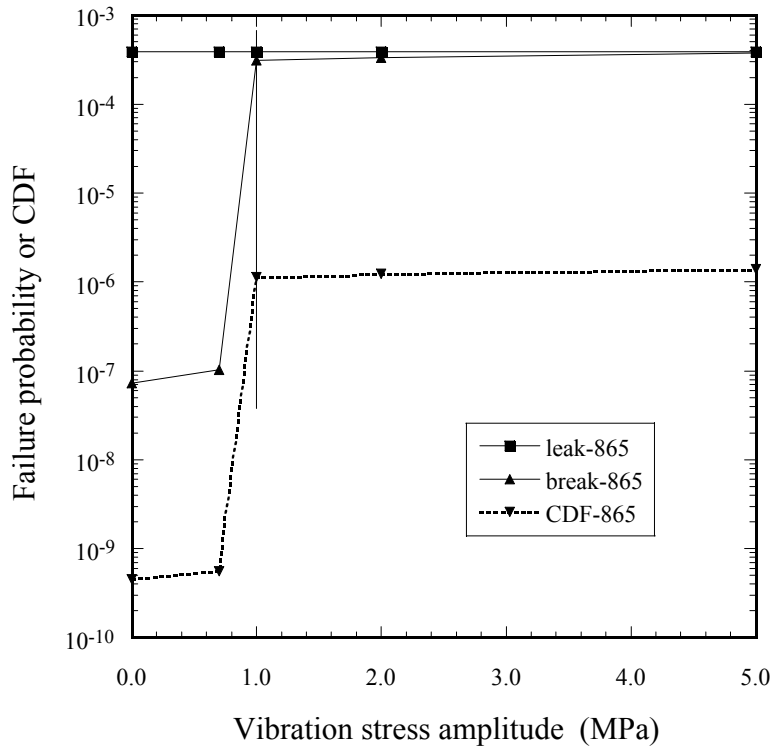


Fig. B7. Failure probabilities and CDF as function of vibration stress amplitude.

As shown in Fig. B7 there is a transition in vibration stress amplitude below which the rupture probability and CDF are small. This has to do with the size of the critical crack length which is limited by vibrations. If the vibration amplitudes are small then the critical crack size will be sufficiently large for the leak rate before rupture to be relatively large which will make the rupture probability small. On the other hand if the vibration amplitude is sufficiently large, the critical crack size at rupture will be small and the high non-detection probability of the leak rate before rupture will cause the rupture probability to approach the small leak probability. Note that the value of the vibration stress amplitude where this transition occurs varies with the particular stress conditions. For this thin-walled pipe with large local bending weld residual stresses and small dead weight and thermal expansion stresses, the vibration amplitudes have to be below about 0.7 MPa in order for the weld not to be more risk significant than those with no vibrations.

B8 Sensitivity of fracture toughness

Fig. B8 shows the sensitivity of the results for different values of the fracture toughness J_c . The reference value of J_c is indicated with a vertical line for the welds.

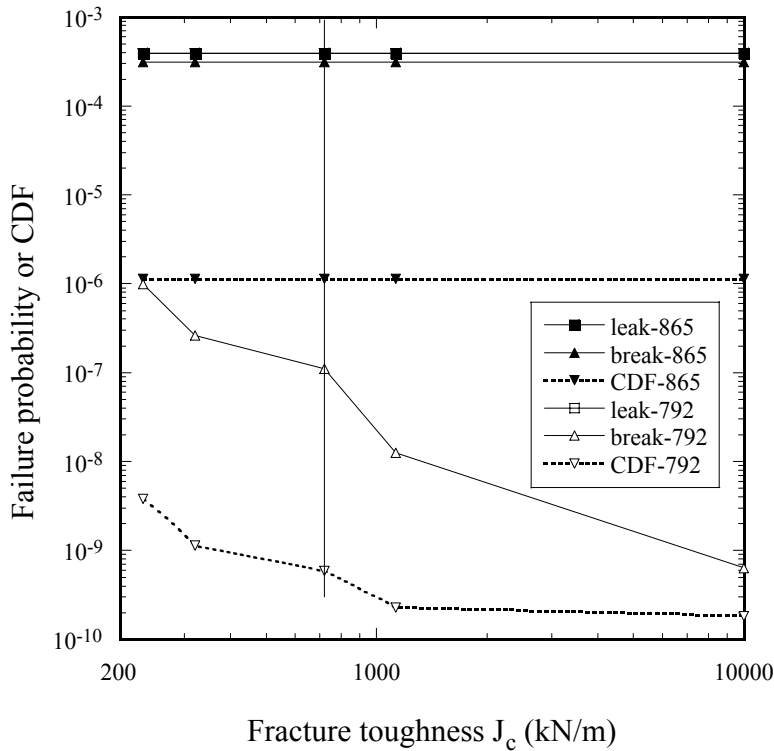


Fig. B8. Failure probabilities and CDF as function of fracture toughness.

The reference case $J_c = 721$ kN/m for GTAW does not correspond to initiation but rather a value of the J -resistance curve after 2 mm of stable crack growth. The fracture toughness level controls the limiting crack size at failure and will influence primarily the amount of leak rate just before rupture. A high fracture toughness will imply a high leak rate and thus p_{ld} will be low for weld no 792. For a sufficiently high fracture toughness, the critical crack size will be controlled by the limit load. Also, for higher J_c -values the risk for core damage will be dominated by the leak probability and thus insensitive to the fracture toughness. The influence of fracture toughness is larger for a large diameter pipe. This is due to the fact that a certain crack angle represents a much larger absolute crack length in a large diameter compared to a small diameter pipe. This will cause a much larger J for the large diameter pipe and thus these pipes are more toughness sensitive compared to a small diameter pipe. This has been demonstrated in Ref. [12].

Weld no 865 is shown to be completely independent of the fracture toughness in Fig. B8. For this case, the critical crack length at rupture is determined by the vibrations and therefore the fracture toughness will have no influence on the risk for core damage.

B9 Sensitivity of yield stress

Fig. B9 shows the sensitivity of the results for different values of the base material yield stress σ_Y . The reference value of σ_Y is indicated with a vertical line for the welds.

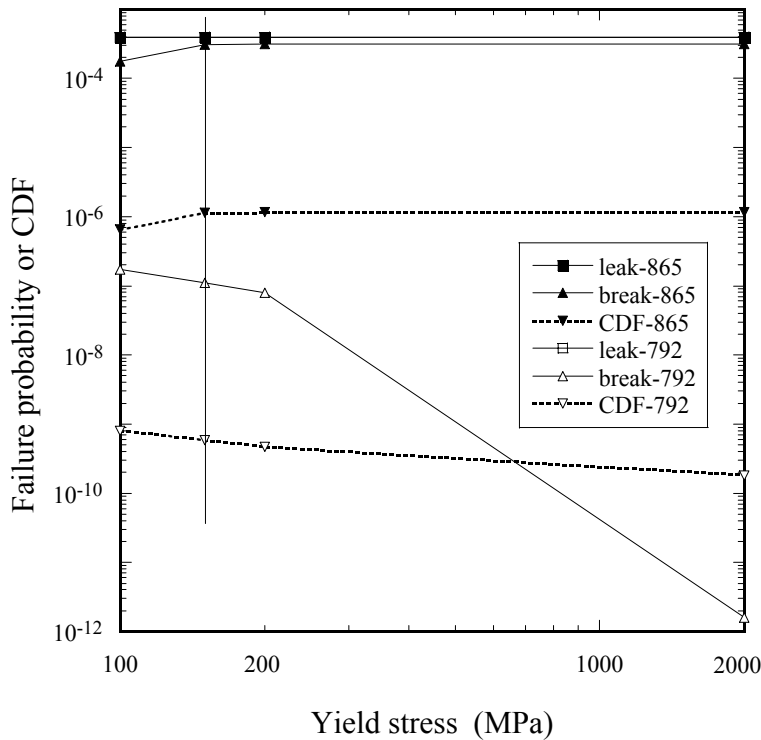


Fig. B9. Failure probabilities and CDF as function of base material yield stress.

If the yield stress is increased from the reference value, the rupture probability is reduced for this small diameter pipe (weld no 792). This is due to diminishing plastic effects which will increase the critical crack size. For a sufficiently large yield stress, rupture will be controlled by linear elastic fracture mechanics alone. For a sufficiently low yield stress, yielding will occur at an early stage and this will also affect J through plasticity effects.

For weld no 865, basically the critical crack size is determined by the vibrations. However, a low yield stress will also increase the plastic effects on the COD and thus tend to increase the leak rate before rupture for the primary stresses. That is why the rupture probability is slightly decreased for the lowest yield stress in Fig. B9. This effect is larger for weld no 865 with vibrations compared to weld no 792.

B10 Sensitivity of initial crack length distribution

Fig. B10 shows the sensitivity of the results for different values of the initial crack length distribution. Only weld no 792 is analysed. The reference value, i.e. mean value of initial crack length $1/\lambda_0 = 10.66\%$ of inner circumference of pipe, is indicated with a vertical line for the weld.

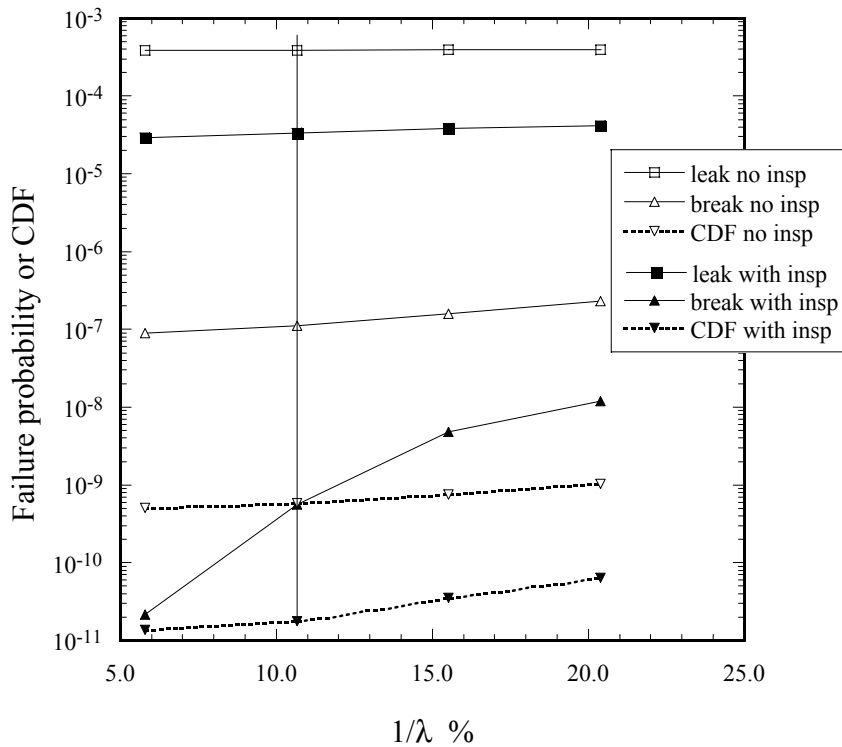


Fig. B10. Failure probabilities and CDF as function of $1/\lambda_0$ in the initial crack length distribution for weld no 792.

Unlike the previous figures (B1-B9), Fig. B10 also considers the effect of inspections. If no inspections are included, the dependence on the initial crack length distribution is quite weak. The assumptions for the inspections are qualified (good team) inspections starting from year 28 and then dependent inspections with an interval of 3 years. Previous non-qualified (poor team) inspections are assumed with a 10 year interval. The reason for that the rupture probability is more sensitive to the initial crack length distribution when inspections are included is that then it may happen that an inspection will occur between leak and rupture. For such cases, $p_{nd} = 0$, i.e. leaking cracks is always assumed to be detected if an in-service inspection is performed between leak and rupture. This is more likely to occur for small initial crack lengths since the time to rupture is longer.

However, in this case for the relatively low stressed weld 792, the CDF is dominated by the probability of small leaks which is not very sensitive to the initial crack length distribution.

B11 Sensitivity of initial crack depth

Fig. B11 shows the sensitivity of the results for different values of the initial crack depth a_0 . The reference value, i.e. an initial crack depth of 1 mm, is indicated with a vertical line for the weld. In this case, to be able to investigate a larger range of initial crack depths, a thicker pipe is considered. Weld no 924 is a low stressed weld in pipe system 315 with a diameter of 229 mm and a wall thickness of 19.5 mm. No vibrations are present.

PIFRAP assumes that an initial crack is present with a deterministic crack depth a_0 and an initial crack length distribution. The probability of this crack to exist is taken care of through

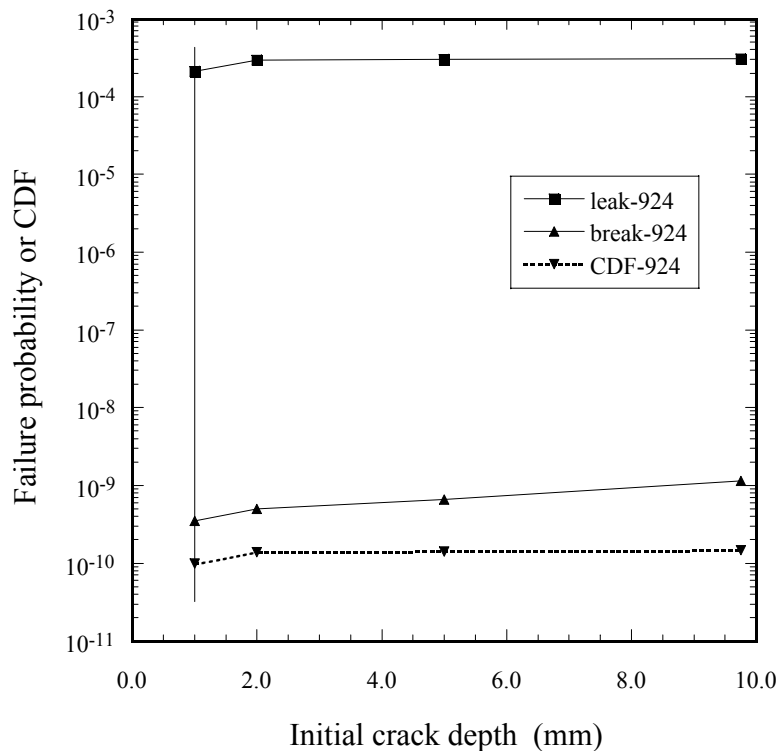


Fig. B11. Failure probabilities and CDF as function of initial crack depth.

the occurrence rate of IGCC, in this case determined by failure statistics to be $f_{i0} = 4.08 \cdot 10^{-4}$ per year, per weld. This value is assumed to be valid for all initial crack depths which should be a conservative assumption for deeper initial cracks. PIFRAP assumes that this initial crack starts to grow with a growth rate given by the growth rate law. If the initial crack size is low, there will take a longer time to leakage and rupture. In this case for the low stressed weld 924, if both the initial crack depth and initial crack length is small, the time to rupture will be longer than the total service life of the plant, 40 years. For such cases, there will be zero contribution to the rupture probability from the small initial crack lengths. If the initial crack depth is larger, also short initial crack lengths will give contributions to the rupture probability. However, the dependence on initial crack depth is rather weak. If inspections are included, the dependence on initial crack depth would be stronger.

To summarise, it can be of some interest to rank the different input parameters in terms of their relative importance for the risk of core damage for the case of no inspections included. This quantity is the basis for risk ranking of components in this study. The following qualitative ranking list has been obtained (with reservation for threshold effects for some of the parameters):

Strong dependence: Pipe stresses P_m , P_b , P_{SRV} , leak rate detection limit d and vibration amplitude.

Moderate dependence: Weld residual stress, thermal expansion pipe stress P_e , fracture toughness and crack growth rate.

Weak dependence: Initial crack depth, initial crack length and yield stress.

APPENDIX C: COLLATION OF IGSCC-CASES IN STRAIGHT PIPE AUSTENITIC STAINLESS STEEL GIRTH WELDS IN SWEDISH BWR-PIPING UP TO 1998

Case Plant, system, year	Pipe dim (<i>D</i> x <i>h</i>) [mm]	Crack depth <i>a</i> [mm]	Crack length <i>l</i> [mm]	$l_0/2\pi R_i$	Reference
F2-321-85	273 x 21	2	20	.0220	C1
R1-354-82	114.3 x 10	9.5	62	.1451	C3
R1-354-82	114.3 x 10	5.7	19	.0257	C3
R1-211-82	114.3 x 10	10	46	.0878	C1, C2
R1-211-82	114.3 x 10	10	35	.0506	C1, C2
R1-354-82	114.3 x 10	10	65	.1519	C1, C2
B1-313-83	114.3 x 8.8	8.8	46	.0935	C1, C2, C3
R1-354-83	114.3 x 10	1.5	5	.00675	C1
R1-354-83	114.3 x 10	1	22	.0675	C1, C2
R1-354-83	114.3 x 10	4.5	45	.1215	C1, C2
R1-354-83	114.3 x 10	3	30	.0810	C1, C2
R1-354-83	114.3 x 10	2	20	.0540	C1
R1-354-83	114.3 x 10	3	30	.0810	C1
R1-354-83	114.3 x 10	1	25	.0776	C1, C2
R1-354-83	114.3 x 10	1	15	.0439	C1
R1-354-83	114.3 x 10	6	65	.1789	C1, C2
R1-354-83	114.3 x 10	5	60	.1688	C1, C2
R1-354-83	114.3 x 10	7.2	24	.0324	C1, C2, C3
R1-354-83	114.3 x 10	3.8	9.6	.0068	C1, C3
R1-354-83	114.3 x 10	3.8	21	.0452	C1, C3
O1-331-83	114.3 x 10	8.6	10	.0068	C2, C3
R1-211-82	114.3 x 10	7.8	70	.1836	C2, C3
R1-211-82	114.3 x 10	6.5	9	.0068	C3
R1-211-82	114.3 x 10	6.5	22	.0304	C1, C2, C3
R1-211-83	114.3 x 10	6	22	.0338	C1, C2, C3
F2-321-85	273 x 21	6	60	.0661	C1, C2, C3
R1-321-83	114.3 x 10	3	10	.0135	C1, C2
R1-321-83	114.3 x 10	1	65	.2127	C1, C2
O2-321-86	230 x 17.5	2.5	30	.0408	C1, C3
F2-321-85	273 x 21	2	7	.00413	C1

F2-321-85	273 x 21	2	55	.07028	C1, C2, C3
F2-321-85	273 x 21	2	170	.2287	C1
F1-321-87	273 x 21	5.1	45	.0480	C1, C3
F1-321-87	273 x 21	6.8	35	.0295	C1, C3
F1-321-87	273 x 21	5.3	25	.01984	C1, C3
O2-331-91	168.3 x 12.5	6.5	55	.0933	C1
O2-331-91	168.3 x 12.5	2.5	75	.1555	C1
O2-331-91	168.3 x 12.5	2.5	90	.1888	C1
O2-331-91	168.3 x 12.5	2.5	30	.0555	C1
O2-331-91	139.7 x 11	2.5	70	.1758	C1, C3
O1-326-91	168.3 x 12.5	7	80	.1466	C1, C3
F2-321-91	323 x 17.5	3.7	150	.1576	C1
F2-321-91	323 x 17.5	1	25	.0254	C1
F2-321-91	323 x 17.5	2	90	.0951	C1
F1-321-94	273 x 21	4	233	.3100	C3
B2-326-95	168.5 x 13	10	110	.2010	C1, C3, C5
B2-321-95	210 x 12.5	5	150	.2409	C1, C3, C5
B2-321-95	210 x 12.5	6	150	.2374	C1, C3, C5
B2-321-95	210 x 12.5	7.5	110	.1635	C1, C3, C5
B2-321-95	210 x 12.5	7	70	.0964	C1, C3, C5
B2-321-95	210 x 12.5	4	122	.1961	C1, C3, C5
B1-313-95	114 x 8	4	60	.1689	C4
B1-321-96	218 x 18	5	100	.1418	C1, C6
B1-321-96	210 x 14	6	150	.2414	C1, C6
B1-321-96	218 x 17	6	95	.1436	C1, C6
B1-321-96	218 x 17	6	40	.04844	C1, C6
B1-321-96	218 x 17	7	330	.5466	C1, C6
B1-321-96	218 x 18	7	71	.0997	C1, C6
B2-321-96	230 x 18	3	85	.1296	C1, C7
B2-321-96	230 x 18	4	95	.1427	C1, C7
B2-321-96	230 x 15	6	60	.07639	C1, C7
B2-354-96	76 x 7	5	26	.0821	C7
B2-321-96	269 x 21	9.1	135	.1482	C1, C7
B2-321-96	269 x 21	5	65	.0771	C1, C7
B2-321-96	269 x 21	9.3	205	.2366	C1, C7
B2-321-96	267 x 22	8	80	.0914	C1, C7
B2-321-95	267 x 19	6	100	.1223	C5

B2-313-97	217 x 16	5	100	.1549	C8
B2-321-96	266 x 17	6	215	.2798	C1, C7
B2-321-95	210 x 15	4	120	.1981	C5
B2-321-95	267 x 22	6	100	.1256	C1, C5
B1-313-88	654 x 52	7.5	25	.005787	C1
R1-354-83	114.3 x 10	3	10	.01350	C1
R1-354-83	114.3 x 10	8.6	50	.1107	C1
R1-354-83	114.3 x 10	4	30	.07426	C1
R1-354-83	114.3 x 10	5.3	110	.3355	C1
R1-211-83	114.3 x 10	5.5	85	.2498	C1
R1-211-83	114.3 x 10	1.5	60	.1924	C1
R1-211-83	114.3 x 10	1.5	22	.06413	C1
R1-211-83	114.3 x 10	5	20	.03376	C1
R1-211-83	114.3 x 10	5	30	.06751	C1
R1-321-83	114.3 x 10	6	62	.1688	C1
O2-321-86	230 x 17.5	1.5	35	.05224	C1
R1-211-82	114.3 x 10	10	35	.05063	C1
R1-354-82	114.3 x 10	10	148	.4321	C1
R1-354-82	114.3 x 10	5	24	.04726	C1
F1-415-85	363 x 36	6	17	.005469	C1
O2-313-97	670 x 35	6	19	.003714	C1
O2-313-97	670 x 35	8	13	.002653	C1
B1-313-92	670 x 35	4.5	18	.004775	C1
B1-313-94	667 x 33.5	5	25	.007958	C1
F2-321-97	273 x 18	8	24	.01074	C1
B1-321-98	125 x 10	7	155	.3327	C1
F2-321-97	273 x 18	8.5	44	.03626	C1
O2-313-96	670 x 35	11	13	.006897	C1
O2-313-96	670 x 35	10	12	.006366	C1
O2-313-96	670 x 35	11	30	.01592	C1
O2-313-96	670 x 35	7	22	.01167	C1

Notation

a	Crack depth	D	Outer diameter of pipe
l	Crack length	R_i	Inner radius of pipe
l_0	Initial crack length	h	Wall thickness

References

- [C1] Damage Data Base STRYK, Swedish Nuclear Power Inspectorate, entry date 1999-03-31.
- [C2] Skånberg, L., "Collation of IGSCC-cases, Project Pipe Break Probabilities", letter dated 1987-08-24 (in Swedish), Swedish Nuclear Power Inspectorate.
- [C3] Bergman, M., "Collation of IGSCC-cases in stainless steel piping welds in Swedish BWR-plants", Report 96-03702 (in Swedish), OKG Aktiebolag, 1996-04-02.
- [C4] Rist, C., "Collation of results from ISI, RA 1995, Barsebäck 1", Report T-9506-72 (in Swedish), Barsebäck Kraft AB, 1995-06-16.
- [C5] Nilsson, J., "Collation of results from ISI, RA 1995, Barsebäck 2", Report T-9509-53 (in Swedish), Barsebäck Kraft AB, 1995-09-26.
- [C6] Nilsson, J., "Collation of results from ISI, RA 1996, Barsebäck 1", Report T-9606-88, rev. 1 (in Swedish), Barsebäck Kraft AB, 1996-06-18.
- [C7] Nilsson, J., "Collation of results from ISI, RA 1996, Barsebäck 2", Report T-9609-14, rev. 0 (in Swedish), Barsebäck Kraft AB, 1996-09-04.
- [C8] Persson, U. and Sandelin, C., "Collation of results from ISI, RA 1997, Barsebäck 2", Report T-9708-68 (in Swedish), Barsebäck Kraft AB, 1997-08-18.